Universiteit Utrecht

The effect of cyclic shoreline dynamics on morphological properties of the downdrift coast

Ameland, The Netherlands

Emily McCullough

Supervisors:

Prof. Dr. Piet Hoekstra

Dr. Albert Oost

Submitted as part of the MSc. Physical Geography

Department of Physical Geography

Faculty of Geosciences

Utrecht University

December 2011

Preface

This research has been submitted as part of the Coastal and Fluvial Systems track of the MSc. programme Physical Geography, undertaken at Utrecht University, the Netherlands.

The aim of this Master thesis is to contribute towards knowledge of the downdrift effects of cyclical ebb-tidal delta behaviour at tidal inlets. The project is based on the island of Ameland in the Dutch Wadden Sea, and the approach varies in both temporal and spatial scale, combining data collected during a period of fieldwork in Autumn 2010, with the long-term Jarkus dataset of coastal profiles. Repeated cycles of large bar attachments to the shoreline have resulted in significant shoreline fluctuations, which can be seen throughout the length of the island. Uncertainty about the sediment volumes involved in this process has prompted this research, while ongoing localised erosion at the coast further emphasises the need to better understand the inlet-coast dynamics through time.

I wish to extend my thanks to Prof. Dr. Piet Hoekstra and Dr. Albert Oost, for providing guidance and feedback throughout the development of this Master project. I also wish to thank Gerben Ruessink, Marcel van Maarseveen and Henk Markies for their assistance before, during and after the fieldwork.

In addition, I thank my fieldwork colleagues and friends, Anouk de Bakker and Aline Pieterse, for the great time we had during the fieldwork on Ameland, including the many early mornings we had 'living with the tide'. I wish to also thank Dirk Visser from Rijkswaterstaat for looking out for us during our stay on Ameland.

Lastly, I am grateful for the support and encouragement of my family and friends, and Dennis in particular, throughout the course of this Master degree.

Contents

List of Figures

List of Tables

1. Introduction

1.1. Problem Analysis

The north and north-west coastline of Ameland, the Netherlands, has been greatly altered by the adjacent tidal inlet over recorded history. It has been observed by various authors (e.g. Israel and Dunsbergen, 1999) that the ebb-tidal delta of the Ameland inlet changes its morphology through a cycle of approximately 50-60 years. This kind of cyclical behaviour is common within tidal inlets and occurs in various situations around the world. At Ameland, this cyclical behaviour permits the bypassing of sand across the ebb tidal delta in the form of a migrating shoal, which migrates onshore and welds to the downdrift beach. This process adds a large volume of sand to the beach, which is comparable to beach nourishment volumes.

It would be expected that, due to wave-driven currents, sand from the welded bar would be dispersed alongshore in the easterly direction and also back into the tidal inlet. This would result in a flattening and lengthening of the profile of the bar, and cause accretion across the downdrift beach. However, there appears to be a longshore limit to this effect. In fact, the central portion of the island downdrift of the welded bar has been experiencing chronic erosion in recent years which has prompted the need for massive beach nourishment to counter this ongoing erosion.

The coastal degradation on Ameland has been a long-term occurrence. The extent of the erosion has been documented by Rijkswaterstaat, who produce maps of shoreline change for the whole Dutch coastline on an annual basis. Figure 1.1 is taken from a recent Rijkswaterstaat coastline report, published in December 2009. This map indicates the recent trend of shoreline movement with reference to the shoreline as it was in 2001, defined in terms of landward-moving trends and seaward-moving trends. The northwest coast, which received sediment from the bypassing event in the mid-1980s, appears to be retreating back toward the reference shoreline. In contrast, the central portion of the northern coastline has shown a seaward-moving trend that exceeds that of the reference shoreline, and indicates a progradation that is unique on the whole island.

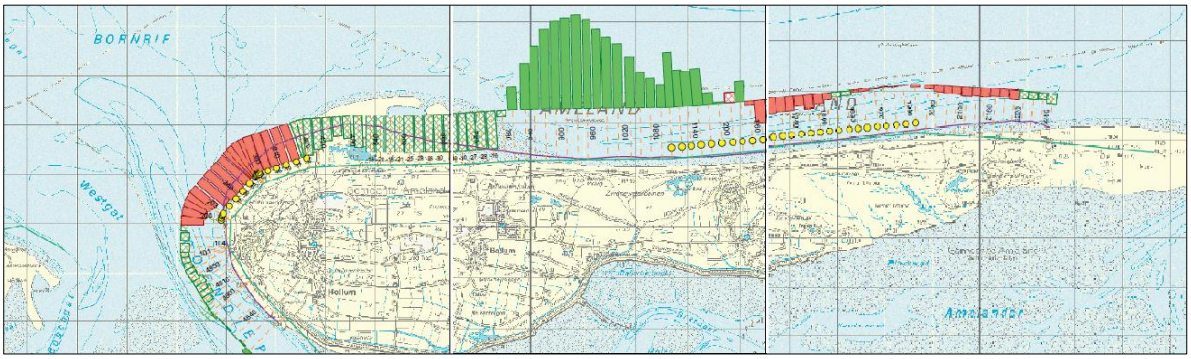

Figure 1.1: Map of Ameland that indicate trends of erosion and accretion: solid red bars indicate shoreline position is seawards of the BKL (reference shoreline position); dashed red bars, landward trend not exceeding BKL; dashed green bars, seaward trend not exceeding BKL; solid green bars, seaward trend exceeding BKL (Rijkswaterstaat, 2009).

While there is a large volume of sand on the western shoreline, the eastern shoreline is suffering a sediment deficit that leads to erosion of the beach. On the other hand, the central portion of the island is accumulating sand which leads to an advance of the shoreline. This pattern suggests that while there is a transfer of sand from the west to the east, it is limited in extent.

The aim of this study is to contribute knowledge towards the workings of this tidal inlet-barrier island system, as little is known about the effect that sediment bypassing has on the island of Ameland. It is the intention of this study to examine the historical trends in morphology to estimate how much volume is contributed to the downdrift beach of Ameland, and to assess the rate of longshore movement associated with the natural beach nourishment.

Chapter 1 aims to place into context the main reason for conducting this research, and addresses the main research questions to be answered as the outcome of this project. The methodology for approaching this research is detailed in Chapter 2, and includes the procedures used to collect both the short-term data from fieldwork surveying methods and the methods used for extracting useful data from the long-term historical record. The analysis of the short-term data is presented in Chapter 3, succeeded by the analysis of the long-term data in Chapter 4. The discussion in Chapter 5 aims to pull together the short- and long-term data and combine it with the knowledge gained from the literature review to address the research objectives. Conclusions drawn within the discussion are presented in the Chapter 6.

1.2. Theoretical Background

Barrier islands and tidal inlet systems are dynamic environments that exist on many coastlines all around the world. The intensity of their study results from an incomplete understanding of how the components within these systems interact, in combination with the threat of increasing beach and shoreline erosion from rising sea-levels. While most research focuses on the dynamics of the tidal inlet itself, one area of research that has not received a great amount of attention is how tidal inlets, specifically the ebb-tidal delta, affect the downdrift coastline.

Tidal inlets interrupt longshore sediment transport by acting as a sink for sediment that is driven past the inlet, preventing it from reaching the downdrift beach. Often erosion occurs on the downdrift beach in response to insufficient sediment supply, as sand that would accumulate is otherwise locked up in the sediment stores of tidal flats and the flood- and ebb-tidal deltas. However, processes of shoal migration from the ebb-tidal delta contribute sediment volumes downdrift, counteracting beach erosion. The ebb-tidal delta itself exerts an influence on the speed and direction of incoming waves, resulting in wave transformation around this topographic obstacle. The morphology of the ebb-tidal delta, and cyclical changes to this morphology, greatly controls the sediment that is supplied to the downdrift beach. Ultimately, the beaches on the downdrift side of a tidal inlet are at the mercy of the processes acting updrift and the influence of the ebb-tidal delta. This can result in a fluctuating response in beach sediment volume, with cycles of accretion and erosion over the long term.

The purpose of this review is to assess how much we understand about tidal inlets, and how much we don't. The general theme is concerning tidal inlets and their impact on adjacent shorelines. In order to gain a complete overview of this topic, this discussion has been divided

into several sections beginning with a brief description and discussion of ebb-tidal delta morphology, a discussion of cyclical behaviour observed at tidal inlets, sand bypassing and downdrift shoreline behaviour, and finishing with a synthesis of the main 'burning questions' in relation to downdrift coastlines.

The aim of this review is to summarise current thought about tidal inlets with respect to adjacent shorelines, with a view to conducting research at a location on the island of Ameland in the Dutch Wadden Sea (Figure 1.2). This literature review is further elaborated with a discussion of a research approach, questions, and objectives based on the conclusions drawn from the review.

Figure 1.2: Northwest beach of Ameland downdrift of the inlet, photo taken in 2007 (www.KustFoto.nl)

1.3. Ebb-tidal Delta Morphology

Tidal inlets are often divided into three broad morphological units: the inlet throat, ebb-tidal delta, and flood-tidal delta (Hayes, 1980). The ebb-tidal delta is a lobate accumulation of sediment on the seaward side of the inlet, while the flood-tidal delta is a similar formation on the landward side. The ebb-tidal delta is formed by the accumulation of sediment washed out from the inlet with the ebb tide, hence the name, ebb-tidal. The size and shape of the ebb-tidal delta represents a morphodynamic equilibrium between the ebb-tidal flow and wave-driven effects.

Longshore sediment transport from one side of the inlet to the other is interrupted by the currents of the inlet, causing sand to flow into and out of the inlet by tidal currents. The sand may settle in the back basin and remain there for a long time, and then it could be transported out of the inlet with ebb-tidal currents and deposited on the ebb delta. In either case, sediment is often taken out of the active system and put into storage, which means that sand is not being directly delivered to the downdrift coast.

Observations of ebb-tidal deltas have shown that they take on a general model comprising of channels and sediment units (Figure 1.3). A typical ebb-tidal delta has a main ebb channel through which the ebb current is focused, and which ends at the terminal lobe. Swash platforms or shoals accumulate on either side of the ebb channel where flow velocity is less. Flood-dominated channels occur between the ebb-tidal delta and the adjacent shoreline, although these are usually less well-defined. Sediment transported by longshore drift enters the inlet by the flood channels adjacent to the updrift beach, and exits the inlet through the ebb channel. As sand continues to be deposited on the terminal lobe, swash platforms (shoals) are built up vertically. There comes a point when deposition has accumulated a sufficient amount of

sediment to reduce the water depth and allows for waves to affect the delta surface. Once waves begin to interact with the ebb delta surface, sediment is transported and shoals of sand develop and migrate towards the shoreline. This process is significant for contributing sediment to the downdrift beach, and the mechanisms will be discussed in further detail in a later section.

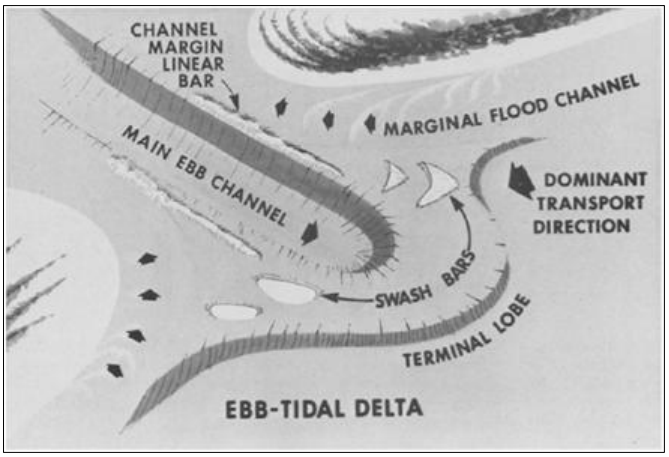

Figure 1.3: Illustration of an ebb tidal delta with accompanying main ebb channel, terminal lobe, marginal flood channels adjacent to the shoreline, and swash bars (Hayes, 1980)

Ebb-tidal deltas are the product of tidal currents and wave action combined (Oertel, 1975; Hayes, 1980; FitzGerald et al, 1984). Their morphology is controlled by these forces acting perpendicular to the coast (waves) and parallel (tides): waves and longshore drift form shoals and bars on the delta, while tidal currents scour out channels (Sha, 1989). Ebb-tidal deltas can be wave-dominated, tide-dominated, or a mixed-energy combination of the two. The morphology of wave-dominated deltas is controlled primarily by the local wave conditions, and while there may be a tidal influence it will be small in comparison to the wave energy. Wave-dominated ebb-tidal deltas are generally pushed closer to the inlet and limited in seaward extent (FitzGerald et al, 2001). Ebb deltas in tide-dominated settings tend to extend much further out to sea due to strong ebb currents and the relatively reduced ability of wave energy to mobilise the sediment. Ebb deltas in mixed-energy settings, however, have a more complex morphology and tend to be skewed either in the up- or downdrift direction. This skewedness results from a combination of oblique angle wave approach and an asymmetry between the ebb and flood tidal currents (Figure 1.4). The concentration of the ebb tide into the main channel shapes the ebb delta into a skewed form in the direction of the current, which also depends on the rate of longshore sediment transport. The ebb-tidal deltas of the Dutch Wadden Sea islands have an updrift asymmetry (Figure 1.5), due to the scouring effect of the shorter ebb tide phase (Sha, 1989) in combination with a low longshore sediment transport rate (Figure 1.4 [B]).

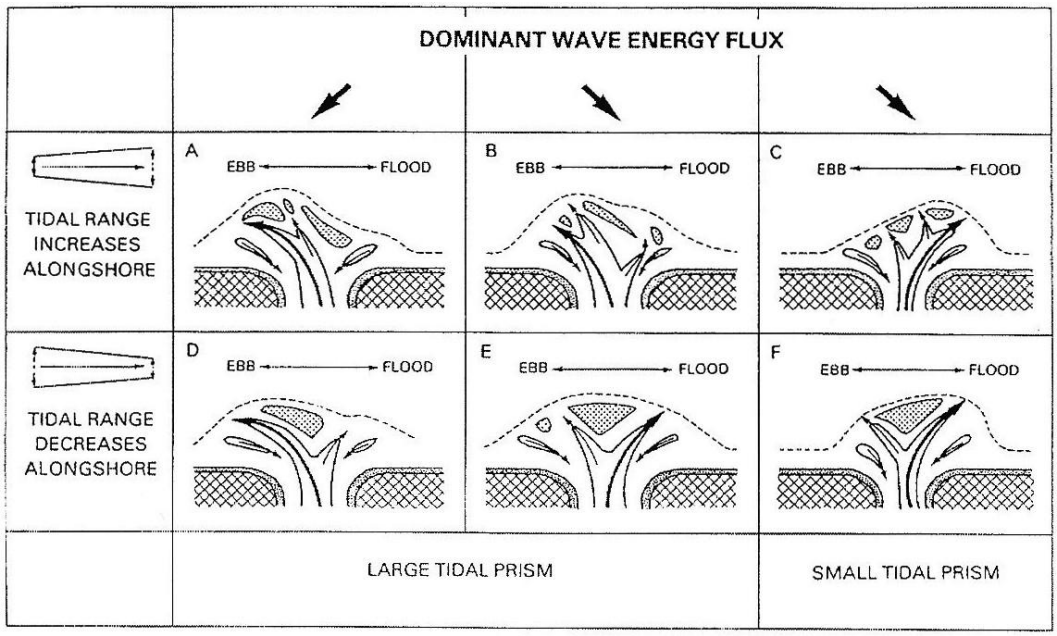

Figure 1.4: Illustration of asymmetric ebb-tidal deltas in response to dominant wave energy flux and the hydraulic gradient generated by fluctuating tidal water levels (after Sha and van den Berg, 1993)

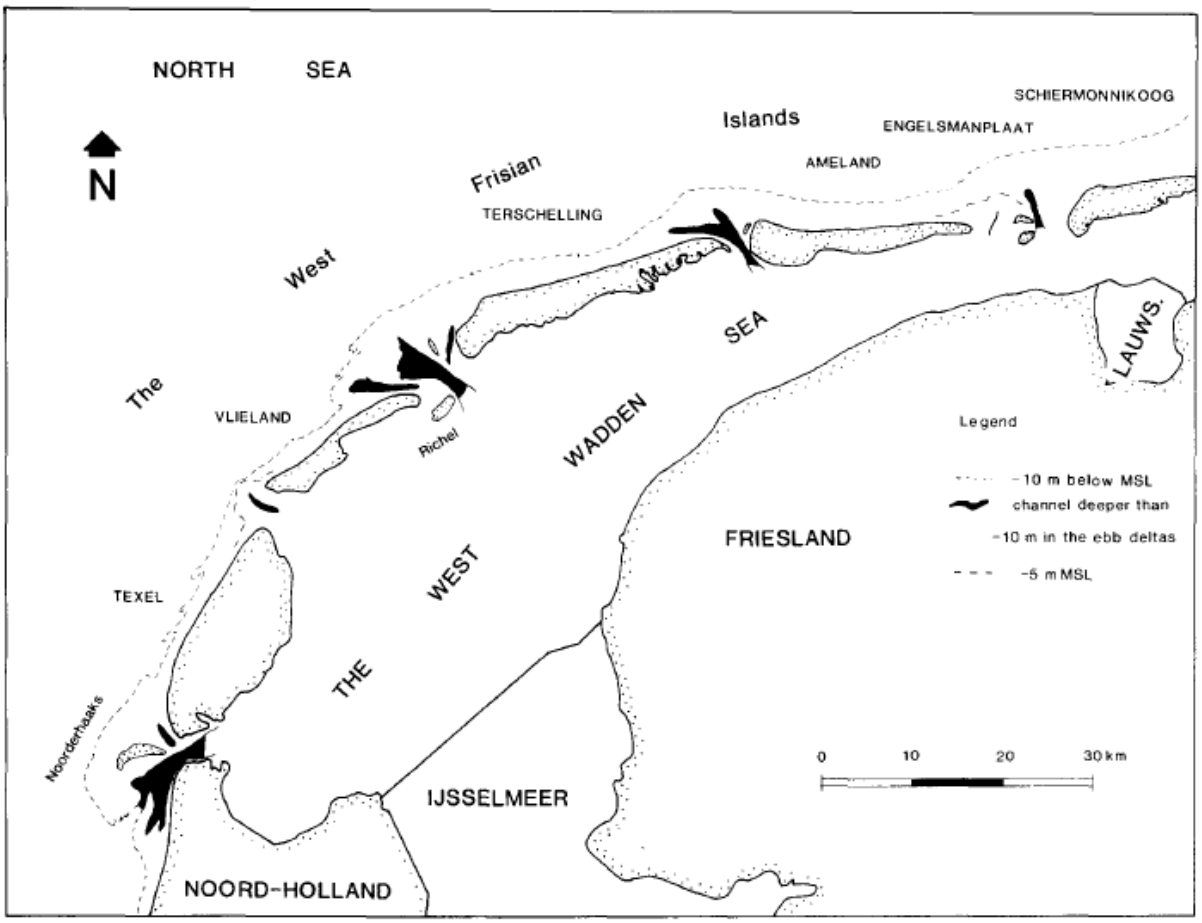

Figure 1.5: General orientation of the ebb-tidal deltas of the Dutch Wadden Sea islands (Sha, 1989)

Davis and Barnard (2003) discussed the sensitive morphodynamics of the highly variable tidal inlets of west-central Florida, USA. On the low-energy coastline of the Gulf of Mexico, this series of eighteen barrier islands varies between wave-dominated, mixed energy and tide-dominated inlets. They highlight the exact delicate balance that makes tidal inlets so dynamic, as a slight change in the relative influence of wave or tidal processes (i.e. tidal prism) can push any of the inlets out of equilibrium and causes rapid morphological change.

Another major contributing factor to morphological changes in ebb tidal deltas is cyclical morphological evolution. The following section addresses this cyclical behaviour, taking examples from real situations such as the Ameland Inlet.

1.4. Cyclic Behaviour of Ebb-Tidal Deltas

Cyclic behaviour of ebb-tidal deltas has been recorded in a wide range of situations (e.g. FitzGerald, 1984; Israel and Dunsbergen, 1999; Cooper et al, 2007). As more research is conducted on the subject authors are reporting that there does not appear to be a universal cause for cyclic behaviour in ebb-tidal deltas, rather they operate as self-regulating systems (Cooper et al, 2007). Cyclic behaviour manifests itself in response to site-specific conditions and occurs on wide temporal and spatial scales, with cycles of periods of 2-3 years at some inlets and ranging to 50-100 years at others. This behaviour can have significant consequences for the adjacent shorelines, which tend to display dynamic fluctuations in response to the changing morphological configuration.

Cyclical behaviour is associated with a change in the hydrodynamics of the ebb-tidal delta and resulting altered morphology in response. Channel switching or migrating involves a dramatic change in direction of the main ebb channel and is often recorded in the literature as a main indicator of cyclical activities. Shoal bypassing is also considered a cyclical occurrence and, although this subject will be dealt with in more detail in the following subchapter (1.5 Sediment Bypassing), it is important to acknowledge the cyclical change in ebb-tidal volume that is associated with shoal migration and the consequences for adjacent shorelines.

1.4.1. Channel Switching

The dynamic nature of ebb-tidal deltas means that the morphology is constantly changing as it is affected by the tides, wind and waves. The main channels are broadly maintained through time by tidal currents, but accumulations of sand can build up at the entrance to the inlet and cause the channels to be deflected. Sand is accumulated in this way by littoral drift which is not subsequently eroded.

Depending on the nature of the channel switching, the downdrift beach can experience periods of erosion and accretion at intervals that coincide with a particular position of the ebb channel. Oertel (1977) observed how the growth of a spit from the updrift side of an inlet could deflect the flow of water against the downdrift beach, before breaching the spit and returning to a previous orientation. This phenomenon has since been reported by several authors (e.g. Michel and Howa, 1997; Cooper et al, 2007). The control on ebb-tidal deltas that display cyclical

channel shifting thus appears to be the sediment input into the system and the morphological feedback that occurs once sand accumulates at one side of an inlet.

Cooper et al (2007) demonstrated how sand within a closed-bay system is recycled between the ebb-tidal delta, the estuary, and the beach-dune system. Sand is deposited and built-up at the ebb-tidal delta, which causes inefficient flow. A diversion from this inefficient flow occurs as the channel flows through a pathway of the least resistance. However once the channel creates a new pathway, erosion of the beach and also the dunes occurs

Michel and Howa (1997) proposed a two-stage conceptual model based on the Arcachon Inlet (France) whereby the ebb delta alternates between a one- and two-channel morphology (Figure 1.6). When there is a single ebb channel, longshore drift on the updrift side of the inlet accumulates sediment into a spit, while sand bypassing delivers sediment to the downdrift shoreline which is subsequently caught in littoral drift reversal and causes a progradation of the shoreline. However, when the two-channel morphology becomes dominant, more sediment is trapped on the ebb delta which leads to a deficit on the downdrift shoreline and subsequently erosion occurs. It is not clear in the article why more sediment remains trapped on the ebb delta during the two-channel phase, but this may be a result of the positioning of the two channels and the delivery of sediment on the ebb delta. They also imply that sand bypassing no longer operates when two channels are present, as the volume of the ebb delta is depleted when the system has a single-channel morphology.

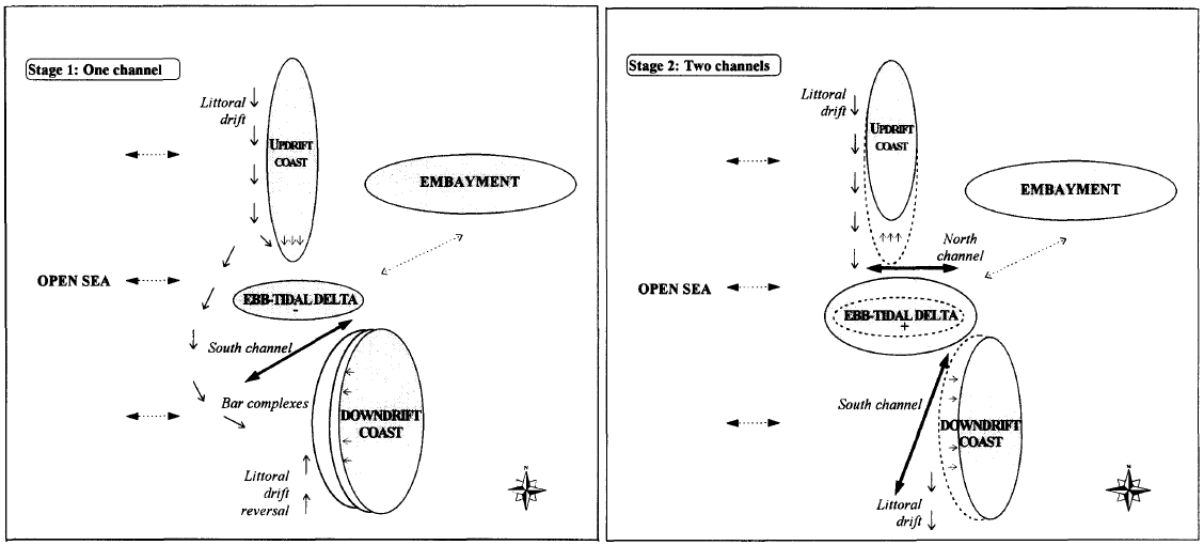

Figure 1.6: Diagram illustrating the one-to-two channel transition and the subsequent impact of sediment supply to the downdrift coastline (Michel and Howa, 1997)

The reason for the observed channel switching is due to an 80-year cyclical morphological evolution of the tidal inlet. Michel and Howa, however, fail to provide an explanation for the mechanism that forces the transition between these stages, stating merely that this transition is "essentially under the control of external hydrodynamic forcing".

The situation at the Arcachon Inlet could be explained by examining similar cyclical ebb-delta morphologies. A one- to two-channel cyclical morphological evolution is also observed in the Ameland Inlet (Figure 1.7). The inlet's main channel, the Borndiep, splits into two channels on the ebb delta, the Westgat to the west (north of the island of Terschelling) and the Akkepollegat. An additional channel, the Boschgat, connects the western side of the tidal basin to the Borndiep. Israel and Dunsbergen (1999) have provided a detailed examination of the four phases of the cycle, which will only be summarised here. In the first phase, the Boschgat migrates northward and interrupts the smooth connection of the Borndiep to the Westgat, creating a 'cross' of the four channels. The Borndiep discharges more directly into the Akkepollegat and this channel becomes dominant over the Westgat, as the significantly larger eastern tidal basin drains through this channel. Sand is brought to the outer ebb delta via the Akkepollegat and swash bars accumulate on the shoal platform on the eastern side. Before the transition to the two-channel morphology, the Bornrif bar emerges and attaches to the downdrift shoreline. The third phase sees the disintegration of the Westgat-Boschgat connection, and the Westgat once again makes a connection with the Borndiep. The addition of the Westgat connection divides the Borndiep flow through two channels and significantly reduces the flow through the Akkepollegat. Subsequently the Westgat becomes dominant, due to the west-to-east tidal current, and the Boschgat migrates to a more southerly position.

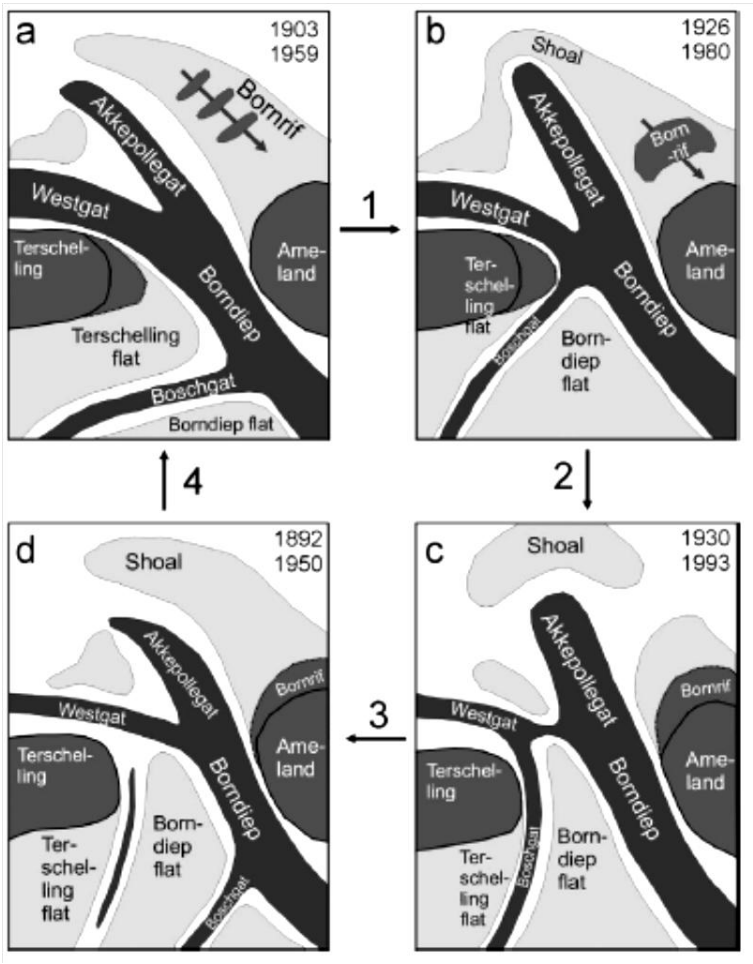

Figure 1.7: The cyclical morphology of the Ameland Inlet, which switches between a one- and two-channel morphology over a 50-60 year cycle (after Israel and Dunsbergen, 1999)

Channel switching also enhances sediment bypassing processes. FitzGerald (1984) notes that a shift in the main ebb channel (similar to a shift back from a two-channel to a one-channel situation) delivers more sediment to the ebb delta, where large bar complexes can accumulate and migrate. Gaudiano and Kana (2001) also observed this phenomenon at Breach Inlet following a periodic shift in the ebb channel. On Ameland, when the one-channel phase is operating, the ebb-dominant Akkepollegat is delivering sand directly to the shoal platform and permitting the formation of swash bars that eventually form the Bornrif shoal.

While there have been several important studies that look at cyclical channel switching behaviour, often the main focus is to report on the morphological behaviour and the timescales involved. The effect on downdrift beaches is evaluated qualitatively, perhaps with a general measurement of beach width, but quantification of volume changes on adjacent shorelines is rarely addressed. Even though Michel and Howa (1997) provided data on the change in ebb delta volume and the longshore sediment transport rate, there was no quantification of the volume changes on the adjacent shoreline. They put an emphasis on the change in volume of sand in the ebb delta and migrating swash bars, but fail to acknowledge the volume change in the adjacent shoreline coinciding with swash bar accretion.

1.4.2. Spatial and Temporal Scales of Cyclical Behaviour

Tidal inlets can vary in width from several hundreds of metres to several kilometres and, concurrently, the scale and response time of cyclical behaviour on the ebb-tidal delta relates directly to the size of the tidal inlet. Walton and Adams (1976) first showed that the volume of an ebb-tidal delta is closely related to the tidal prism of the inlet basin, and therefore related to the cross-sectional area of the inlet itself.

Gaudiano and Kana (2001) demonstrated with a selection of South Carolina inlets how predictable relationships exist between the volume of the ebb tidal delta, the migrating shoals, the mean event interval and the tidal prism. Their results suggest that as the cross-sectional area of the inlet increases (thus the tidal prism), so does the volume of the ebb delta, the volume of the shoals and the time interval between shoal migration events. Larger inlets undergo shoal bypassing less frequently than smaller inlets, but they also produce greater shoal volumes. This is logical because inlets with larger tidal prisms have a greater carrying capacity for sediment, thus are able to transport larger volumes of sand than smaller inlets. More about delta and shoal volumes from this study can be found in the subchapter, “Impact of the size, shape and volume of the ebb-tidal delta”.

There appears to be a bias in the literature concerning the tidal inlets that are studied. While many inlets undergo cyclical changes, large and small, the majority of studies that examine this behaviour tend to be small. In their study, Gaudiano and Kana (2001) discuss Stono Inlet as a ‘large inlet’ with a tidal prism of 70 10^6 m^3. However, this is comparable to inlets such as Ameland Inlet where the tidal prism is 480 10^6 m^3 with bypassing intervals ten times longer than that at Stono Inlet. And yet there is little discussion about the shoal volumes and adjacent shoreline changes at Ameland Inlet. Part of the reason for the bias toward smaller inlets is probably due to the lack of data about shoal events, particularly if they take place very infrequently. But, this means that there is a gap in our knowledge about sediment bypassing that occurs on much longer timescales.

As cyclical behaviour is inherently linked to sediment bypassing in most inlets, the next subchapter discusses why it occurs and the mechanisms by which bypassing is achieved.

1.5. Sediment Bypassing

As previously mentioned, tidal inlets restrict the transport of sediment from one side of the tidal inlet to the other. A process by which this downdrift sediment deficit is reversed is sediment bypassing. Sediment bypassing is an important process which permits the transport of sand from the updrift side of the inlet towards the downdrift side.

Cycles of erosion and accretion on downdrift beaches are often reported in literature in association with the migration of shoals from the ebb tidal delta in combination with the pattern of wave refraction around the inlet and the resulting sediment transport along the adjacent shoreline (subchapter 1.6) (Oertel, 1977; FitzGerald, 1984).

1.5.1. Mechanisms

Although sediment bypassing is known to occur, the exact mechanism which operates is uncertain and little is known about the volumes involved (Gaudiano and Kana, 2001). The backbarrier and ebb-tidal delta represent the two main reservoirs of sediment in the inlet system. As sediment is accumulated in these reservoirs, there must also be a balanced loss of sediment in order for the inlet to be stable (O'Brien, 1931).

The process of sand bypassing was first recognised by Bruun and Gerritsen (1959). They suggested that shoals were formed by littoral drift along the terminus of the ebb tidal delta, which coalesced to form migrating shoals. Although this mechanism may be applicable in wave-dominated inlets, at much larger ebb tidal deltas with deep channels this is not a feasible mechanism (Kana et al, 1999). At larger inlets, the channels of the ebb delta are wider and deeper and it would not be possible to have a transport of sediment in this way. Instead, sediment is brought into the tidal inlet by wave action and transported either into the backbarrier by flood currents or out onto shoals of the ebb delta by ebb currents (FitzGerald et al, 2000).

FitzGerald et al (2000) describes some of the mechanisms by which natural sediment bypassing occurs on sandy shorelines with tidal inlets. The nine conceptual models presented in the article relate to ebb tidal deltas in different circumstances, such as migrating inlets or stable inlets, developing spit platforms, or those inlets which have hard engineering structures preventing natural evolution. Of these models, only three are potentially similar to the situation at the Ameland Inlet (Figure 1.8). The first concerns sediment bypassing at stable inlets, the second is ebb-tidal delta breaching, and the last outer channel shifting. Each of the models consists of three phases which indicate the evolution of the ebb tidal delta through time.

A stable inlet is one where migration does not occur either in the inlet throat or the main ebb channel. Sediment accumulates on either side of the main ebb channel, and is bypassed across the inlet with the flood and ebb tidal currents. Swash bars are formed adjacent to the ebb channel and as these become larger they are more and more subjected to sub-aerial processes. Wave breaking and swash action permits the migration of these bars towards the shore. As the bars migrate, they are stacked up against each other and coalesce to form a singular bar form.

The reason they merge is because as they move closer to the shore, they are subjected to an increasingly shorter period of the tidal cycle over which wave action permits their migration.

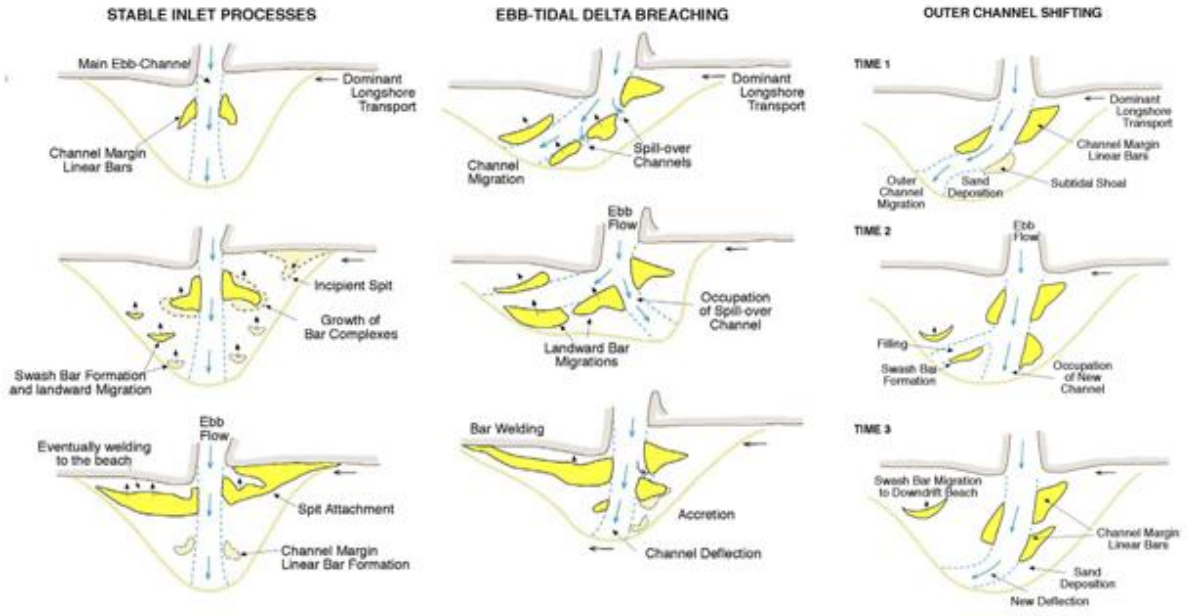

Figure 1.8: Three conceptual models of sand bypassing: L-R, stable inlet processes, ebb-tidal delta breaching, and outer channel shifting (after FitzGerald et al, 2001)

Ebb-tidal delta breaching occurs at inlets that are fixed or stable in time, but whose main ebb channels periodically migrate. The main control at these deltas is the, often great, influx of sediment from longshore transport, which builds up on the updrift side of the inlet and forces the migration of the ebb channel toward the downdrift coast. This mechanism was also described by Hubbard (1977) who envisaged bypassing occurring in three stages: ebb delta growth, channel extension, and abandonment. When the channel is extended on the downdrift side, sediment is transported along its margin. When the extended channel is abandoned, this sediment forms shoals which are then transported to the downdrift coast, completing the bypassing process. Thus the process is cyclical in time and results in large volumes of sediment accreting on the downdrift beach as the newly-extended channel is breached and abandoned.

Sediment bypassing that occurs as a result of outer channel shifting tends to be smaller in volume than ebb-tidal delta breaching, but the mechanism is similar. Sediment built up on the updrift side deflects the ebb channel, but for deep channels the deflection may only occur at the outer part of the channel. Otherwise, as can be seen in Figure 1.8, both mechanisms are largely the same except for the volume of sand bypassing occurring.

The morphological evolution at the Ameland Inlet means that sand bypassing occurs as a combination of these three mechanisms. The inlet is known to be stable in position, while the main ebb flow switches between two channels rather than a significant movement of the channel in space (Israel and Dunsbergen, 1999). When the main ebb flow is more or less perpendicular to the shoreline, the ebb delta is receiving greater amounts of sand and sediment bypassing processes are most active. When the main flow diverts to the west, less sediment is able to accumulate at the terminal lobe. Thus, in their attempt to classify specific models,

FitzGerald et al (2001) have only considered single-channel inlets and the classification system does not cover the complexities of dual-channel inlets such as Ameland.

1.5.2. Shoal Migration Processes

There remains some discussion about the actual process that is responsible for the migration of shoals from the ebb-tidal delta, and this discussion reflects the difficulty in directly measuring and confirming the processes in the field. In the literature, three mechanisms of shoal migration have been identified: surf processes, swash, and a combination of surf and wave bores.

Oertel (1975) and Gaudiano and Kana (2001) attribute bar migration to surf processes, where shoaling and breaking waves are primarily responsible for the movement of sediment. Gaudiano and Kana (2001) in particular make reference to the influence of surf processes as a shoal or bar become increasingly subject to sub-tidal processes during portions of the tidal cycle. Alternatively, FitzGerald (1984) and FitzGerald et al. (2000) believe that swash processes dominate a bar's movement onshore. This process is made more complex as swash operates in very limited water depths, and thus would be greatly affected by the stage of the tidal cycle and local wave climate.

Both Oertel (1972) and FitzGerald (1984) recognised surf processes associated with tidal current asymmetry as the influential mechanism for shoal migration. Wave shoaling and breaking over the terminal lobe generates landward-directed currents which, in combination with flood tidal currents, enhance movement of sediment landward. Ebb tidal currents are inhibited by wave breaking. Greater sand suspension during an asymmetric flood tide enhances the migration of shoal bars (FitzGerald, 1984). Interestingly, Schwartz (2005) states that wave shoaling and breaking is the dominant process for sediment transport at the terminal lobe, while swash action permits the migration of bars in the reduced water depth on the swash platform.

The existing debate concerning the dominating mechanisms of shoal migration is a result of the lack of hydrodynamic data collected for migrating shoals. Many studies concerning ebb-tidal delta bar processes are based on observations rather than on hydrodynamic conditions during the tidal cycle (Robin et al, 2009). This is partly due to the limitation of time, as many studies of sand bypassing concern events that have already taken place over decadal timescales, but also practical limitations. Ebb-tidal deltas are often in water that is too shallow for boats to cross, making echo-sounding data collection hazardous, and too deep for the installation of fixed tripod devices. Robin et al (2009) attempted to address these limitations by studying the movement of intertidal bars in the macrotidal setting of northwest Normandy, France. The exposure of the bars during low tide meant that topographical data could be collected directly. This study is significant as it was conducted in a macrotidal environment, whereas most studies of ebb tidal deltas are conducted in micro- and mesotidal settings. They were able to conclude that surf processes and the associated currents were the dominant mode of bar migration, and that swash action was negligible due to the short duration of time where swash took place over the bar. However, they conclude that it would be necessary to conduct similar experiments on bars in the upper beach profile where water depths are shallower and the bar is exposed to a greater influence of swash action. Additionally, they highlighted the importance of the duration of hydrodynamic processes acting on the bar, which contributes to the slow migration of bars in the macrotidal setting but may have a greater effect in micro- and mesotidal environments.

Although the point was made that conclusions are varied with regard to bar migration in micro- and meso-tidal settings, the author did not address the difficulty in extrapolating this information to apply to other tidal settings. Tidal inlets in macrotidal environments have a tendency to be unstable in time, and thus applying this knowledge to similar environments might not be valid.

One of the most significant aspects of sediment bypassing is that shoal attachment acts as a new sediment supply to the downdrift beach (Oertel, 1977; Kana, 1995; Gaudiano and Kana, 2001) which would otherwise be starved of sediment derived from the updrift beach. The sand volume of the downdrift beach, therefore, is controlled by the location, frequency and size of shoal bypassing events in combination with sand dispersal processes.

1.6. Downdrift Coastal Behaviour

Ebb tidal deltas are known to be the controlling factor in downdrift coastal behaviour (FitzGerald, 1988). In addition to sediment bypassing processes, wave refraction effects, ebb delta volume changes and sediment dispersal all dominate the volume and morphology of downdrift shorelines.

1.6.1. Impact of Size, Shape and Volume of the Ebb-tidal Delta

The presence of the ebb-tidal delta itself has an important impact on the downdrift shoreline, by influencing wave refraction patterns and wave sheltering. The volume of the ebb-tidal delta is therefore an important control over the development of the downdrift shoreline, and cyclical fluctuations in the delta volume have shown to be related to fluctuations in the beach volume.

FitzGerald (1984) shows that the volume of the ebb tidal delta has a direct relationship with the stability of the adjacent shoreline. He demonstrated that the ebb tidal delta of the Price Inlet underwent cycles of growth and decay which were associated with the growth and release of bypassing shoals to the adjacent shorelines. The ebb tidal delta experienced a gain and loss of around 15-20% of its total volume, indicating a significant amount of sediment is being transported during each cycle. Moreover, 300m of shoreline erosion occurs when the delta is accumulating sediment following shoal welding, which FitzGerald (1984) suggests is due to the lack of sediment input combined with greater wave attack over the reduced ebb delta. In contrast to the results of FitzGerald (1984), Gaudiano and Kana (2001) indicate that the mean shoal percentage of the ebb tidal delta at Price Inlet is approximately 3.59 ± 2.25% which is a much lower percentage than the 15-20% estimated by FitzGerald. However, the authors address the issue of shoal calculation error as both authors used aerial photography to estimate shoal volume, and had to estimate depth of the shoal. The large error value associated with Gaudiano and Kana's figures emphasises the uncertainty involved in calculating shoal volume remotely. It is thus difficult to have confidence in the shoal volumes calculated by these authors, and further investigation would be required to improve the accuracy.

The dynamic volume of the delta contributes another control on shoreline development. In their study of the relationships between ebb tidal delta volume and shoal volumes, bypassing interval, and tidal prism, Gaudiano and Kana (2001) found that shoals in larger inlets are of

greater volume than those in smaller inlets, but they migrate at a much reduced rate. Therefore the volume of the ebb tidal delta, which is related to the tidal prism and the size of the inlet, is an important control on shoal migration. In larger ebb deltas there is a wave-sheltering effect as waves shoal over the surface of the delta, providing less energy for sediment transport and slowing shoal migration. Further, large ebb deltas can extend several kilometres out to sea and shoals migrating have a greater distance to travel, which also increases the interval time between bypassing events. Lastly, large ebb deltas tend to have shoals with a greater volume, which means more mass to be moved by wave action. They were able to quantify this relationship to allow predictions to be made about these variables:

$I = 0.046Tp + 4.56$

Where, I = average shoal bypassing event interval yrs; Tp = tidal prism in 10^6

$S = 6.42Tp + 113.4$

Where, S = average bypassing shoal volume (10^3 m^3); Tp = tidal prism

In order to derive these equations, a selection of nine tidal inlets from South Carolina, USA, were analysed from a series of vertical aerial photographs and bathymetry data. The inlets studied ranged in size (tidal prism, cross-sectional area of inlet), but all were classified as mixed-energy environments with significant sand bypassing events. It is particularly useful to see how the bypassing interval and volume increase with larger tidal inlets, and the selection of inlets chosen allows for comparisons to be made with a variety of sizes (see Table 1). Although they found the relationships to be statistically significant, they also warned that there is a considerable error involved, as discussed previously. Improvement of these relationships would come with physical measurements and long-term recording of the evolution of the shoals rather than relying on infrequent aerial photography and the subsequent estimation of volumes. The authors do, however, illustrate the importance of temporal and spatial scales with regard to bypassing intervals and volumes.

FitzGerald and Pendleton (2002) also illustrated the close relationship between the tidal prism and the equilibrium volume of the ebb tidal delta in their study of sediment bypassing processes during the formation of New Inlet, Cape Cod. A storm overwash breach on Nauset Spit formed a tidal channel that dramatically widened as it accessed an increasingly larger proportion of the tidal prism. Sand that previously would comprise littoral drift is captured by the inlet and transported into Pleasant Bay to form shoals and pumped into the ebb tidal delta, causing a deficit downdrift. Over ten years the shoreline immediately south of the inlet eroded by 100-300 metres due to lack of sediment. When the inlet achieved an equilibrium volume, sand bypassing processes restarted and began to nourish the downdrift shoreline. This study is unique in that the authors were able to follow the evolution of the ebb tidal delta before and after the storm breach, with the intention of also studying the downdrift effects. The idea of the 'equilibrium volume' of the ebb tidal delta also pertains to downdrift beach stability, which is achieved through regular sand bypassing once the ebb tidal delta has achieved an optimum volume.

Table 1: Summary of the variables associated with bypassing events at the South Carolina inlets. Standard deviation is indicated by ±; total number of shoals per inlet studied is denoted by (n) (after Gaudiano and Kana, 2001).

Inlet	Cross-sectional area (m^2)	Tidal prism (10^6 m^3)	Ebb-Delta Volume (10^6 m^3)	Mean Bypassing Shoal Volume (10^3 m^3)(n)	Mean Shoal Percentage of Ebb Delta	Mean Event Interval (yrs)	Mean Annual Contributions (10^3 m^3/yr)
Pawleys	42	0.66 ± 0.13	0.9	61 ± 45 (23)	6.61 ± 4.87	4.1 ± 2.6	15
Midway	168	1.96 ± 0.39	2.0	50 ± 27 (22)	2.51 ± 1.34	4.3 ± 2.7	12
Captain Sams	231	2.29 ± 0.46	3.8	155 ± 90 (20)	4.08 ± 2.36	4.5 ± 3.1	35
Capers	906	5.81 ± 1.16	6.9	208 ± 173 (22)	3.02 ± 2.51	5.6 ± 3.4	37
Breach	948	12.8 ± 2.57	6.8	199 ± 156 (19)	2.93 ± 2.30	5.0 ± 3.8	40
Price	894	13.8 ± 2.75	6.1	219 ± 137 (43)	3.59 ± 2.25	4.3 ± 1.6	51
North	1475	14.9 ± 2.99	10.6	225 ± 188 (21)	2.12 ± 1.77	5.8 ± 3.7	39
Dewees	3506	24.6 ± 4.92	15.7	315 ± 285 (27)	2.01 ± 1.82	6.6 ± 2.1	48
Stono	5600	70 ± 14	95.6	561 ± 356 (24)	0.59 ± 0.37	7.6 ± 2.8	74

The shape of the ebb delta, particularly the degree of overlap of the delta with the adjacent islands, influences the location of bar attachment on the downdrift shoreline and the resulting shape of the island. Figure 1.9 shows how the shape of barrier islands is dominated by inlet morphology, combined with sand bypassing, in mixed-energy settings. The size of the inlet relative to the length of the barrier island, and the position of the main ebb channel within the inlet determines the extent of the overlap of the ebb delta.

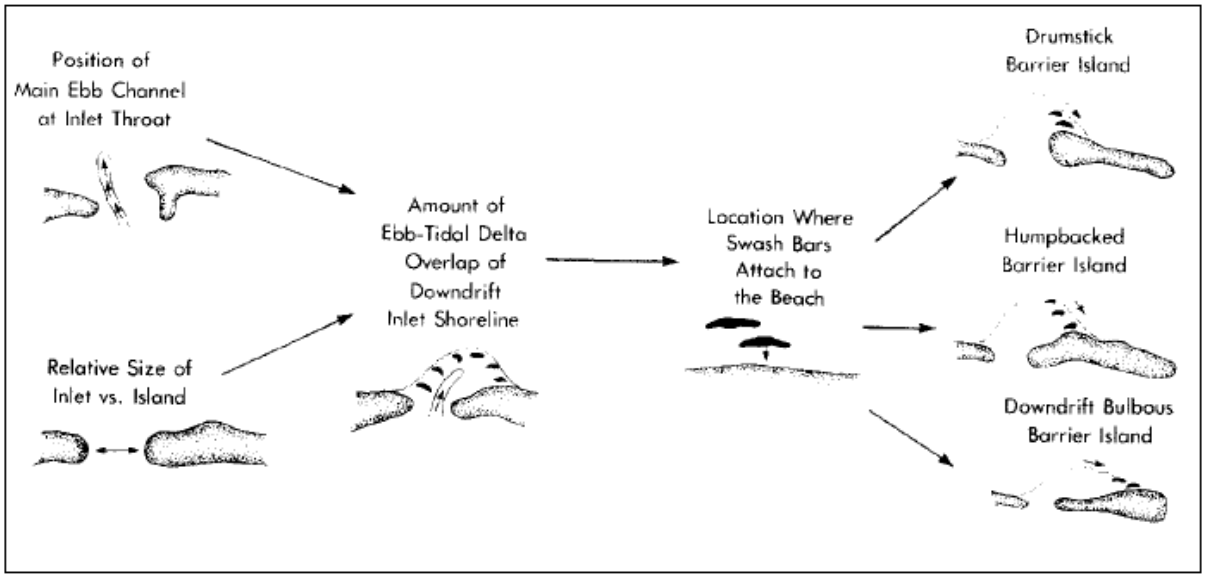

Figure 1.9: The factors of main ebb channel position and relative size of the inlet vs. the island affect the degree of overlap of the ebb tidal delta, and subsequently the resultant shape of the island (FitzGerald et al, 1984)

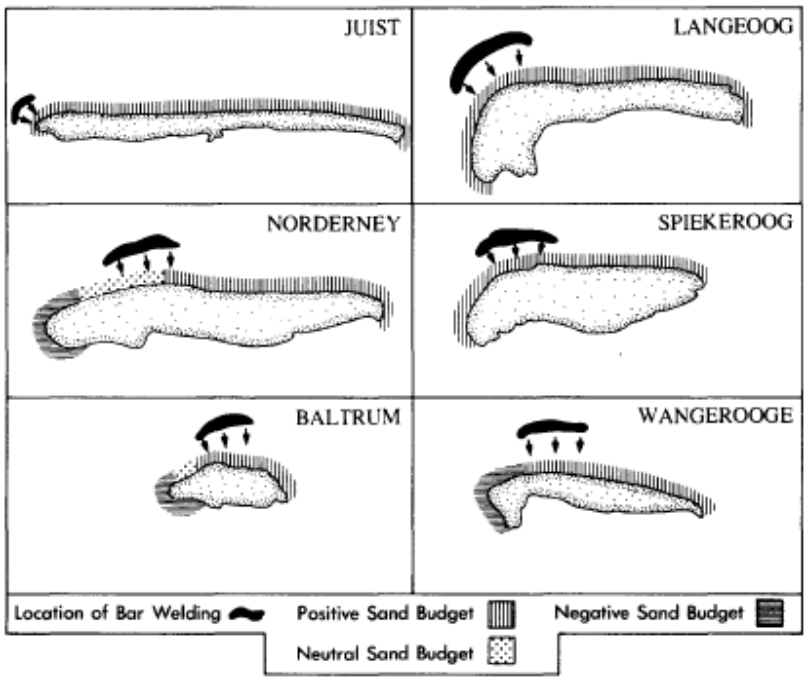

Figure 1.10: The location of cyclical bar attachment to the downdrift coasts of the German East Wadden Islands, resulting in a specific island shape (FitzGerald et al 1984)

A large degree of overlap produces a 'bulbous' or humpback-shaped island, such as Norderney or Spiekeroog in Figure 1.10. The 'drumstick' shape is prominent in the Dutch Wadden Sea as bypassed bars migrate toward the western ends of these islands, reflecting the updrift-oriented position of the ebb delta and the downdrift-offset island. While one end of the island is accreting, the central part of the exposed northern coastline experiences erosion and the shoreline forms a curved arc that extends for several kilometres. The eastern ends of the islands, like in the west, fluctuate depending on the phase of the ebb tidal delta, with a recurved spit forming during periods when the main ebb channel is not eroding the adjacent islands.

The changing morphology of the downdrift beach is controlled not only by its sediment supply, but also by wave action acting on the shoreline. Waves passing the ebb tidal delta are influenced by the fluctuating seabed topography, and these effects can be noticed on the downdrift beaches.

1.6.2. Wave Transformation Processes and Sediment Transport Directions

Wave transformation occurs as waves encounter shallower water in the area of the delta, causing the wave crest to slow down and bend oblique to the shoreline, parallel to the depth contours. When refracted wave crests encounter migrating bars on the downdrift side of the ebb delta, an additional effect has been observed. Littoral drift reversal has been recognised as an important process for sediment transport in the lee of ebb tidal deltas (Hayes et al, 1970; Goldsmith et al, 1975; Hayes and Kana, 1976; FitzGerald et al, 1984; Sha, 1989; Kana et al, 1999).

Initially, several authors (Hayes et al, 1970; Hayes and Kana, 1976) proposed that littoral drift reversal was the most important mechanism that contributes to the 'drumstick' shape of barrier islands such as those of the Dutch Wadden Sea. They claim that littoral reversal around the ebb delta reduces the rate by which sand bypasses the inlet and contributes to the 'bulbous' head of the island. Although agreeing that this factor is important, FitzGerald et al (1984) made the point that accretion downdrift of ebb-tidal deltas is primarily by sand bypassing, even if littoral drift reversal is not occurring, and it is the degree of overlap of the ebb tidal delta with the downdrift barrier island that determines the welding location of migrating bars, and thus the shape of the island. This conclusion is also reached by Hicks et al (1999) for the drumstick-shaped Matakana Island barrier in New Zealand.

That said, littoral drift reversal prevents sand from being dispersed downdrift and instead cycles it back to the ebb tidal delta. Prior to bar welding on the shoreline, FitzGerald (1984) indicates that littoral drift reversal is more significant with intertidal bars than with subtidal bars, as intertidal bars are larger and more likely to generate this reversal current (Figure 1.11).

Wave refraction around the attaching shoal can also draw in sand from the shoreline to which it is attaching. Kana et al (1985) demonstrate how an alongshore pattern of erosion and accretion at the Dewees Inlet (South Carolina) could be attributed to wave refraction drawing in sand from the shoreline on either side of an attaching shoal. After welding to the beach, the opposite effect occurs as wave divergence causes erosion of the bulge and eventually nourishment of the beaches.

The detachment and migration of shoals occurs in three stages (Figure 1.12). In stage one the shoal is detached from the ebb delta as wave breaking exceeds ebb-directed currents, and wave

refraction around the shoal causes it to take on a crescentic shape. Stage two occurs when the shoal attaches to the shoreline, with one or both apexes. Between the shoal and the shoreline a runnel remains trapped and waves push the shoal up further against the shoreline. In stage three the shoal spreads laterally as waves break and disperse the sand in either direction (flow divergence: into the inlet and toward the downdrift beach). They claim that the migration is complete when the attached shoal is dispersed and there are no more shoreline changes.

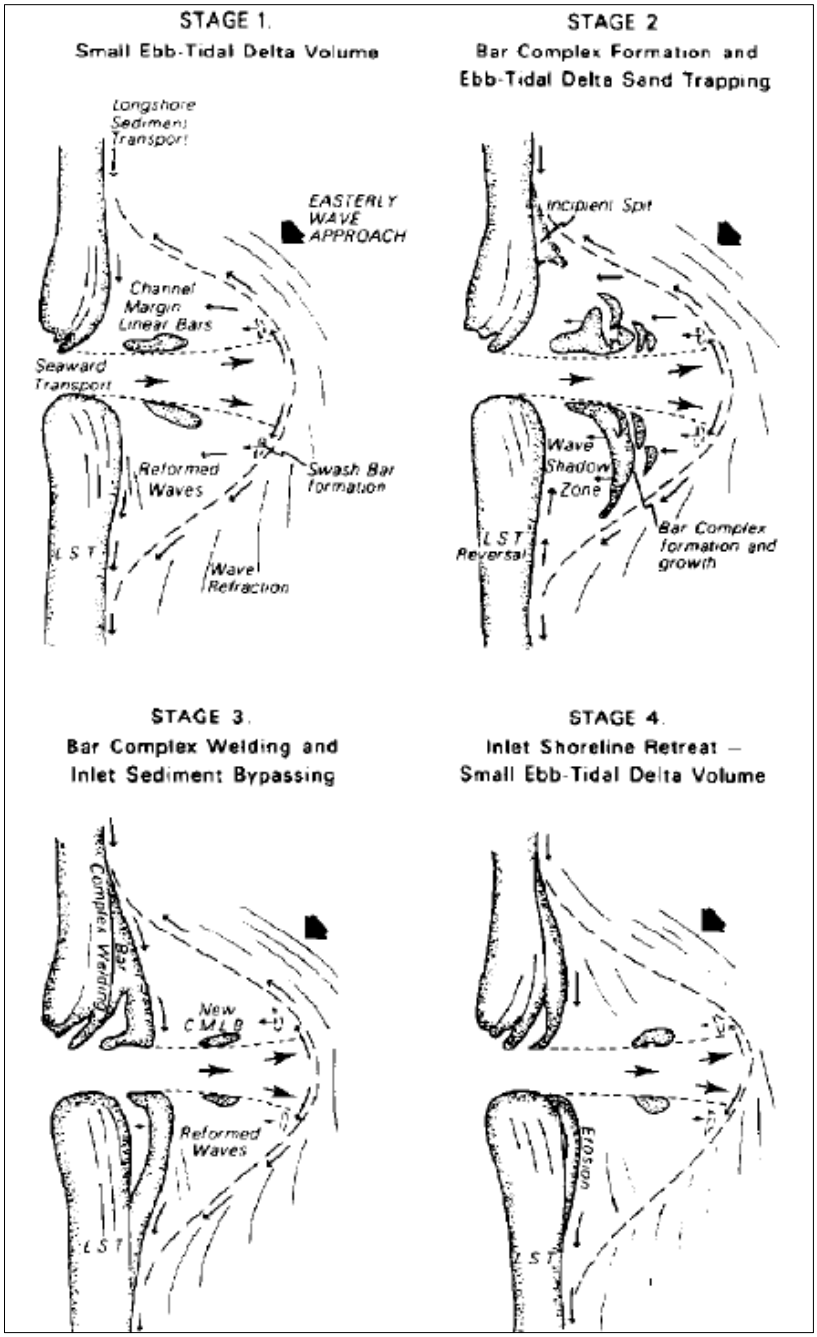

Figure 1.11: Wave transformation around the ebb-tidal delta – note littoral drift reversal in Stage 2, and drumstick-shape of downdrift island (FitzGerald, 1984)

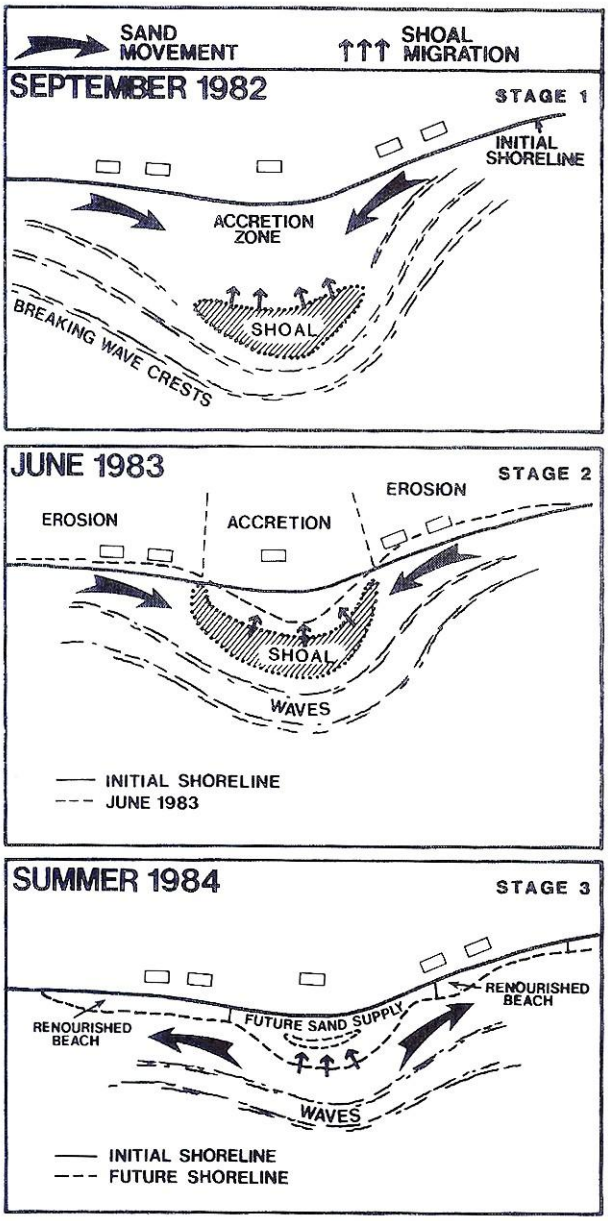

Stage 1: Shoal migrates toward the shore; waves refract and bend around the shoal, causing sand to be transported alongshore towards the attaching shoal (longshore sediment reversal).

Stage 2: Before the shoal attaches, shoreline erosion occurs on either side as sand accretes in the vicinity of the attachment site; and the shoal is formed into a crescentic shape.

Stage 3: The shoal is attached to the shoreline; wave action transports sand away from the 'bulge' and re-nourishes the adjacent eroded beaches; and the attached shoal is completely eroded before the next shoal attachment.

Figure 1.12: The process of shoal migration and attachment to the coast (after Kana et al, 1985).

1.6.3. Sediment Dispersal Mechanisms

Following welding to the shoreline, the sand contained in the shoal will be dispersed until the shoreline reaches equilibrium with the wave climate and tidal conditions, as mentioned previously in subsection 1.6.2 (*Wave Transformation Processes and Sediment Transport Directions*). It is assumed that sand is dispersed from the initial 'bulge' by the following mechanisms: cross-shore and longshore distribution, as a singular unit or "sand wave", or by diffusion. These mechanisms will be discussed in relation to the effect observed on the downdrift beach.

- Cross-shore and longshore distribution

Cross-shore sediment transport occurs as both onshore-directed movement and offshore-directed movement, varying throughout the year in response to seasonal wave and wind climate. The transport of sand in these directions can be difficult to measure in the field, but the response on the beach over a period of time can indicate which direction of movement is dominant over the other. Wave-driven cross-shore sediment transport is facilitated by swash motion, comprising of asymmetric uprush and backwash phases with decelerating and accelerating velocities, respectively. The uprush phase permits the transport of sediment with larger velocities in the landward direction, while the backwash transports sediment seawards with slower velocities over a longer duration (Masselink and Hughes, 2003). During storm events, more energetic waves can promote the transport of sediment seawards and cause a flattening of the beach profile. Cross-shore movement of sand is particularly important to assess the beach and dune response to storms, the equilibration of beach nourishment, the seasonal change of the shoreline, and the beach response to sea level rise (Dean et al, 2006).

Longshore sediment transport occurs where incoming waves break at an oblique angle to the shoreline, setting up an alongshore current. It is assumed that downdrift of an attached bar, longshore drift will nourish the otherwise sediment-starved beaches. However, there doesn't seem to be much evidence of this occurring at large inlets and, in particular, the chronic erosion problem at Ameland has prompted the need for artificial nearshore nourishments.

In the case of the beach at Ameland, the effect of wave-driven dispersal of sand is clear when examining the evolution of the shoreline through time (Figure 1.13). Shortly after its attachment to the northwest beach, the shoreline in 1986 shows a distinct outline of the sand bar which, by 1995, has decreased in cross-shore width and smoothed towards the east of the beach. While the beach 'hook' spit-like feature dominates the appearance of the shoreline, it can also be seen how the shoreline extends further around the western coast simultaneously. This indicates that there is a bifurcation in sediment transport across the beach, driving sand in toward the inlet at the same time as it is driven eastwards. This bifurcation in sand transport occurs due to the oblique angle of breaking waves which, at the most curved point of the beach, causes a divergence in longshore current towards the east and also in towards the inlet in the west. The opposing directions of sediment transport have also been modelled by Rijkswaterstaat (2005) in Figure 1.14.

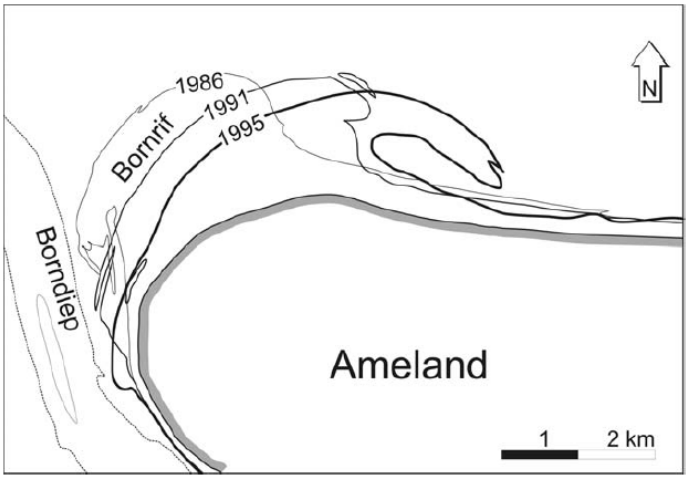

Figure 1.13: Former shorelines of the northwest beach of Ameland (Cleveringa et al, 2005)

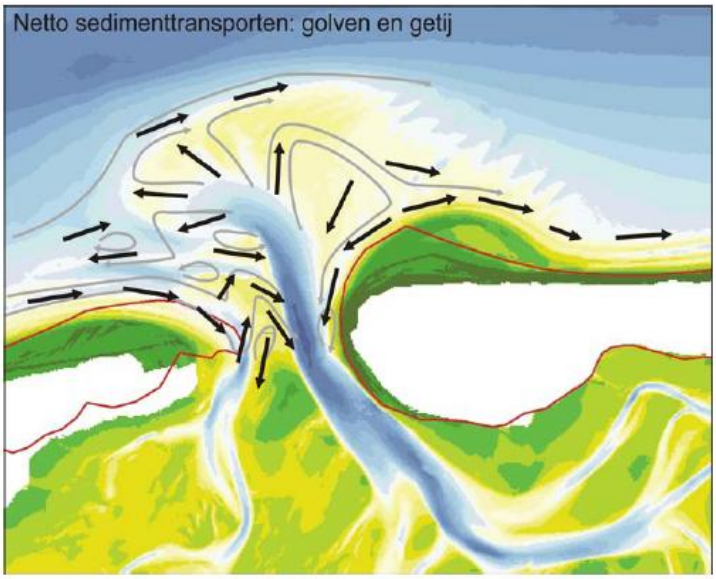

Figure 1.14: Net sediment transport by waves and tides combined, indicating bifurcation of sediment transport on the northwest beach (Cleveringa et al, 2005)

On the backshore, aeolian transport of sand can occur in both cross-shore and alongshore directions depending on the weather conditions. The prevailing north-westerly winds on Ameland permit the growth of new dunes high on the backshore, in front of the existing dune foot. These new dunes exist predominantly on the south-east side of the beach, where the long fetch from the north-west allows sand to accumulate.

The progradation of the dune foot implies that there is more than sufficient sand being transported and added to the dunes to encourage growth of new dunes. Increased availability of sand on the beach is often the reason for new growth, and periods when bypassed sediment bars attach to the beach could indicate dune growth if there is sufficient aeolian activity.

- Unit or Diffusion Sediment Transport

A distinction can also be made in the manner by which sediment is transported: migration as a singular unit, or as diffusive behaviour. A sand wave (Figure 1.15) is defined as a local irregularity in beach form that moves along the shore as a singular mass, in the direction of net littoral drift, and which can be tracked downdrift as the propagation of an accretion/erosion wave (Schwartz, 2003). The downdrift migration of sand waves produces a temporal variation in beach width at any point along the shoreline (Davidson-Arnott et al, 2003). In contrast, diffusion transport of sediment breaks down the original form of the bar and sand is progressively removed from the accretional bulge in existing transport pathways.

Initial investigations into the situation on Ameland have suggested that sand wave migration may be the main mode of sediment dispersal acting on the northwest beach. Louters and Gerritsen (1994) and Cheung et al (2007) have both indicated the presence of an eastward-migrating attenuating sand wave.

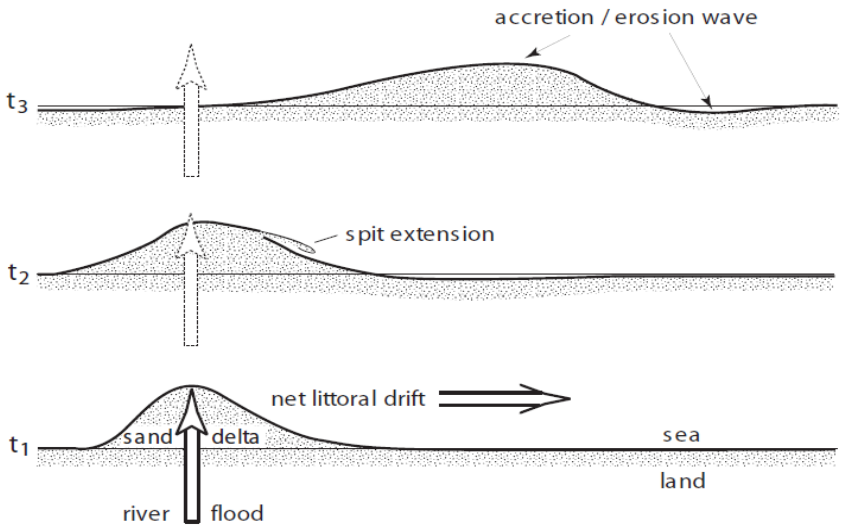

Figure 1.15: The propagation of a sand wave (Schwartz, 2003)

The significant effect on the downdrift shoreline occurs while the ebb delta and associated swash bars are accumulating sand in the growth phase of the cyclical behaviour. The downdrift shoreline is starved of sediment from updrift, which leads to erosion as the sediment budget experiences net loss (Hicks et al, 1999). Once the swash bar amalgamates and attaches to the coast, it is transported by longshore transport processes and migrates downdrift. There is very little available information regarding the timescales or the volume of sediment involved in this process.

1.7. Morphological Response of the Shoreline

1.7.1. Shoreline Response

Some literature has focused directly on the consequences of ebb-tidal delta dynamics on morphological response of adjacent shorelines. Reacting to reports that shoreline erosion decreases with distance from a tidal inlet, Fenster and Dolan (1996) attempted to combine shoreline change data with an analytical even/odd method developed by Dean and Work (1990, 1993) to determine the spatial extent and magnitude of an inlet influence. They found that, based on their three criteria for delineating magnitude of change, there was a large degree of variability in the spatial range and suggested a barrier zone in which inlet processes *dominate* shoreline change, and one where inlet processes *influence* shoreline change.

Hicks et al (1999) investigated patterns of beach change at Katikati Inlet on New Zealand's North Island. Their aim was to identify the spatial extent, causes and timescales of change as seen in beach volume measurements and dispersal diagrams. The authors found that changes to beach volume and shoreline position were three to four times larger at near-field beaches than at far-field ones, which seems to be a logical finding.

They found that the inlet/delta system acts as a "non-return valve" for beach sand and that erosion can occur for several years before a sand bar eventually migrates onshore from the ebb delta and a 'sand slug' is released alongshore. Strong tidal currents are claimed to be capable of

aiding transport of sand alongshore. This means that a multi-year pattern is induced on the far-field beach, which is phase-locked to the bypassing cycle although lagged in time with distance from the inlet.

Cyclical fluctuations in shoreline have also been recorded on Schiermonnikoog (Figure 1.16) where sediment bypassing has led to the welding of sand bars to the beach. Rhythmic fluctuations in beach width are recorded in the mean low tide and mean high tide positions, reflecting the passage of sand waves (Stive et al, 2002). The high-water line responds slower than the low-water line to the changes, and the amplitude of difference is less. This time lag occurs as sediment transport processes act on the lower foreshore during most of a tidal cycle but at the high-water line for a much reduced period of time. The dune foot experiences gradual progradation which is due to the increased sand supply and beach width, allowing for sand to be picked up and transported by aeolian processes. However, there is no strong correlation between specific sand wave occurrences and progradation of the dune foot. Generally, the advancing dune foot shows that Schiermonnikoog has net coastal accretion and the accreting trend results from a positive sediment budget.

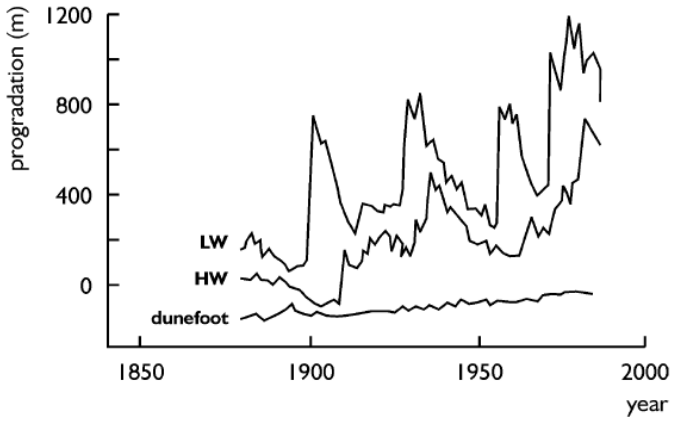

Figure 1.16: Natural oscillations in the shoreline of Schiermonnikoog, resulting from the passage of sand waves derived from the welding of ebb tidal delta shoals to the downdrift shoreline (Stive et al, 2002).

1.7.2. Shape of Beach Profile

Beach volume changes primarily occur in the dynamic foreshore zone, which is routinely affected by wave action and the tides. During storms and periods of increased set-up, the backshore can also lose sediment volume. On a seasonal scale, summer months are generally regarded as periods of net gain while winter months are periods of net loss. Superimposed on these short-scale volume changes is a combination of medium-term re-equilibration, such as the shoreline evolution at Ameland, and to a lesser extent, long-term sea level rise.

Thus, the beach profile (Figure 1.17) is expected to alter with increasing spatial extent relative to the timescale, i.e. daily volume changes occurring in the intertidal zone are small compared with the medium-scale re-equilibration associated with cyclical behaviour over several years.

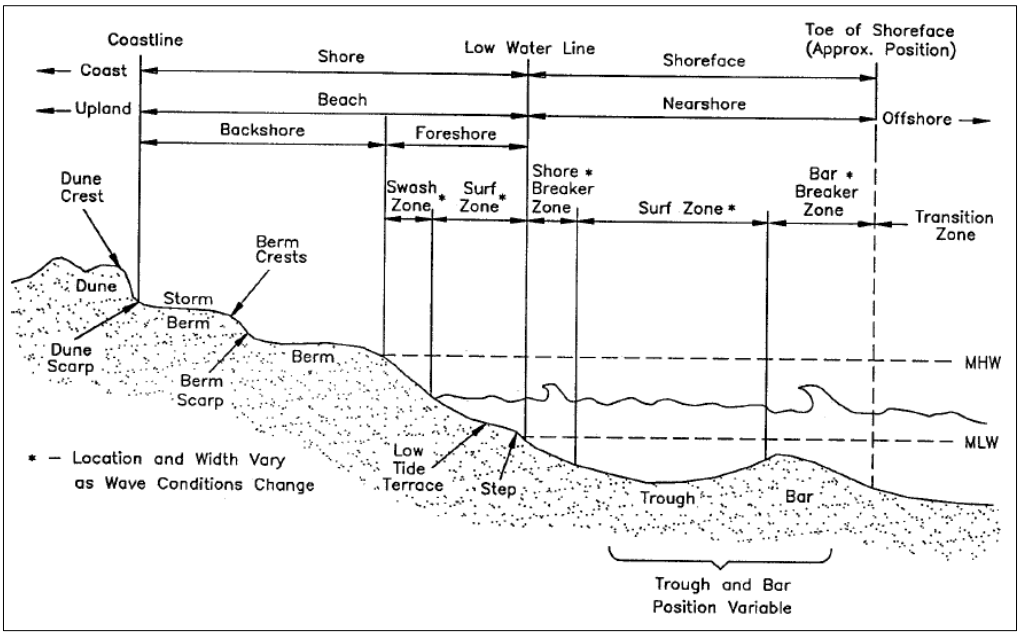

Figure 1.17: Classification of a barred beach profile (Morang, 2002)

1.7.3. Sediment Volumes and Budgets

The vast majority of tidal inlets studied tend to be comparatively small in size, with short bypassing cycles of only a few years (see Table 1; page 15). There is a tendency for authors to broadly assume that longshore drift will disperse sand downdrift towards an eroded beach, providing a form of natural nourishment and re-balancing the shoreline equilibrium. While this may occur downdrift of small inlets, which also bypass relatively small volumes of sand, the process takes longer at larger inlets and downdrift beaches erode for longer periods of time. The character of the dispersal processes may also be different to those at smaller inlets and dispersal pathways may include a bifurcation in transport (whereby sediment is transported in opposing directions) which cycles sediment back into the inlet instead of downdrift. Knowledge about bypassed bars and the subsequent effects is scarce, and while we attempt to 'fix' the downdrift erosion problem through repeated nourishment projects, it would be more beneficial to understand the spatial and temporal scales of sediment movement at these larger inlets.

1.8. Synthesis

This literature review has attempted to illustrate that while our knowledge of tidal inlet processes has grown and developed, there are still areas of research that have yet to be studied. Most literature focuses on the tidal inlet itself, rather than the downdrift coastline. Numerous case studies from North America focus on migrating inlets and storm impacts, reflecting the dynamic nature of their native tidal inlet systems, but which leave stable inlet processes somewhat neglected in the literature. Additionally, many authors believe that the downdrift welding of shoals act as a natural form of beach nourishment on the downdrift shoreline, and indeed this may be the case for small inlets. For larger inlets, however, the situation is complicated by the larger scale of operation and the time taken for accretion to occur is much greater.

The sediment volumes involved in sediment bypassing, particularly in attachment shoals, and the subsequent dispersal of that sediment on the downdrift beach, appear to be relatively unknown. This is certainly true when considering large, slow-responding tidal inlets such as the Ameland Inlet. A bias appears in the literature as smaller, faster-response inlets are more intensively studied due to the greater availability of data and quick turnover of cyclic morphology and sediment bypassing. However, this means that the morphodynamics of larger inlets are less well understood, particularly in terms of sediment volume contained in shoal bypassing events.

Knowledge of volumes involved in bypassing is crucial, as they are often comparable to volumes of nourishment projects (Kana et al, 1999). It is particularly important to understand cyclical variations in beach sediment budget; because while it might appear that a beach is eroding over a long period it may simply be part of a larger cycle that will involve accumulation through shoal bypassing. Therefore, shoal bypassing volumes, and the time it takes for the dispersal of welded shoals, are vital pieces of information for coastal management practice.

The disagreement in estimated volume of migrating shoals at the Price Inlet (FitzGerald, 1984; Gaudiano and Kana, 1999) highlights the uncertainty of how much sediment is bypassed at large inlets, and in particular emphasises the need for better, more accurate volume calculations. However, one of the greatest limitations for projects that attempt retrodiction of shoal volumes is the temporal resolution of data available for the area in question. Collection of data is a limiting factor for projects such as this, particularly when some inlets have a long response time. Qualitative measurements may be made based on aerial photography, but knowledge of volumes is restricted. The timing of aerial photographs also plays a role, as images taken at high tide may cover shoals that would otherwise be visible at lower tide, and photographs are not always taken at the optimal timing for research.

Understanding sediment dispersal following shoal attachment is important for predicting the evolution of the barrier island shoreline in the long-term. Unfortunately there are very few papers that deal with dispersal mechanisms, and it is often assumed that once a shoal is attached to the shoreline then wave-driven longshore transport will disperse the sand into the inlet and alongshore (FitzGerald, 1984; Kana et al, 1999; Gaudiano and Kana, 2001), providing a source of nourishment to the sediment-starved beaches downdrift.

Finally, it is important to emphasise that the topic of this thesis only comprises a small portion of a much larger, dynamic system that we still do not totally understand. Observations of processes are made but, as has been discussed, it is very difficult to provide empirical data to verify processes in place.

1.9. Research Objectives

The central aim of this research is to contribute towards scientific understanding of the role that cyclical dynamics at tidal inlets have on the downdrift coast of barrier islands. Specifically, this thesis will study the barrier island of Ameland in the Wadden Sea, the Netherlands, in order to address this topic.

Two main aspects of uncertainty have been drawn from the previous discussion: knowledge about sediment volumes involved in sediment bypassing, and the subsequent dispersal from the downdrift shoreline. These aspects will form the focus of research within this project.

The main objective is to investigate the effect of cyclical shoal attachment on the downdrift shoreline sediment budget, at various spatial and temporal scales:

- To observe and record the short-term morphological change on the downdrift shoreline, using beach surveying methods.
- To calculate the long- and short-term change in sediment volume and identify patterns of accretion and erosion.
- To analyse long-term morphological data to determine the long-term trend and influence of sediment bypassing on the shoreline.

The approach considers different time scales, namely short- and long-term. Short-term refers to data that was collected during fieldwork, whereby measurements were taken daily for a period of several weeks during the storm season. The long-term time scale refers to data from the Jarkus dataset, which contains a single representative profile for each year since 1965. Short-term changes are therefore occurring on a day-to-day, week-by-week basis, and the long-term changes over a period of years.

Considering the theories surrounding downdrift morphological effects of tidal inlet dynamics, and the problem of ongoing erosion on the island of Ameland, the following hypothesis has been developed for this research project:

"Insufficient eastward sediment dispersal from the bypassed shoal causes a downdrift sand deficit and erosion trend on the exposed northern Ameland coastline."

The research questions that will be used to address this hypothesis are the following:

1. How much sand was added to the beach when the shoal attached to the shoreline?
    a. How does the downdrift beach volume change over time?
    b. How do properties of coastal profiles change in time and space?
    c. Where in the profile does most change occur?
    d. Is there a cyclical component to volume fluctuations over time?
    e. During a previous shoal attachment, did the shoreline respond in the same way as currently?

2. How is sediment dispersed along the coastline following attachment of the shoal?
    a. In which direction is sand dispersed at the coastline?
    b. What is the pattern of dispersal: as a unit, or diffusion?
    c. Can a diverging sediment transport be identified from morphological changes?
    d. What is the rate of sediment transport?

e. Does the rate of sediment dispersal remain constant over time?

3. What is the impact of fluctuating beach width on dune development?
    a. Does a phase of shoreline accretion and beach widening correlate with dune building processes and vice versa?
    b. Are aeolian processes dispersing sand cross-shore and contributing to dune formation?
    c. How much dune advance has there been since attachment of the shoal?
    d. What is the change in volume of the dunes since attachment of the shoal?

Due to the long timescales involved in the cyclical behaviour of both the ebb tidal delta and the downdrift shoreline, it is necessary not only to investigate the short-term sediment budget fluctuations, but also to collate historical long-term morphological data in order to fully address the temporal extent of shoreline change. Long-term (annually-measured) morphological data is augmented by short-term data derived from fieldwork, with the intention of analysing morphological changes over the short period of six weeks, and the longer period of 45 years.

2. Methodology

In order to address the research questions with consideration to the cyclic changes occurring at the inlet, it is necessary to study the evolution of the downdrift beach over varying timescales. In the short term, it is possible to conduct surveys of the beach to examine the response to the waves, tides, and perhaps storm activity. In the long term, it is necessary to consult historic survey data to examine the trend over the past four decades.

2.1. Study Location

Ameland is one of the barrier islands that comprises the western Wadden Sea, and is situated between Terschelling and Schiermonnikoog. The area of interest for this research is the north-western coastline (Figure 2.1), which is immediately downdrift of the Ameland Inlet. This beach is characterised by a very wide cross-shore width, relative to the rest of the island, and the existence of a tidal channel. Figure 2.1 also indicates transect numbers 304 to 1000, which are referred to as transects 3 to 10 in this project.

Figure 2.1: Location map of the research area on Ameland (Google Earth image, 2005).

2.2. Short-term Morphological Data

For this project, cross-shore profiles of the foreshore on the North Sea coast of Ameland were measured daily for a period of five weeks, between September and November 2010. The aim of beach surveying is to record the profile of the beach by identifying the X, Y, and Z component of each measuring point. In this way, it should be possible to gain a fairly representative view of

the topography of the beach surface, which, when repeated over a widespread area of the beach, will be used to calculate changes to the volume of sediment on the beach.

The area of interest is a stretch of the Ameland coastline on the North Sea side, immediately adjacent to the Ameland inlet (Figure 2.2). This delimitation was made on the basis of the proximity to the inlet, but confined within a 2 km range due to equipment limitations and also to avoid known areas of quicksand. In total, nine transects spaced approximately 200 metres apart were measured (Figure 2.3). The spacing of the transects deliberately and directly coincides with the existing official beach marker sequence, making it possible to easily compare the short-term morphological data with the longer-term Jarkus dataset.

It is assumed that the 'active' part of the beach, between high and low water position, experiences daily morphological change in response to waves and the tides, and thus the intertidal area was surveyed on a daily basis. Profiles were taken of the whole section of beach (from the dune foot to low water position) at the beginning, middle, and end of the fieldwork period. In addition, a location distant from the main beach was surveyed to compare the short-term response at this location with the profiles from the main study area. Surveying took place between transects 9 and 10, approximately 4 km distance from the more intensively-measured site, and measurements were taken once per week of this entire downdrift section of beach.

This project coincides with two other Master projects which were undertaken at the same location on Ameland. As part of these two projects, instruments were placed in a cross-shore array at beach transect 5.0, positioned in the intertidal zone and oriented to north. The cross-shore distance was around 200 m, and the maximum water depth was around 2.5 m at high tide at the most seaward sensor. The equipment typically operated continuously when submerged. The dataset that was obtained consists of six weeks of measurements of pressure, cross-shore and alongshore velocities and sediment concentrations.

Figure 2.2: Ameland's North Coast annotated with transect numbers and red boxes with indicate the locations of fieldwork measurements (Google Earth image, 2005).

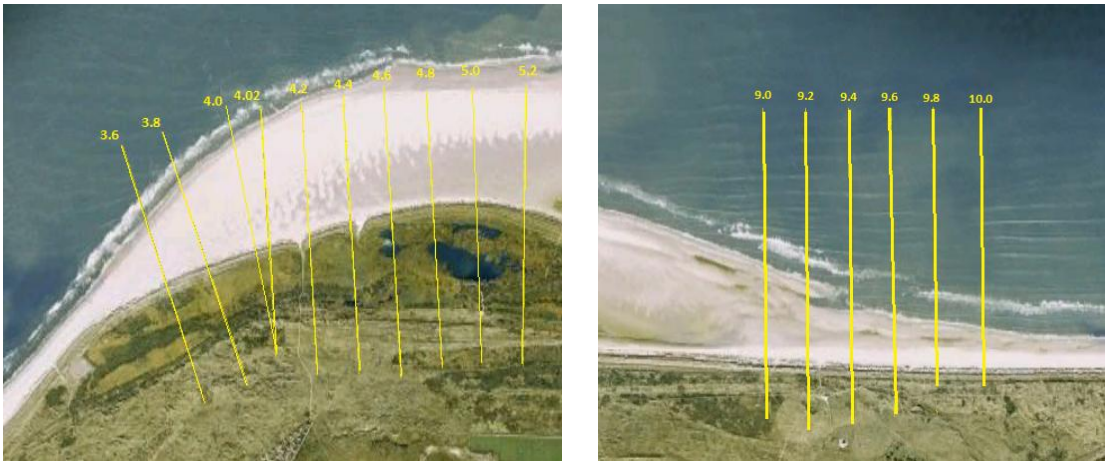

Figure 2.3: Location of transects 3.80 to 5.20, and 9.0 to 10.0, the distance between transects is approximately 200 metres (Google Earth image, 2005).

2.2.1. Time Management for Data Collection

The time period for the undertaking of data collection was divided between three spatial areas. The beach adjacent to the inlet is deemed the main study area and the focus of this research project. Thus, most priority was given to surveying this area. This stretch of coastline was further sub-divided into the foreshore and backshore areas. It is assumed that the actively changing part of the beach is the foreshore, as it is directly subject to wave energy and the tides. Subsequently, this part of the beach was surveyed on a near-daily basis for the duration of the campaign. Emphasis on this part of the beach was also made due to the extreme cross-shore width of the beach (up to 750-800m), which means the backshore is only flooded during spring tide and surges. Furthermore, the logistical requirements of two other students also conducting research on the beach needed to be met, and additional time was required in the field to account for errors with the equipment used.

The backshore is assumed to undergo much reduced rates of change due to the absence of the aforementioned controlling factors of waves and tides, and so measurements were only conducted on three occasions during the campaign: at the start of the campaign on 24th September 2010, at halfway through on 15th October 2010 (upon observation of increased aeolian activity), and at the end of the campaign on 1st November 2010. Lastly, and by way of gaining some comparison, measurements were also taken of a nearby section of the beach at a distance of about 4 km away, approximately 7 km distance from the inlet channel. The purpose of this secondary location is to observe profile changes in an area that is somewhat distant from the inlet and on the opposite side of the shoal beach. Measurements in this location were only made about once per week of the campaign, and due to the narrower width of the beach it was possible to combine foreshore and backshore measurements in one session.

Data collection was undertaken during a window of time coinciding with low tide, typically an hour before and after, with preference for surveying of the lowest points during low tide itself. Due to the time of the year and with ever-decreasing daylight hours, some days during the campaign were allocated as no-survey days. Often this was because low tide was too early in the morning and too late at night, whereby daylight hours had not begun or had ended, respectively. This decision was made prior to the start of the campaign and ensured our safety.

2.2.2. Measurement Equipment and Technique

The short-term morphological data was collected using a Trimble differential GPS, with real-time kinematic global positioning system (RTK-GPS) capability, which was mounted on a quad vehicle. A small base station structure was temporarily installed at a high position in the dunes, and the Trimble GPS receiver was carried in a backpack (see Figure 2.4). Each day the base station was set up and a new data collection session was initiated and tested before data collection could begin. Surveying aimed to cover a grid over the beach, with cross-shore profiles intersected by evenly-spaced longshore transects. The intention was to create an even coverage of measurements for eventual interpolation procedures and the creation of accurate digital elevation models (DEMs).

Unfortunately for the majority of the data collections days, problems were experienced with the DGPS which reduced the time available for data collection. Issues that occurred ranged from loss of rover-base station communication, extended periods of time where no satellite signal could be found, and the ceasing of functionality of the DGPS rover radio. One week out of the six-week allotted fieldwork time was unavoidably lost due to required repairs, however data collection was able to continue once the equipment was replaced. During surveying, planned surveying time was lost as the quad needed to be slowed down or stopped to re-connect the rover-base station signal, and considering the time constraints this meant that distance between measured points had to increase. Short-term data quality, therefore, could have been improved if there was more time available to compensate for errors with the equipment.

Figure 2.4: The base station and quad set up for data collection.

2.2.3. Deriving coastal profiles from measurement data

The raw data that was collected during the survey campaign first had to be organised into layers in a GIS map, using the program ArcMap. The next step was to remove erroneous measurement points lying outside the area of interest. Once each set of measurements was organised and sorted by date, Triangulated Irregular Networks (TINs) were created for each set of points which produced a surface based on the spatial data. Figure 2.5 shows an example of this process; the overlying layer contains the point measurements used to create the TIN. The process to create a TIN involves the creation of triangles of various sizes interpolating the space between data points. Thus, the intention was to create a grid of measurement points so as to improve the accuracy of the TIN. However, this does result in some areas of strange morphology (e.g. the centre of Figure 2.5 with long 'spikes' of higher elevation), as the TIN is better suited to

fluctuating surfaces. For the purposes of this project, creating TINs was adequate to produce coastal profiles. Once the TIN surfaces were created, cross-shore profiles for each transect were derived and it is these profiles which form the basis for the analysis.

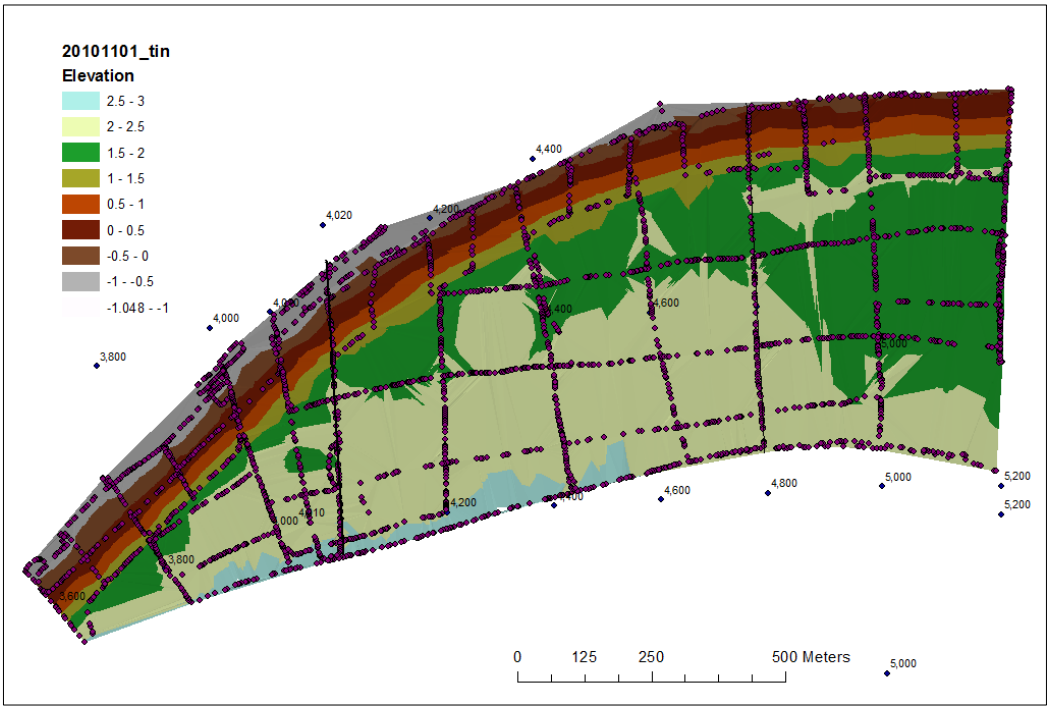

Figure 2.5: An example of a TIN created from the survey data from 01.11.2010; the measurement points are overlain on the TIN to show how the surface is derived from the original measurements.

2.3. Long-term Morphological Data

To make an assessment of the long-term, decadal, trends of shoreline change, it was necessary to examine historic morphological data. Beach profiling in the Netherlands has been conducted on an annual basis in recent years, and every 2-3 years at the beginning of surveying in the 1965. It is collated by Rijkswaterstaat into the Jarkus data set. This surveying was conducted at intervals along the entire Dutch coastline, and so is possible to access data that covers a wider alongshore section of the coastline than the fieldwork. This longer temporal framework and larger spatial scale permits an assessment of volume changes and sediment dispersal from the attached bar to the downdrift shoreline.

The long-term analysis considers the RSP (**R**ijks**S**trand**P**alen: official beach markers) transects that are most directly affected by the bypassed shoal attaching to the beach. These transects are at RSP 3, the most north-westerly transect and the closest to the inlet, through to transect 10 at a distance of approximately 7 km from the inlet (Figure 2.6). In total, 8 transects were analysed (RSP 3 to 10) over the period 1965-2010, with a temporal resolution that varies from 1 to 3 years. Temporal resolution of the data was affected by years where no data collection occurred (such as during the early 1970s, parts of 1980s), and also the spatial resolution was voluntarily reduced to cope with the volume of data. Initially an overview of the data was conducted to get an idea of the morphological developments at each transect. From there, years from the dataset

were chosen to be included in the analysis, often with a gap of 2-3 years from one set of data to another. Data resolution was increased during periods which were seen to have increased morphological development, and then data from each year was used.

Figure 2.6: Location of transects 3 to 10: these were the only transects considered for the long-term analysis (Google Earth image, 2005).

2.4. Data Analysis

2.4.1. Analysis of Short-Term Morphological Data

Three characteristics were used to quantify the changes occurring to the beach over the short-term period: profile volume, beach slope, and surface analysis (cut and fill).

- Profile Volume

The beach profile visualises the change of elevation of the beach surface with distance from a known position. The profile is derived from a cross-shore transect, typically perpendicular to the general trend of the shoreline as in this case, but it can also be conducted perpendicular to beach contours. Beach profile campaigns over a period of time allow the researcher to observe morphological changes occurring.

The short-term morphological data permitted detailed observation of the day-to-day changes in profile shape and volume, and a qualitative description of these changes is included in the analysis.

Dean and Dalrymple (2002) defined a technique of estimating beach volume by calculating the area under a profile graph, multiplying this value by a certain width (i.e. 1 metre), then multiplying the resulting figure with the longshore length of the beach (Figure 2.7). This technique should produce a good estimate of the total beach volume as derived from profile data, without the necessity for reproducing the actual beach surface.

However, in this project, the beach surface has been interpolated using cross-shore profiles and additional spot heights derived from dGPS measurements. This means that it is possible not only to estimate the beach volume from the profiles, but also to recreate a surface and interpolate new profiles.

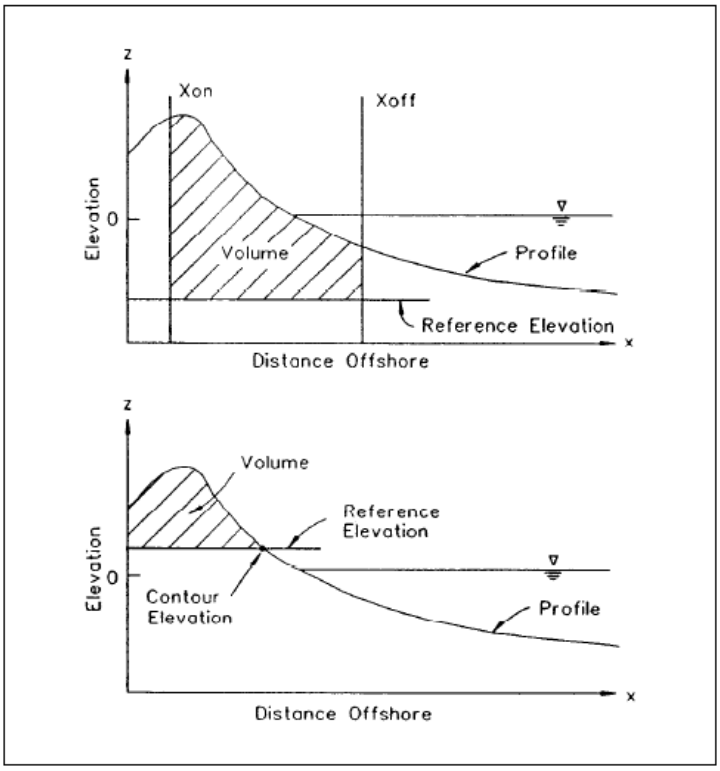

Figure 2.7: Methods for estimating cross-sectional profile volume of a beach (CETN, 1999)

- Slope

The slope of the beach can be divided into the foreshore and the backshore, separated by the berm (the highest point reached by waves). In the cross-shore profiles, this distinction can be made visually as a break in the slope of the beach. Thus, calculations of slope derived from the foreshore could be separated from the lower-sloping backshore.

- Surface analysis (Cut and Fill)

The Cut and Fill functionality within the GIS software ArcGIS allows the subtraction of one DEM surface from another, with the intention of determining locations where material has been gained or lost between the surfaces. Further, the volume of material gained/lost can be calculated as a net volume. The product of this analysis is a raster classified into areas of net gain, loss or unchanged, thus spatial data is also a product.

For the purposes of this project, DEM surfaces for the entire beach (main location and secondary location), derived from data collected at the beginning and the end of the measurement campaign, are used to provide a 'before-and-after' snapshot of the beach morphology. Using this Cut and Fill function, the total volume change can be calculated and the spatial pattern of change identified.

2.4.2. Analysis of Long-Term Morphological Data

- Profile Volume

The profile volume method was utilised once again in order to extract useful volume data from the long-term record. Each profile, per transect, per year, had to be separated from a single large text file containing every transect profile for the entire period from 1965-2010. To be able to calculate the profile volume, each profile was plotted as a graph within the software program Surfer. Due to the time required to convert the data from its original form into an organised form that could be used in Surfer, the number of transects and data years used had to be reduced.

Each profile for transect x and year y was initially separated from the entire record and saved as a simple text file. A conversion process within Microsoft Excel transformed and re-ordered the data into two columns: X as the distance from a known RSP point increasing in the seawards direction, and Y as the deviation in surface elevation. Once in this format the text file could be imported into Surfer and converted to a .BLN file, recognisable within the program as a file with an ordered set of points, not unlike the original text file but the first line includes the number of X-Y points within the file. Only then could Surfer recognise and plot the data as a graph of surface elevation over distance.

To derive the profile volume, each profile had to be converted from a simple line graph to a polygon graph. The boundaries for each volume were identified by comparison with each transect's historical morphology, i.e. much of the coastline from transect 7 had boundaries of dune foot at +3 m NAP and an offshore boundary of -6 m NAP, as these boundaries included all the fluctuations over time.

Once the boundaries were known, new files were created from the .BLN files that only included the relevant morphological data within the boundaries. This data was "closed off" by inserting the first set of coordinates at the end of the file, thereby creating a polygon rather than a line. The properties of the polygon indicated its area, which we take to be the cross-sectional profile volume.

- Beach width

Measurement of beach width was simple after the boundaries for dune foot position had been identified. The seaward boundary was designated as +1 m NAP, which corresponds roughly with the high tide position. This contour was chosen because while much variation occurs in the lower foreshore zone on a daily basis, the +1 m NAP does not change quite so much as it is exposed to wave and tidal currents for a much shorter time. A change in position of this contour therefore signified a change in morphology brought about through an extended period of accretion or erosion.

Calculation of beach width identified where the surface crossed the relevant contour and a calculation of the distance between these contours produced a value for beach width.

- Dune properties

Cross-sectional volume of the foredune, its height, and the dune foot position give enough information about the dimensions of the active dune at a given time, as each is inherently linked

to the other. For each transect this data has been collated and analysed for patterns and trends in dune development.

Assessing the dunes is conducted in the same manner as the beach and nearshore. The dune foot is estimated at the +3 m NAP contour, or as otherwise stated (at lower elevations when the foredune height was lower than the +3 m NAP threshold, i.e. transect 3 in the earliest profiles). The first dune at the dune foot is usually termed the foredune, and is the most active part of the dune system. Often the general form and position of the landward side of the dune does not change through time, as the dune progrades from the front, seaward side. With this in mind, analysis of the dunes considered this first dune only within the following calculations.

Dune volume calculations involved an initial general examination of the trends in dune behaviour throughout the historical period, in order to identify suitable boundaries for the foredune. As the dune foot is determined as +3 m NAP, this contour was used (unless otherwise stated) as the minimum contour above which the volume would be classed as the dune volume. This method is also included in Figure 2.7. Generally, a fixed position behind the foredune could be used throughout the entire record for a particular transect as little migration or change to this side of the dune was noticed.

On occasion the foredune from the earliest records was succeeded by the growth of another foredune later in the record. In these circumstances the original landward position remained in use despite the development of a new foredune.

Dune height could be derived, rather simply, from the heights of the foredune. Where the foredune was replaced by a younger dune, the highest dune height would be recorded until the younger foredune overtook the height of the older.

Lastly, dune foot position was identified from the profiles as the major break in backshore slope between the beach and the dune. This position usually coincided with +3 m NAP, but as previously mentioned, this threshold did not apply to all transects and the dunes closest to the inlet had a dune foot position of +2.5 m NAP. Dune foot is taken to be at +2.5 m NAP for these locations and this ensures inclusion of the earliest records when the dunes were less developed in height and volume, and to enable a good comparison of profiles through time. The fluctuations in the dune foot position were represented as the change in position since the start of the record, which was assigned a zero value. All deviations in position away from the original resulted in a distance measurement that was either positive (progradation) or negative (retrogradation). This data is best presented in combination with high water mark (HWM) fluctuations to give an idea of how the beach width is evolving through time at the foreshore and at the dunes.

3. Analysis of Short-Term Morphological Behaviour

Observations of the short-term morphological changes can give us an idea of the long-term response of the shoreline. Three zones can be defined based on morphological response: the backshore, the berm, and the foreshore. It is assumed that the foreshore is the most morphologically active part of the entire beach as it undergoes continual reworking by waves and tides. Similarly the berm, or high tide position, is a dynamic feature which shifts position according to the intensity of wave action and the highest reach of waves. The backshore is generally assumed to be the least active zone of the beach, but although it may only receive large storm wave energy, backshore morphology may be largely under the control of aeolian processes in the right circumstances. Certainly on Ameland in the process of data collection, descriptive observations were made about the state of the beach in response to day-to-day changes in weather, and it is particularly noteworthy for Ameland that aeolian processes dominated the backshore morphology to an extreme extent.

Analysis of the short-term data will examine the measured changes in the surface of the beach over the six-week period of data collection. Transect and spot dGPS measurements were used to create digital elevation models (DEMs), one per data collection session (per day), from which it was possible to derive cross-shore profiles, estimate volumes, and calculate slope. Further, the DEMs can be used to determine where on the beach sand has been lost and gained by subtracting one DEM from another.

3.1. Characteristics of the Study Sites

The beach downdrift of the Ameland Inlet has a distinctive morphology characteristic of barrier island coastlines. The most north-westerly beach (the main study site) has a convex planform which results from the welding of large onshore-migrating bars. This comprises the 'drumstick' head of the island as discussed in the literature review. The beach width increases considerably over a short distance from the inlet; from a low-tide width of 200m to nearly 800m at its widest, just over a kilometre's distance away. Further eastwards from the inlet and the beach width again decreases with the furthest extent of the attachment shoal.

The secondary study site is located six kilometres from the inlet, also on the North Sea coast. This beach has a concave planform, forming the furthest edge of the most recently attached shoal, and the point where beach width decreases from 500m in the west to 300m in the east. From this point eastwards the beach decreases to less than 150m for a substantial portion of the coastline.

The elevation of the north-west beach fluctuates from 2.0 m at the berm to approximately 2.50 m at the dune foot. Similarly, the secondary beach elevation ranges from 1.75m to 2.25m at the dune foot. The difference between these beaches is that while the north-west beach has a convex cross-shore profile, the secondary beach location has a very clearly defined concave profile which sees the mid-section of the beach lowering by 0.5m.

Dune height varies with distance from the inlet, ranging from 14.0m at the closest to the inlet to 8.0m over a kilometre away. Dune height reduces progressively in the alongshore direction from the inlet. At the furthest measured point on the north-west beach, the beach environment

in front of the dunes is very different to that close to the inlet; here, the beach takes on a 'quick-sand' character and is highly vegetated. This substantially reduces the availability of sand to contribute to dune-building, and so the dunes at this location are 'older' in character than those towards the inlet. At the secondary location dune height averages at 13.0m elevation in the second line of older dunes, which is fronted by more open, active dunes of a reduced height.

3.2. Hydrodynamic Conditions during Fieldwork

The following two diagrams contain data about the offshore and onshore wave conditions during the fieldwork campaign in September-October 2010. Julian days 265-305 refer to 23rd September to 1st November 2010. The offshore data (Figure 3.1) refers to measurements made from an offshore buoy, while the onshore data (Figure 3.2) was measured within the intertidal zone by instruments mounted on a frame.

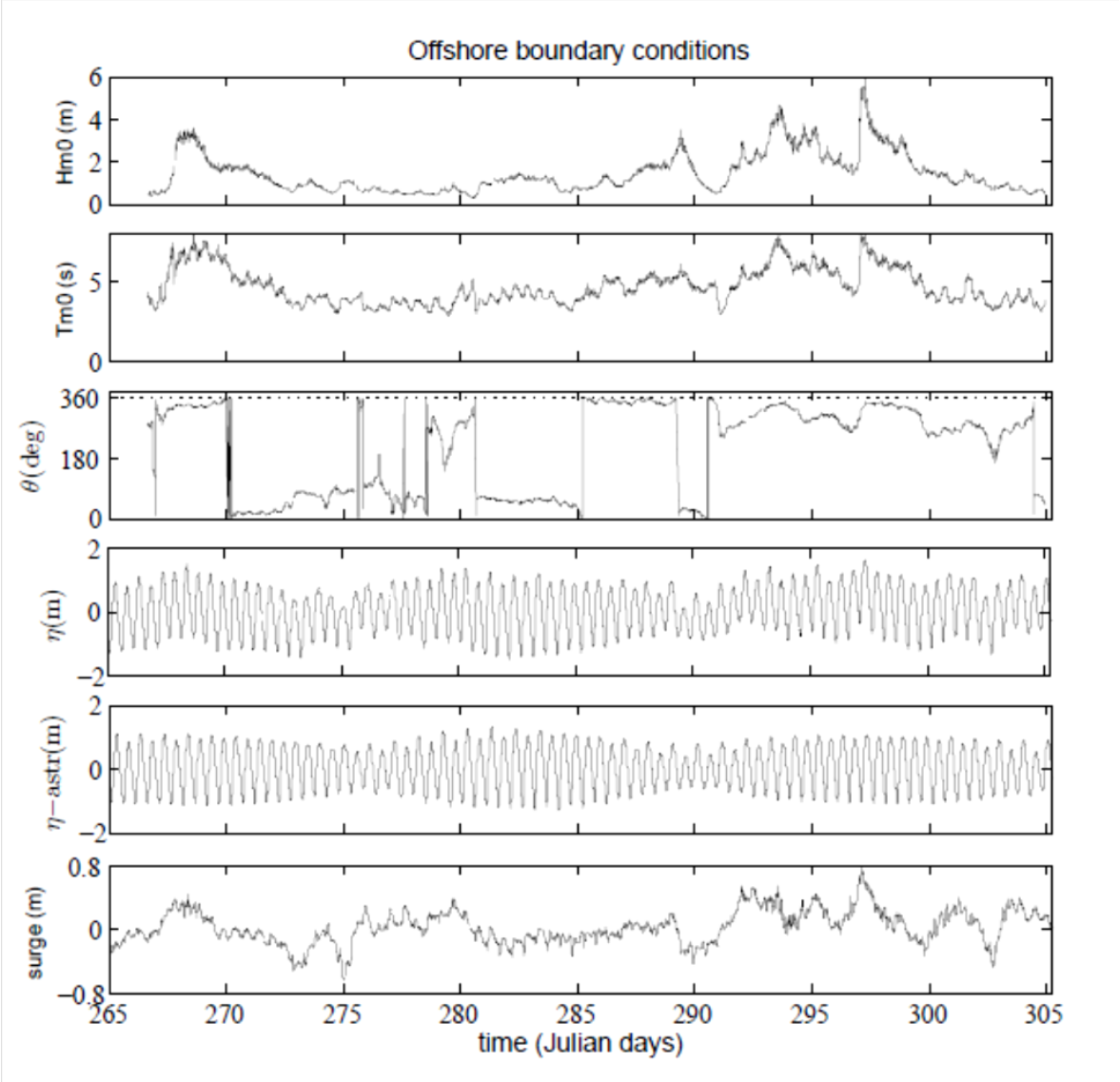

Figure 3.1: Offshore boundary conditions during the Ameland campaign. a) Significant wave height (Hm0), b) significant wave period (Tm0), c) wave direction (θ), d) measured offshore water level fluctuations (η), e) astronomical tide and f) the local surge.

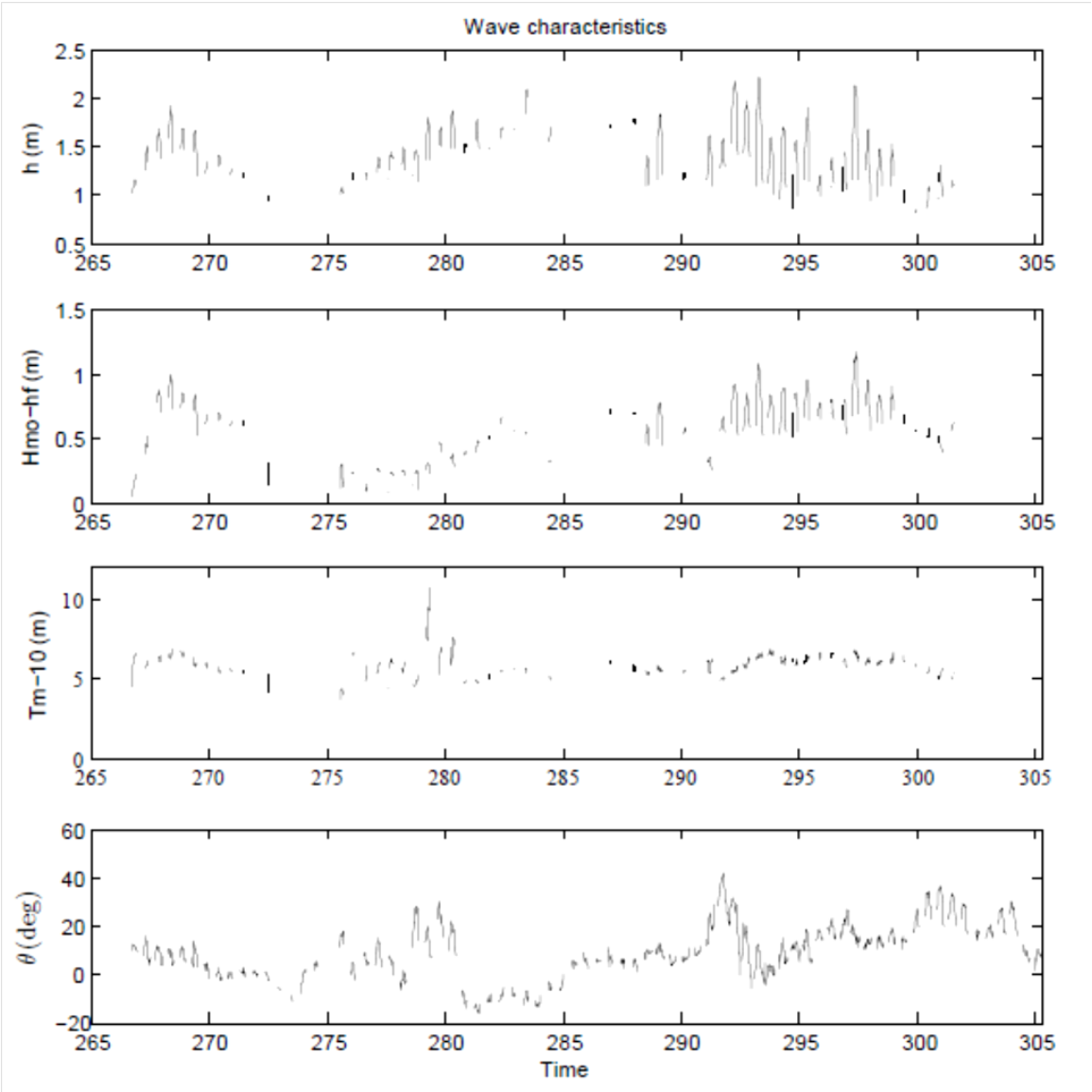

Figure 3.2: Onshore wave characteristics during the fieldwork campaign on Ameland.

Table 2: Hydrodynamic conditions during storm events that occurred in the course of the fieldwork period.

Storm event	Julian day	Hm0	Tm0 (sec)	Wave direction ^{0} (offshore)
1	268	3	5.5	340
2	288	3.8	5	350
3	293	4.5	6	350
4	297	6	6	355

Generally, periods of higher significant wave height, wave period and local surge coincide with extended lengths of time where the dominant wave direction is from the north-west. Four storm events are seen in the offshore and onshore data and are summarised in the Table 2. Occurring sequentially the later storm events were stronger than the first two, producing higher

significant wave heights. Wave direction is from the north-west as seen in Figure 3.1, and north-east in Figure 3.2. This disparity is likely to be due to the position of the measurement tract which was orientated towards north at transect 5, and means that north-westerly waves that refract around the curved coastline appear to approach from a more north-easterly direction onshore.

3.3. General Changes and Trends in Beach Profiles

The morphological behaviour of the beach can be observed by analysing cross-shore profiles in terms of change in profile shape, volume and slope. Short-term fluctuations in volume and slope are discussed in the following sections, while general descriptive changes are dealt with here.

3.3.1. Profile Description: Transects 3.80 to 5.20

The north-west beach at low tide exposes approximately 100m of foreshore which, considering the uncommonly wide beach, is a rather small proportion of the total beach. The foreshore profiles of the main study area (north-west Ameland) generally show very flat, smooth slopes with only a slight concavity towards the water's edge, and berm around +2 m NAP. A clear break in slope is evident from most profiles which indicate the position of the berm, but it becomes less pronounced close to the inlet (e.g. profile 3.80; Figure 3.3).This analysis covers only the foreshore above 0 m NAP due to inconsistent measurements below this level, and thus does not include subtidal or nearshore bars.

A prominent trough and subtidal bar existed for much of the campaign below 0 m NAP (below low tide water level), with the trough exceeding 1 m depth. Due to the depth and additional water level changes caused by waves and strong winds, measuring spot heights on foot with the dGPS could not be accomplished consistently for each profile throughout the campaign and is thus left out from this analysis. Observations made during the course of the measurement campaign can provide some idea as to the morphology of the subtidal bar. It appears somewhat oblique to the shoreline between profiles 4.00 and 4.20, while straighter and less interrupted between 4.80 and 5.20. The depth of the trough and height of the bar are reduced nearest to the inlet, but are more defined with distance from the inlet at profiles 4.80 to 5.20. Indeed the reduced depth of the trough on one side of the beach made it possible for measurements to be taken, but the depth also inhibited the collection of data where the trough had a more pronounced, deeper morphology. Thus, there was a certain degree of alongshore variability in the intertidal bar-trough system with a clear distinction made from one side of the beach to the other, from within the inlet throat to a point distant from it. Furthermore, it should be noted that onshore migration of the subtidal bar has not been clearly identified in the cross-shore profiles.

The foreshore closest to the inlet, between profiles 3.80 and 4.02, displays significant variability in the day-to-day fluctuations of the elevation of the foreshore, while the beach between profiles 4.20 and 5.20 displays a lesser degree of variability.

Profiles 3.80 and 4.00 show a loss of vertical elevation in the order of 0.30 metres between the start and the end of the campaign, but also displays a distinct cross-shore shift of the berm sea-ward and subsequently land-ward. This can be seen clearly in profile 4.00 from the drop in

foreshore elevation between 24/09/2010 and 15/10/2010 (storm event 2, Julian day 288) coinciding with a storm occurrence and increased aeolian activity on the backshore (Figure 3.4). In the period following, the elevation of the foreshore decreases while the berm moves landward and increases in elevation. This behaviour is typical of sediment re-distribution and the re-equilibration of the profile following storm action, where deposition of sediment takes place higher in the profile and causes an increase in berm elevation. This behaviour is seen most clearly in profile 4.00 (Figure 3.4), but less so in profiles 3.80 (Figure 3.3) and 4.02 (Figure 3.5). Berm features are not recognisable in these profiles, but a distinct 'recovery' period after 15/10/2010 can be seen whereby an increase in the upper foreshore elevation is evident coinciding with a lowering of the lower foreshore. The upper foreshore displays a variation in elevation in the order of 0.50 metres in profiles 4.00 and 4.02, reflecting the impact of wave action on this side of the beach in combination with aeolian activity.

The variability in cross-shore profiles is less dramatic between 4.20 and 4.40 (Figure 3.6 and Figure 3.7). Both profiles show an increase in upper foreshore elevation on 25/10/2010 (the day after storm event 4, Julian day 297) followed by a subsequent decrease. Profile recovery after the storm event is evident but less pronounced than the foreshore to the west. Lower foreshore variability is in the order of 0.10 to 0.15 metres.

Lower foreshore measurements for profiles 4.60 and 4.80 (Figure 3.8 and Figure 3.9) indicate low variations in elevation change throughout the campaign, with elevation excursions in the order of 0.10 metres. Once again, both profiles display increasing elevation of the berm in the second half of the campaign which results in greater variation in the profile. Lack of measurement points in the upper foreshore part of profile 4.60 during 24/09/2010 and 15/10/2010 reduce the accuracy of the estimated elevation. However by comparing profile 4.60 with the similar profile 4.80 it is possible to see that the upper foreshore as reproduced in the graph isn't incorrect in elevation but only by shape (i.e. this part of the profile is too straight).

Profiles 5.00 and 5.20 (Figure 3.10 and Figure 3.11) also demonstrate little variability over the lower foreshore profile, similar to that seen in profiles 4.60 and 4.80. Likewise, the landward-moving and increasing elevation trend of the berm in the second half of the campaign is evident in both profiles.

The alongshore variation in beach profiles can be divided into two sections: the three profiles closest to the inlet (3.80, 4.00, 4.02) display large variations across the profile, but particularly in the upper foreshore/berm area; while profiles 4.20 to 5.20 show a much reduced degree of variability, with most differences occurring in the upper foreshore, but to a lesser extent than 3.80 to 4.02. Similarities throughout all profiles are seen in the evolution of the berm after 15/10/2010 (Julian day 288). The development is clearest in profile 4.00, which shows how the berm feature changes from the beginning of the campaign by a lowering of the upper foreshore by 0.25-0.30 metres and shifting approximately 10-15 metres seaward. Subsequent profiles show a decreasing vertical elevation of the lower foreshore profile occurring coincidently to an increasing elevation of the berm and a shift landward.

The trend of upper-foreshore erosion can be attributed not only to increased wave energy levels and higher wave reach caused by storm weather, but also to the changing water levels associated with the spring-neap cycle of the tide. The transition between neap to spring tide raises water levels by as much as 0.50m and this could cause increased upper-foreshore erosion due to the higher elevation reach of waves.

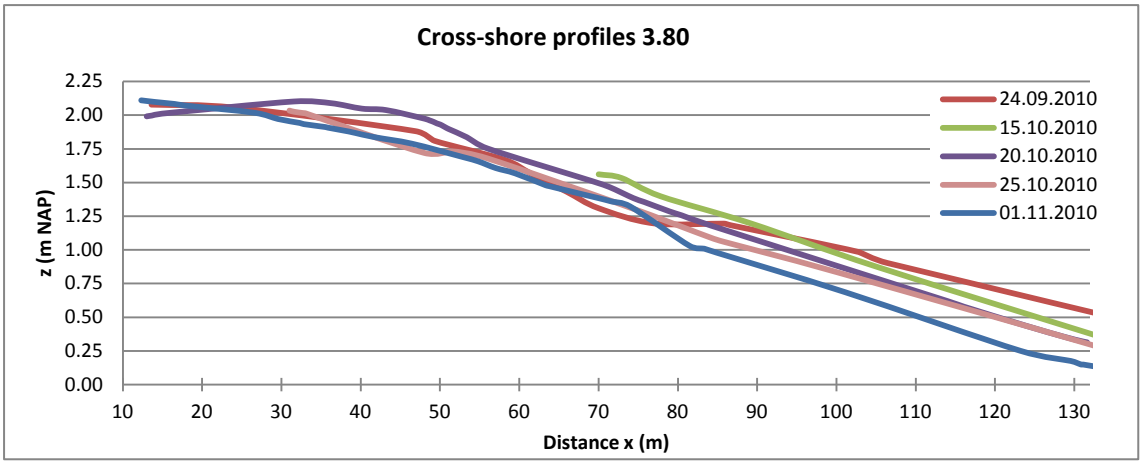

Figure 3.3: Cross-shore profiles of the foreshore of transect 3.80

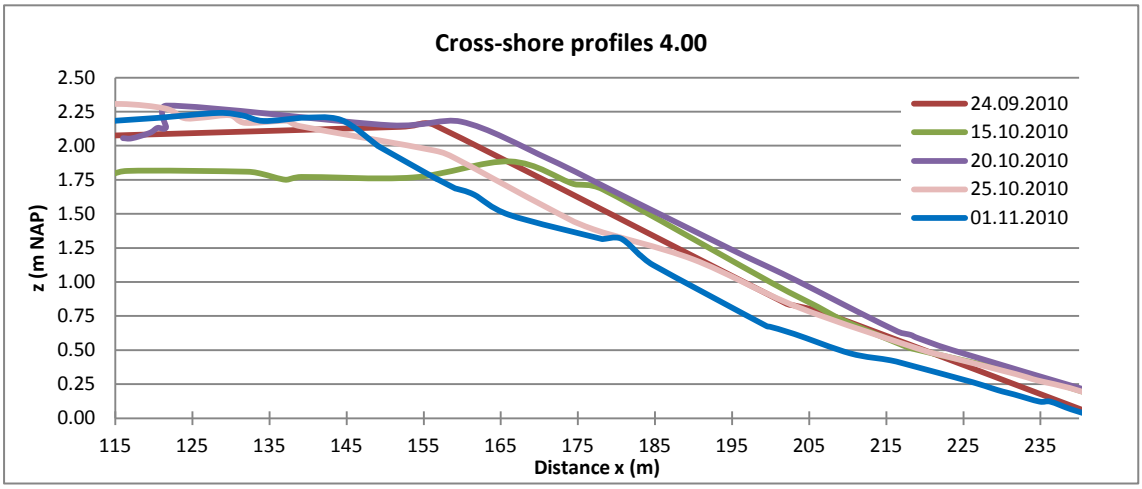

Figure 3.4: Cross-shore profiles of the foreshore of transect 4.00.

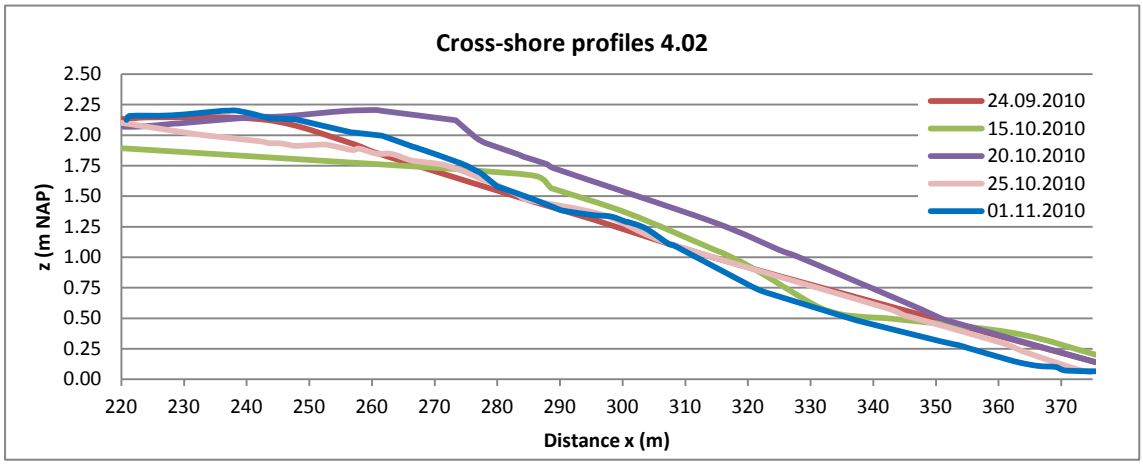

Figure 3.5: Cross-shore profiles of the foreshore of transect 4.02.

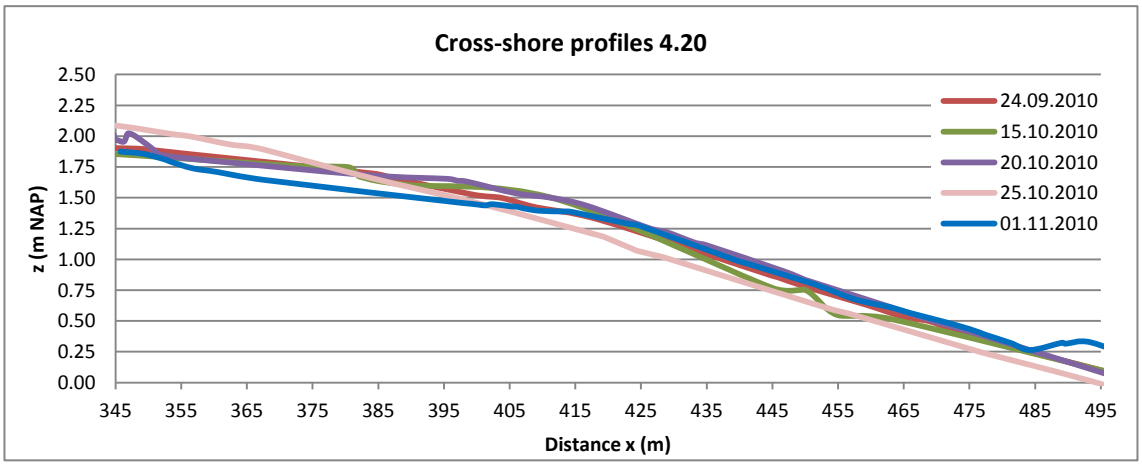

Figure 3.6: Cross-shore profiles of the foreshore of transect 4.20.

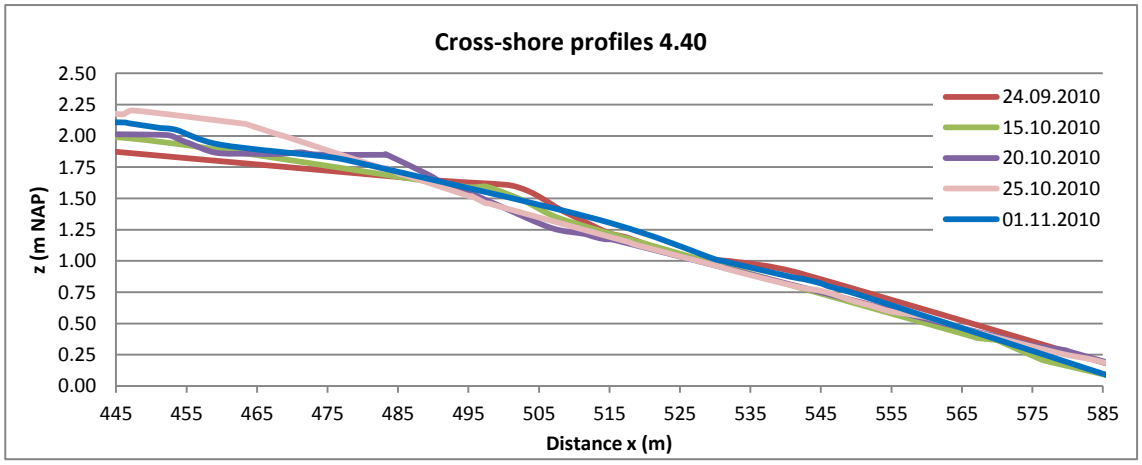

Figure 3.7: Cross-shore profiles of the foreshore of transect 4.40.

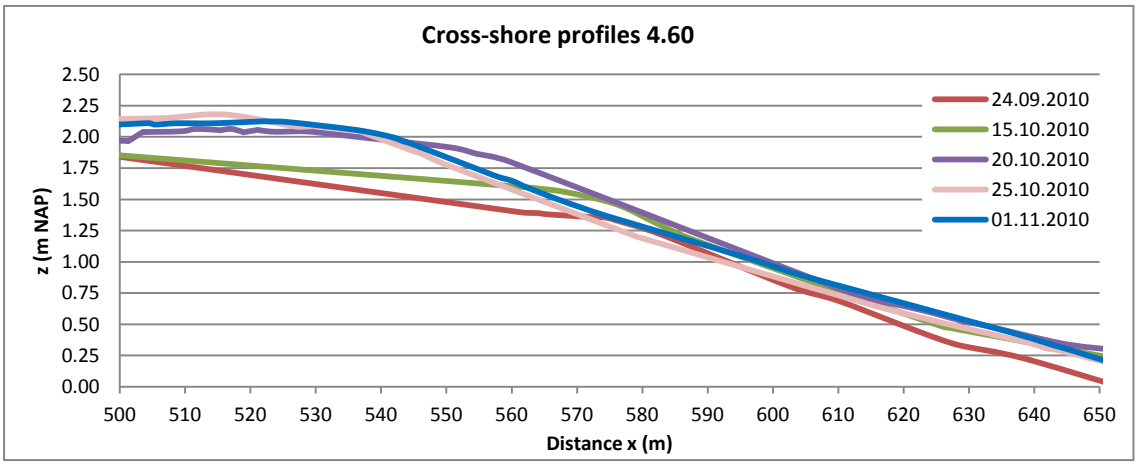

Figure 3.8: Cross-shore profiles of the foreshore of transect 4.60.

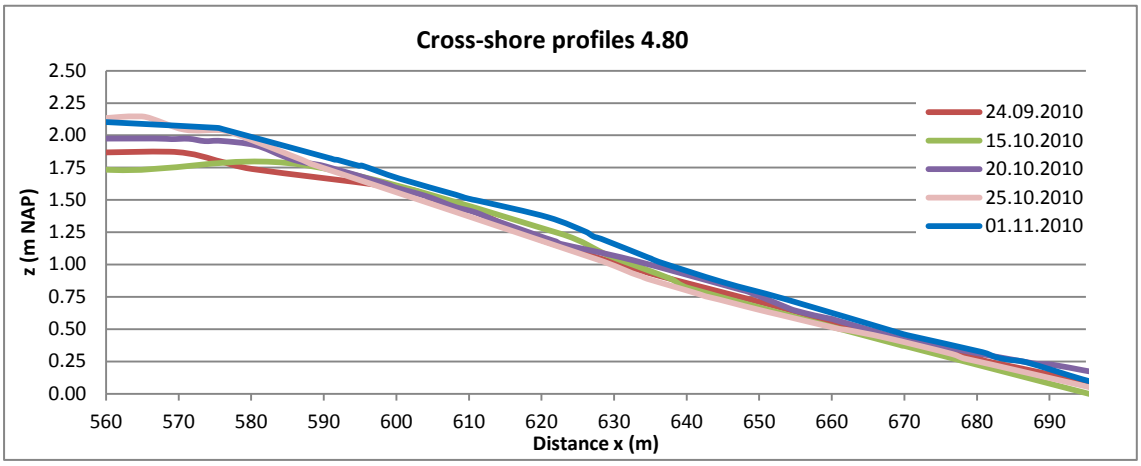

Figure 3.9: Cross-shore profiles of the foreshore of transect 4.80

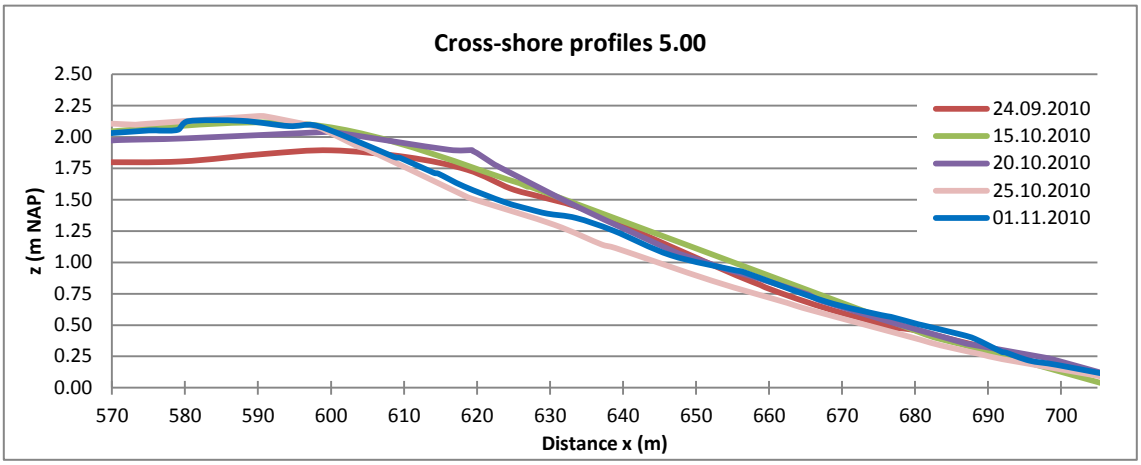

Figure 3.10: Cross-shore profiles of the foreshore of transect 5.00.

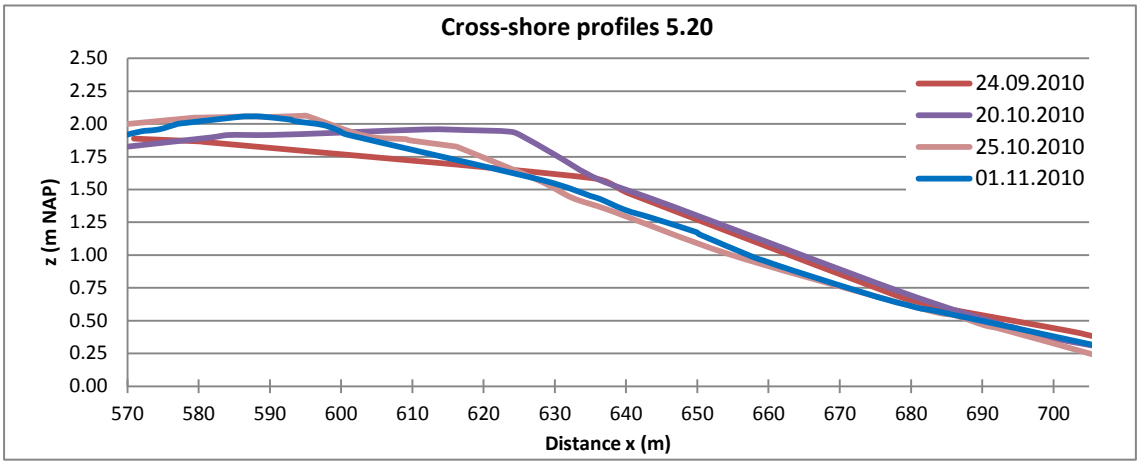

Figure 3.11: Cross-shore profiles of the foreshore of transect 5.20.

3.3.2. Profile Description: Transects 9.20 to 10.0

While the focus of this research is on the north-west Ameland beach, another section was monitored at the same time to determine if there is a relationship between the responses observed on each part of the beach. The beach at transects 9 to 10 experiences the same wave impact as transects 3 to 5, however this beach is in a more exposed location downdrift of the ebb tidal delta.

There are several differences between each section that are important to mention. The main study site is located immediately adjacent to the tidal inlet, while the control section is located at a distance of several kilometres away. It is assumed that wave energy is reduced near to the inlet due to the presence of the ebb tidal delta, but further away from the inlet this mitigating structure is not present and thus the coastline receives the full impact of wave energy.

The control beach itself is different in morphology compared to the main study beach. The general trend of the shoreline is slightly concave, and likewise the beach curves in a concave manner from west towards the east. Due to this shape the cross-shore width of the beach decreases by approximately 130 metres over 1 kilometre alongshore width. The beach of the main study site is convex in shape.

Figure 3.12 to Figure 3.16 show the profiles of transects 9.20 to 10.0 as measured on the 17th, 24th and 30th October 2010. While the profiles of transects 3.80 to 5.20 only covered the foreshore area, transects 9.20 to 10.0 feature the full cross-shore profile from near the dune foot to around 0 m NAP. Measurements of this area were made possible due to the relatively narrow cross-shore width of the beach. At transect 9.20 the beach width is approximately 450 m, narrowing to ≈320 m at transect 10.0.

The profile in each figure begins not at the dune foot itself but at a small distance just in front of the dunes on the backshore (the dune foot occurs at 3 m NAP), as dGPS was installed on the quad. The cross-shore profile, until the raised berm at the foreshore, features a low depression across all transects that was often occupied by standing water during fieldwork. This depression is the remaining morphology of a former channel that once existed when the bar-spit dispersed alongshore and towards the shoreline (see later discussion on this morphology; Chapter 4). The deepest part of the depression occurs around +1.50 m NAP at 9.20, lowering to +1.25 m NAP at 10.0. The berm part of the beach exists at all transects around +1.75 m NAP, which means this feature stands at a higher elevation than the whole backshore.

A distinctive trough feature appears alongshore in all profiles on 17.10.2010 with the exception of profile 9.20. The trough exists around the 300 m point (distance from dune foot) and while it can be distinguished from adjacent profiles, it becomes shallower, narrower, and also higher in elevation towards the western side of the section. It is no longer visible in profile 9.20, the westernmost side of the control section. At its most pronounced, in profile 10, the trough reaches -0.14 m NAP and is over 20 metres wide. At profile 9.60, approximately 400 m distance from profile 10.0, the trough feature is reduced to 10 m wide and it is now at an elevation of +1.1 m NAP, an increase in elevation of 1 m (≈25 cm/100 m alongshore). The feature remains more or less in the same alongshore band of about 300 m from the dune foot. It is likely that this feature is a migrating intertidal bar and the reason for the alongshore variability is due to wave refraction around the convex shoreline to the west. Incoming waves predominantly from the north-west are refracting around the shoreline and breaking earlier on the most westerly point of the control section where the angle between the wave crest and the shoreline is highest. The

intertidal bar is subsequently pushed onshore by swash action, but there exists an alongshore gradient which is shown in the cross-shore profiles.

By examining the change in profile position from the first to last surveys, transects 9.20 to 9.60 show clearly a retreating trend as the berm and foreshore shift landwards. Transects 9.80 and 10.0 have a less well-defined trend, but the profiles appear to shift seawards over this period. This produces an alongshore disparity: one side of the beach is eroding, the other accreting. As there was no significant transport of sediment to the backshore, the conclusion based on profile development over this period is that sediment is being transported alongshore from the updrift to downdrift locations.

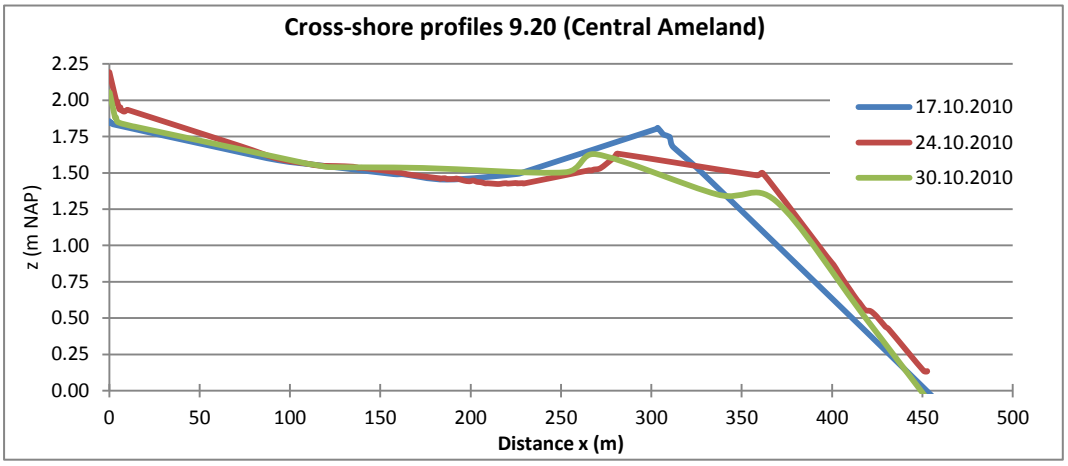

Figure 3.12: Cross-shore profiles of transect 9.20.

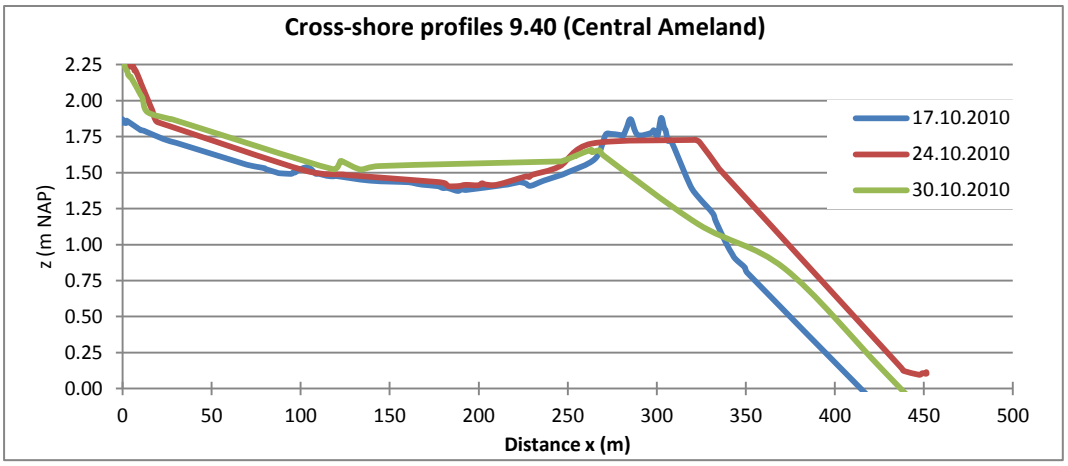

Figure 3.13: Cross-shore profiles of transect 9.40.

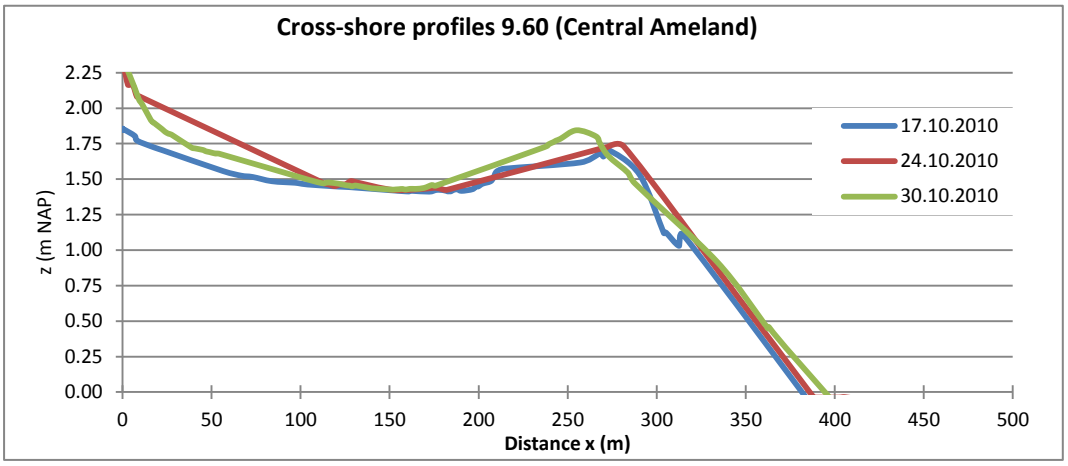

Figure 3.14: Cross-shore profiles of transect 9.60.

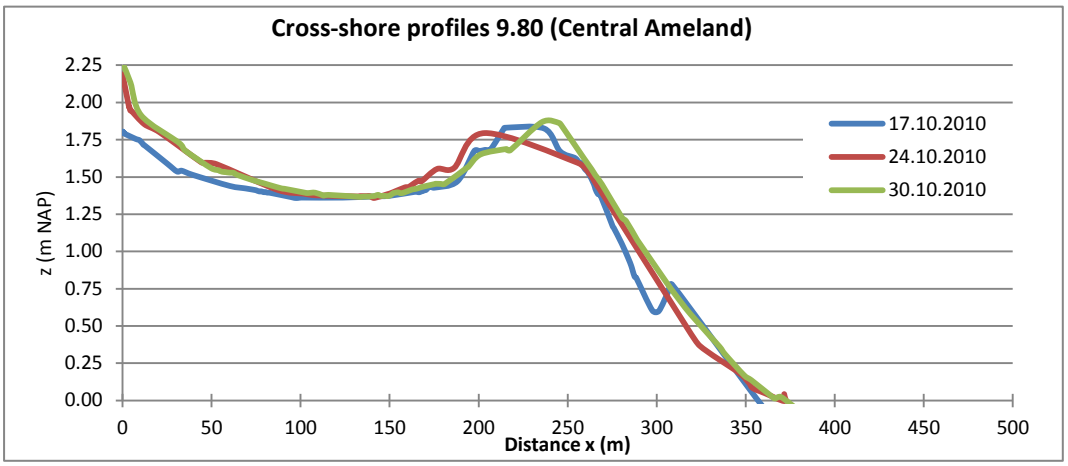

Figure 3.15: Cross-shore profiles of transect 9.80.

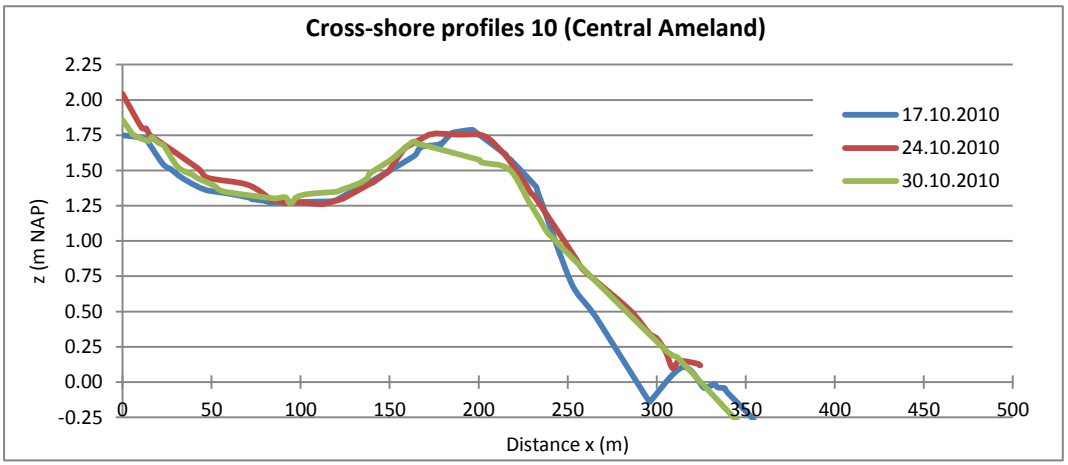

Figure 3.16: Cross-shore profiles of transect 10.0.

3.4. Beach Profile Volume

The profile volume was calculated by determining the area underneath a profile and multiplying this value with an alongshore distance, in this case by 1 metre, producing a value of m^3/m (volume per unit of alongshore length). It is a useful means of not only comparing profile change over time, but also for calculating total beach volume.

3.4.1. Transects 3.80 to 5.20

Five survey days were chosen to represent the fluctuations in the beach volume during the measurement campaign, and the results for profile volumes and the percentage change in volume from the total are presented in Table 3.

One of the first observations of the profile volume data is that there is little consistency or clear pattern occurring between the data on each day. Some profiles may experience net loss at the same time as adjacent profiles experiencing net gain, on the same day. By looking at the average of gains and losses, a division can be seen either side of profile 4.20: to the west of this marker, the beach volume was calculated to have an average loss, while to the east there was average gain.

The standard deviation of the percentage change in volume indicates that the largest deviations in volume change occur at 4.80 and 4.02 respectively.

Over the period, the biggest decrease in volume between the first and last surveys occurs at transect 3.80 with a total net volume loss of 19 m^3/m. This is also the location for increased erosion over recent years, so it is not surprising that greatest loss over this period occurs in this transect. Additionally, transect 4.00 undergoes a similar net volume loss totalling 16 m^3/m over this period. The highly variable transect 4.02 indicates a gain and subsequent loss of volume of 34 and 32 m^3/m over a 10-day period during the campaign, causing this transect to stand out as the most variable. Transects 4.40 to 5.00 undergo net gain in volume, with 4.60 gaining the most with 35 m^3/m during the period. Transect 5.20 indicates no difference in volume from the start to the end of the campaign, but experiences equal gains to losses throughout.

To make an estimation of the net coastal erosion and accretion during the campaign, it is possible to upscale the net loss and gain per alongshore length by the distance between the transects. The total net loss is calculated as 9,100 m^3 (transects 3.80 to 4.20) and the net gain 12,500 m^3 (transects 4.40 to 5.00), over the 6-week period of the campaign. These figures only cover the coastal change at the foreshore, with a total alongshore distance of 1770 metres at 0 m NAP.

Table 3: Beach profile volume per profile, 3.80 to 5.20.

Beach Profile Volume per Profile									
	3.80			4.00			4.02		
Date	Vol m^3/m	Gain/Loss m^3/m	% change	Vol m^3/m	Gain/Loss m^3/m	% change	Vol m^3/m	Gain/Loss m^3/m	% change
24.09.2010 (1)	165		0	173		0	192		0
15.10.2010				164	-9	-5	189	-3	-1
20.10.2010	163	-2	-1	189	24	15	223	34	18
25.10.2010				171	-18	-10	191	-32	-14
01.11.2010 (2)	146	-17	-11	157	-14	-8	191	0	0
v2-v1	-19 m^3/m			-16 m^3/m			-1 m^3/m		
AVERAGE	158		-6	171		-2	197		1
STDEV			7			11			13
	4.20			4.40			4.60		
Date	Vol m^3/m	Gain/Loss m^3/m	% change	Vol m^3/m	Gain/Loss m^3/m	% change	Vol m^3/m	Gain/Loss m^3/m	% change
24.09.2010 (1)	175		0	168		0	167		0
15.10.2010	172	-3	-2	164	-4	-2	184	17	10
20.10.2010	180	8	5	167	3	2	205	21	11
25.10.2010	167	-14	-8	171	5	3	195	-10	-5
01.11.2010 (2)	172	6	3	171	-0	-0	202	7	4
v2-v1	-3 m^3/m			+3 m^3/m			+35 m^3/m		
AVERAGE	173		-0	168		0	191		5
STDEV			6			2			7

	4.80			5.00			5.20		
Date	Vol m^3/m	Gain/Loss m^3/m	% change	Vol m^3/m	Gain/Loss m^3/m	% change	Vol m^3/m	Gain/Loss m^3/m	% change
24.09.2010 (1)	144		0	162		0	177		0
15.10.2010	142	-2	-1	172	11	7			
20.10.2010	151	9	7	172	-1	-1	187	10	6
25.10.2010	147	-4	-3	160	-12	-7	177	-10	-5
27.10.2010							159	-18	-10
01.11.2010 (2)	160	13	9	168	8	5	177	18	12
v2-v1	+16 m^3/m			+6 m^3/m			No difference		
AVERAGE	149		3	167		1	175		0
STDEV			6			6			10

3.4.2. Transects 9.2 to 10.0

Due to the overall narrower cross-shore (≈500m) and longshore width (≈1000m) of the control beach section, it was feasible to take measurements from the dune foot to around 0 m NAP. Thus the following profile volume results represent the 'full' beach cross-shore volume, unlike profiles 3.8 to 5.2 which dealt mostly with foreshore measurements only. The results from profile volume analysis can be seen in Table 4.

The control beach has a stronger alongshore trend in the profiles, and volume fluctuations tend to operate in tandem with adjacent profiles. In the first profile on 17/10/2010 (Julian day 290) an intertidal bar-trough system is evident in each of the profiles except 9.2 and 9.4 (see Figure 3.14 to Figure 3.16). By the second survey, on 24/10/2010 (Julian day 297), this feature has disappeared but there is a consistent increase in volume alongshore which suggests that the intertidal bar has migrated and amalgamated with the foreshore, adding the observed additional volume. By 30/10/2010 (Julian day 303) there is a loss of volume in profiles 9.2, 9.4 and 10.0, but a smaller loss in profile 9.6 and gain in 9.8. One main difference between these profiles is that the berm in profiles 9.6-9.8 is higher than in the other three transects. Berm height in profiles 9.2, 9.4 and 10 is around 1.65-1.70m while in 9.6-9.8 it is 1.84m and 1.86m respectively. There could be a number of explanations for this alongshore variability, but wind-blown sand towards and building up on the berm may contribute both volume and height to the berm where the profile is otherwise similar to adjacent profiles.

All profiles from 9.2 to 10.0 display a clear trend of sediment redistribution throughout the profile during the measurement campaign. Following the addition of sand in the form of the proposed intertidal bar (17/10/2010), the profiles show increased volume across all five profile locations (24/10/2010), coinciding with the storm on the same day (day 297, see Table 2 page 39). By 30/10/2010 the redistribution of this additional sand has manifest itself as a filling-out of the lower foreshore and coincident erosion of the upper foreshore/berm area. This trend is observed at each of the profile locations for 30/10/2010 but is most clear in profile 9.4. This redistribution may be a result of the lowered tidal water levels as the period between 24/10 and 30/10 was a transition between spring and neap tide.

To make an estimation of the total net accretion across this 1 km stretch of the coastline, the same upscaling approach as used for the NW beach is applied to this area. Each transect experienced net coastal accretion, which amounted to a net accretion of 21,000 m^3 over the 1 km alongshore distance.

In order to make a direct comparison with the foreshore of the NW beach, profile volume measurements were calculated for the foreshore area only, and the results presented in Table 5. Here, it is possible to see the effect that cross-shore re-distribution of sediment has on the profile volume, as two of the transects indicate a loss of volume when the full-profile volume showed an increase. Volume decrease from the start to the end of the campaign at transects 9.40 and 10.0 amounts to 1200 m^3 when upscaled across the area, while volume increase at transects 9.60 and 9.80 amounts to 3800 m^3.

Table 4: Beach profile volume per transect, 9.20 to 10.00.

	9.20			9.40			9.60		
Date	Vol. m^3/m	Gain/Loss m^3/m	% of total	Area m^3/m	Gain/Loss m^3/m	% of total	Vol. m^3/m	Gain/Loss m^3/m	% of total
17.10.2010 (1)	620	-	-	554	-	-	514	-	-
24.10.2010	644	24	4	611	57	10	552	38	7
30.10.2010 (2)	628	-16	-3	587	-24	-4	548	-4	-1
v2-v1	8 m^3/m			33 m^3/m			34 m^3/m		
Average Vol.	631			584			538		
STDEV	12			28			21		
Beach Width x	450m			400m			375m		

	9.80			10.00		
Date	Vol. m^3/m	Gain/Loss m^3/m	% of total	Vol. m^3/m	Gain/Loss m^3/m	% of total
17.10.2010 (1)	463	-	-	377	-	-
24.10.2010	478	15	3	395	18	5
30.10.2010 (2)	486	8	2	383	-12	-3
v2-v1	24 m^3/m			6 m^3/m		
Average Vol.	476			385		
STDEV	12			9		
Beach Width x	350m			275m		

Table 5: Foreshore profile volume measurements for transects 9.20 to 10.0.

Date / Transect	17.10.2010 (m^3/m)	24.10.2010 (m^3/m)	30.10.2010 (m^3/m)	Net Change 17.10 – 30.10 (m^3/m)
9.20	-	213	195	-
9.40	144	180	140	-4
9.60	116	126	126	10
9.80	171	170	180	9
10.0	152	160	150	-2

3.5. Slope

The slope of the beach is divided into the foreshore and the backshore, separated by the berm which is distinguished in the beach profile as a break in slope. The slope results in Table 6 and Table 7 were derived from the cross-shore beach profiles using the berm as the point to begin and end slope measurements for the foreshore and backshore respectively. Slope was calculated directly from the data using the slope function in Microsoft Excel, with data points manually selected from the highest point on the berm to ensure accuracy. Average slope (foreshore and backshore) was calculated per profile with the five chosen dates representing the short-term campaign.

3.5.1. Transects 3.60 to 5.20

The slope results show that the beach has a low gradient with some differences in slope alongshore (Table 6). The foreshore of profiles 3.60 to 4.02 is consistently steeper through time than the foreshore of profiles 4.20 to 5.20 (with the exception of profile 5.00). The lowest average gradient of -0.013 is found in profile 4.20, whereas the transects on either side of 4.20 are considerably steeper.

Similarly, the backshore is flat with a very low gradient and, as anticipated, not much change occurred during the campaign. It is interesting to note that the backshore profile of 4.00 indicated a slightly positive slope by the end of the campaign, whereas all other profiles are negative. This is due to an increased volume of sand held above the high water level which results in a higher berm and a positive slope in the seaward direction. Backshore slope was not calculated for profiles 3.60 and 3.80 as the beach became very narrow at this point, there was no distinguishing berm feature and there was no evident break in the slope. What data there is available for 3.60 and 3.80 can be assumed the same for both foreshore and backshore slope.

One day of the campaign produced markedly steeper slope values than other days. The 20.10.2010 results show an increased steepness in most transects, with the exception of 4.20 to 4.60 which actually indicated a flatter slope than the previous measurements. In the steeper transects, the cross-shore profiles from 20.10.2010 also indicate a higher, more seaward-located berm. In the days preceding this survey strong winds had increased aeolian sediment transport and decimetre-scale barchan-type dunes accumulated above the high water position on the top of the berm. Additionally, the measurement equipment installed on the foreshore for the other Masters projects was significantly buried by sediment. These factors all indicate significant movement of sand, accumulation on the upper foreshore, and ultimately a steeper profile measured on this day. The flatter mid-section of the beach, transects 4.20 to 4.40, likely remained flat due to its exposed position with strong winds from all directions easily dispersing sediment away from this foreshore.

Table 6: Calculation of slope for foreshore and backshore, profiles 3.60 to 5.20.

Foreshore Slope Results: 3.60 to 5.20										
	3.60	**3.80**	**4.00**	**4.02**	**4.20**	**4.40**	**4.60**	**4.80**	**5.00**	**5.20**
24.09.2010	-0.017	-0.014	-0.014	-0.014	-0.011	-0.014	-0.016	-0.016	-0.017	-0.013
15.10.2010	-	-0.018	-0.016	-0.016	-0.015	-0.013	-0.018	-0.014	-0.017	-
20.10.2010	-	-0.020	-0.024	-0.019	-0.013	-0.014	-0.015	-0.015	-0.020	-0.017
25.10.2010	-	-0.018	-0.019	-0.015	-0.014	-0.015	-0.015	-0.016	-0.019	-0.016
01.11.2010	-0.019	-0.018	-0.019	-0.016	-0.010	-0.015	-0.016	-0.016	-0.017	-0.015
Average	-0.018	-0.018	-0.018	-0.016	-0.013	-0.014	-0.016	-0.015	-0.018	-0.015
Backshore Slope Results										
	3.60	3.80	4.00	4.02	4.20	4.40	4.60	4.80	5.00	5.20
Average	-	-	0.000	-0.001	-0.002	-0.002	-0.001	-0.001	-0.001	-0.001

3.5.2. Transects 9.2 to 10

Slope data for transects 9.2 to 10 are presented in Table 7. The first set of slope data measured on 17.10.2010 shows an alongshore pattern of increasing slope from transect 9.20 to 10.0. This foreshore steepening coincides with measurements taken on 20.10.2010 at the NW beach: steeper beach slopes were measured from 3.80 to 4.02 and from 4.80 to 5.20, but between 4.20 and 4.60 the slope was flatter than previous measurements. This alongshore pattern of increasing steepness must similarly be a product of the strong winds noted during this period of the fieldwork, in combination with the presence of a trough feature. In Figure 3.13 (page 46) the top of the berm as measured on 17.10.2010 includes measurements of the barchan-type dunes which were also present on this beach, as they were on the NW beach at the same time. This produces a 'bumpy' surface on the berm and indicates that accretion was taking place on the upper foreshore. Additionally, the trough feature mentioned in the previous section is noticeable between transects 9.60 to 10.0 and contributes to the steepness of the slope at these transects. After the stormy period, the trough has disappeared from the profiles and there is a generally flatter foreshore.

Slope values of these transects on 24.10 and 30.10 are similar to transects 4.60 to 5.20 on the 25.10 and 01.11, suggesting that similar processes are underway at each location that act to re-equilibrate the foreshore slope following the stormy weather.

Generally speaking, the average slope values per transect are more similar to each other than at the NW beach. Unlike the NW beach, however, the slope of the backshore for this beach was not calculated due to the depression in the surface.

Table 7: Foreshore slope results

Foreshore slope results: 9 to 10					
	9.2	**9.4**	**9.6**	**9.8**	**10**
17.10.2010	-0.013	-0.014	-0.016	-0.019	-0.021
24.10.2010	-0.015	-0.014	-0.017	-0.015	-0.015
30.10.2010	-0.016	-0.011	-0.014	-0.014	-0.013
Average	-0.015	-0.013	-0.016	-0.016	-0.016

3.6. Cut and Fill

3.6.1. Transects 3.60 to 5.20

Figure 3.17 is a raster derived from the subtraction of one DEM surface from another in the GIS program ArcGIS. The result shows where the second DEM surface differs from the first: in this case the diagram shows how the surface of the beach has changed between the start and the end of the fieldwork campaign using DEMs of measurements taken on 24.09.2010 and 01.11.2010. The "cut" function identifies areas where the second surface has been eroded compared to the first, while the "fill" function identifies areas in the second surface that have accumulated volume. The two DEMs thus act as the "before and after" with the resulting raster providing both volume change data and spatial information. The net volume change data is presented in Table 8.

Overall there is a widespread pattern of erosion interspersed with areas of accretion, with almost no areas remaining unchanged since the beginning of the campaign. The volume eroded over this period is calculated as 99,250 m^3 while the accretion is only 26,750 m^3, meaning that there was a total loss calculated at -72,500 m^3 during this period.

By visually examining the diagram of accretion and erosion, it is possible to suggest that there is a higher proportion of accumulation on the eastern side of the beach (profiles 4.40 to 5.20) than the west (3.60 to 4.20). In order to further examine the spatial trend of loss and gain over the beach surface, the entire area was subdivided into profile sections for individual study.

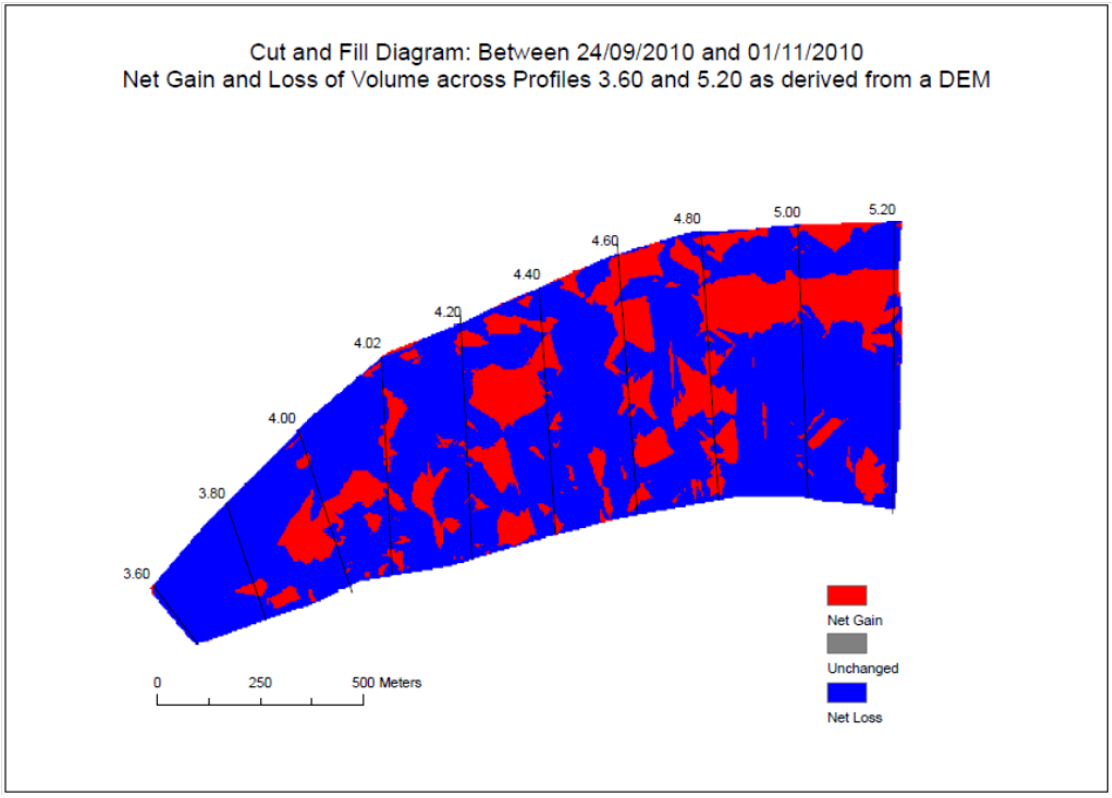

Figure 3.17: A "cut and fill" diagram derived from two DEM surfaces, indicating the spatial trend of gains and losses in volume between 24.09.2010 and 01.11.2010.

Table 8: Net volume change between 24/09/2010 and 01/11/2010 as derived using the "cut and fill" functionality of ArcGIS.

Net gain (m^3)	Net loss (m^3)	Total (m^3)
26,750	99,250	-72,500

The original DEMs were divided into profile sections where the profile transect runs through the middle of each section, i.e. the section for profile 3.80 covers half the distance to 3.60 and 4.00. The same cut and fill operation was conducted for each section and the results presented in terms of both volume and area involved. The volumes involved in the cut and fill are presented along with the net budget per section (cut volume subtracted from fill volume), and additionally the areas designated as cut and fill are also presented. The relative proportion of cut vs. fill per section is provided in Figure 3.18 and Figure 3.19, whereby the volume (area) change is displayed as a percentage of the total.

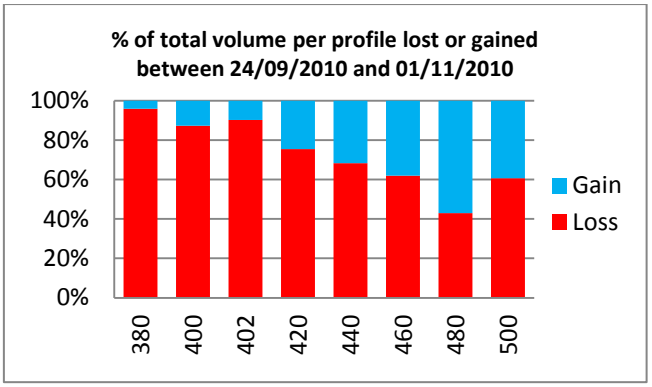

Figure 3.18 Gains and losses of volume per profile section are presented as a percentage of the total volume change of the beach (not total beach volume).

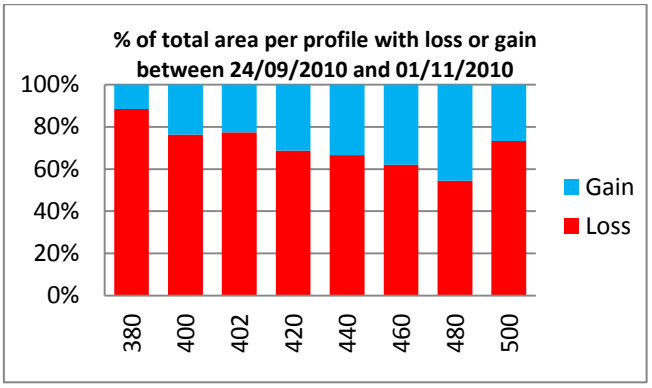

Figure 3.19 Areas of gain and loss per profile section are proportionally represented as a percentage of the total area per section.

The results confirm the suggestion that there is more accumulation on the beach in the eastern side than there is in the west, as seen in the increased relative proportion of gain compared with loss in sections 4.40 and 4.80.

Further, the change of volume related to surface area for each section has been calculated by dividing the total volume (either loss or gain) by the surface area. The results are shown in Table 9. The volume related to surface area (depth) ranges from 0.06 m to 0.24 m, which indicates that the degree of change is larger than the error associated with the DGPS.

Average depth, or volume related to surface area, for volume loss decreases with distance from the inlet, while average depth of volume gains increases with distance from the inlet.

Table 9: Average volume change related to surface area (estimation of depth of accretion and erosion), transects 3.80 to 5.00.

	Loss (m)	Gain(m)	Net Difference (m)
3.80	0.24	0.08	-0.16
4.00	0.19	0.09	-0.10
4.02	0.18	0.07	-0.11
4.20	0.11	0.08	-0.03
4.40	0.08	0.22	+0.14
4.60	0.07	0.07	0
4.80	0.06	0.09	+0.03
5.00	0.09	0.15	+0.06

Based on the previous figures, and in particular Figure 3.17, it is possible to see that most accumulation of sand occurred above the high water level in the zone that forms the berm. During the campaign, decimetre-scale barchan-type dunes formed on the upper foreshore, above the highest water level, during periods of extreme wind speeds and increased aeolian activity. It is highly likely that the widespread change (loss and gain) observed across the beach is due to these high wind speed events which caused much movement of sand and accumulation in certain areas depending on wind direction. Wind from the south and south-west accumulates sand in the berm and foreshore, while northerly winds transport sand towards the foredunes. Aeolian activity from the north and north-west contributes to the increased depth of sediment accumulating in the east compared with the west, which is also reflected in the deeper erosion on the westernmost, inlet side.

3.6.2. Transects 9.20 to 10.0

The cut and fill analysis was applied to the DEM surfaces representing profiles 9.20 to 10.0 of the control beach, using data collected on 17.10.2010 and 30.10.2010. The result can be seen in Figure 3.20.

A visual check of the diagram indicates that between these two dates there is very little surface of the beach that has remained unchanged. There is widespread net gain, or accumulation, which seems to concentrate on the backshore area. Observations during fieldwork noted an increase in sediment accumulation at the dunes after 24/10/2010, which corroborates with the accretion trend shown in this figure. Net loss is evident mostly on the foreshore, and is interspersed with areas of net gain, which matches with the results from volume calculations. Four profile sections were analysed and the results presented in Figure 3.21.

The average volume lost and gained as a layer between the surfaces is estimated and presented in Table 11. The volume of loss over the surface area averages more volume than that which is gained. Comparably more volume is lost and gained in sections 9.60 and 9.80, with the smallest change occurring in 9.20.

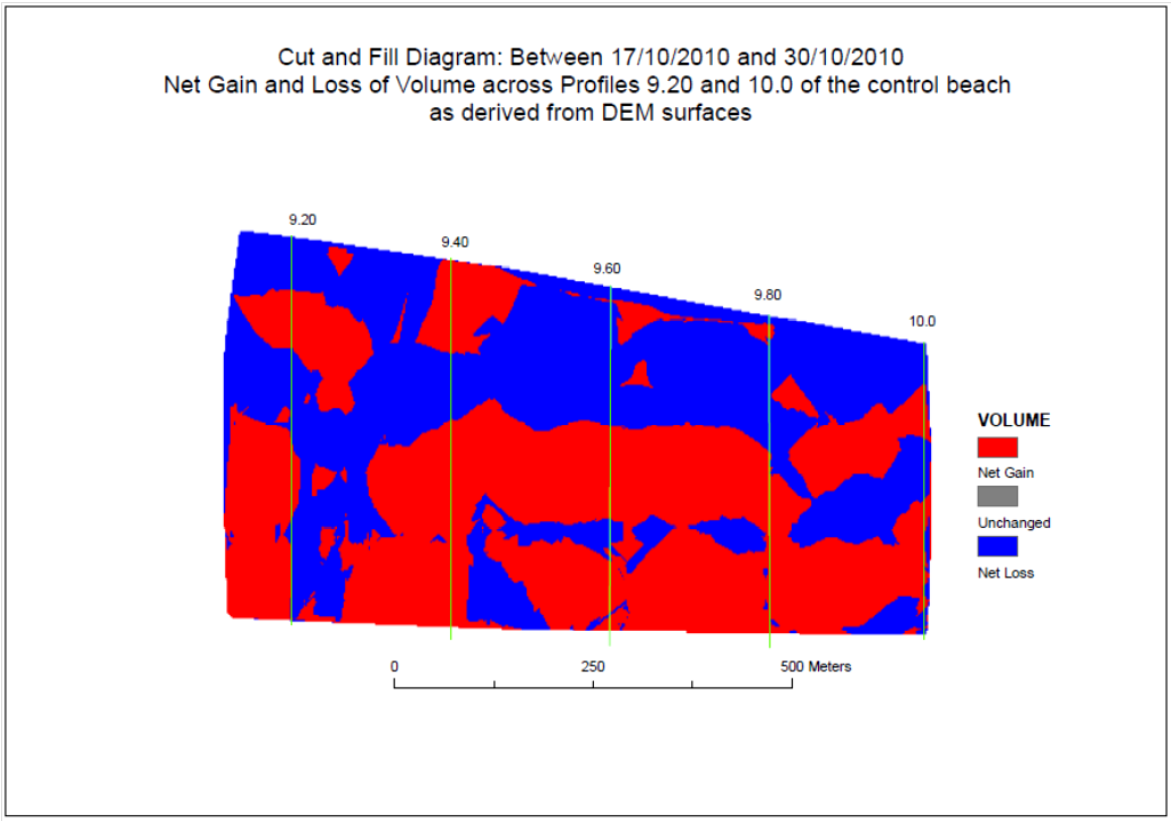

Figure 3.20: A "cut and fill" diagram derived from two DEM surfaces, indicating the spatial trend of gains and losses in volume of the control section between 17.10.2010 and 30.10.2010.

Table 10: Volume and area statistics based on cut and fill analysis of DEMs for 17.10.2010 and 30.10.2010

Volume of Net Gain m^3	**Volume of Net Loss m^3**	**Total m^3**
16,100	21,600	-5,470
Area of Net Gain m^2	**Area of Net Loss m^2**	**Total Area m^2**
181,500	152,400	333,900

Table 11: Average volume change related to surface area (estimation of depth of accretion and erosion), transects 9.20 to 9.80.

	Loss (m)	**Gain (m)**	**Net Difference (m)**
9.20	0.09	0.06	-0.03
9.40	0.16	0.09	-0.07
9.60	0.17	0.10	-0.07
9.80	0.17	0.10	-0.07

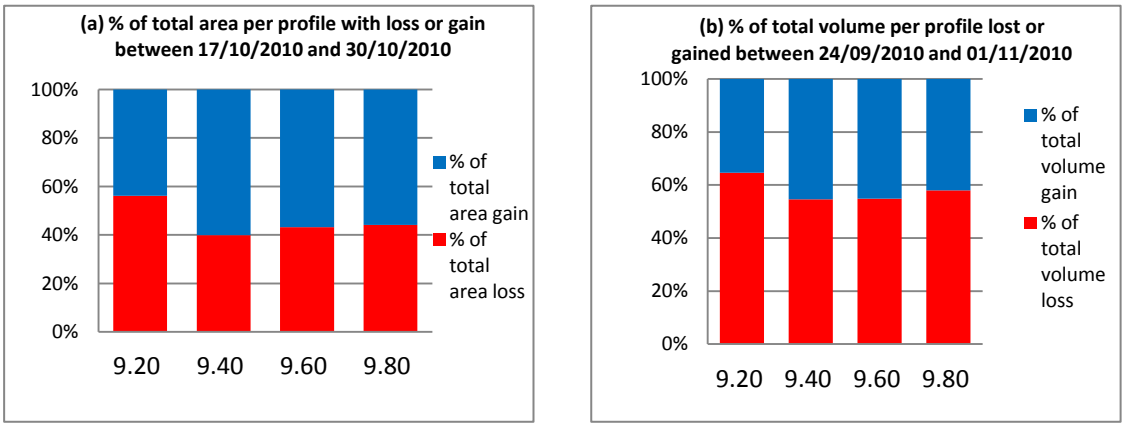

Figure 3.21 Gains and losses: (a) volume per profile section as a percentage of the total volume change of the beach; (b) area gain and loss per section proportionally represented as a percentage of the total area per section.

Figure 3.21 (a, b) shows a more balanced proportion of erosion and accumulation across the control beach, but ultimately the net budget is negative. Interestingly, while there is higher net loss than net gain there is also a greater area involved in accumulation than there is with erosion, as seen in Table 11.

3.7. Summary of Short-Term Data

The morphology data collected during fieldwork has shown several short-term trends. At the near-field beach, transects 3.80 to 5.20, there exists an alongshore pattern of erosion and steep foreshore slope nearest the inlet that changes to accretion at the more easterly transects. Overall there is a landward-directed trend in profile position for transects 3.80 to 4.20, while the trend at 4.40 to 5.20 is less clear. Profile changes that occur due to the phase of the tide, in combination with storm events, means that it is difficult to derive a clear trend from these transects. A division was found either side of transect 4.20: estimated net foreshore erosion of 9100 m^3 between 3.80 and 4.20, and net foreshore accretion of 12500 m^3 between 4.40 and 5.20. At transects 4.02 and 4.20, the beach is oriented SW-NE, meaning that incoming wave crests approach parallel to the shore. This can set up a divergent wave pattern that leads to a bifurcation in sediment transport, which may be enhancing erosion.

At the far-field beach, there was a trend of re-distribution of sediment throughout the profile where erosion was focused on the foreshore and accumulation on the backshore. A similar trend of accumulation at the foreshore occurred at both the near-field and far-field beaches on the 24th October 2010 (Julian day 297), coinciding with a storm event. In the days afterwards, both beaches show a recovery and landward shift of the profile again. Therefore, the shoreline response at both beaches can be similar during storm events, but otherwise there appears to be a different reaction taking place at each location. Additionally, the amount of erosion and accretion is more evenly balanced across the far-field beach than the near-field, with a small net loss of -5500 m^3 from the start to the end of the campaign.

4. Analysis of Long-Term Morphological Behaviour

4.1. Introduction

The long-term behaviour of the North Sea coast of Ameland can be interpreted by analysis of the trends in coastal profiles over a long time period. Moving up in scale from the short-term data, this analysis covers the same alongshore stretch of beach but instead examines the annual trends in 8 transects spaced one kilometre apart. The major perturbation to the shoreline is the attachment of a shoal from the ebb-tidal delta to the 'drumstick' head of Ameland, with the subsequent sediment dispersal and adjustment of the beach to this new feature. The large dimensions of the shoal means that it takes a number of decades for the entire feature to attach and disperse, thus it is necessary to examine the trends in beach morphology over a long decadal timescale. The data used for this analysis is freely-available Jarkus data which was collected, by various means, since 1965 to the present day by Rijkswaterstaat, the governing body in charge of maintaining and protecting the Dutch shoreline. The data is collected annually, but for the purposes of this project the analysis examines beach profiles over an interval of 1-3 years depending on the variability of the morphology.

This chapter will deal with the analysis of the morphological evolution of Ameland's North Sea coast, from 1965 to the present day. A summary of the morphological developments of the inlet and adjacent coast are presented first, to give an impression of the association of inlet dynamics with the downdrift beach. This summary draws its main points from the study by Israel and Dunsbergen (1999). The main analysis begins with the most basic beach property, beach width development, and is followed by the presentation of beach volume results. Lastly, consideration is made for dune development with respect to morphology changes on the beach.

4.2. Summary of Morphological Development: 1965-2010

This summary adopts the phase system proposed by Israel and Dunsbergen (1999) which describes the so-called cyclical dynamics of the Ameland Inlet. Previously discussed in Chapter 1.4 (page 6), the figure depicting each phase of the 'cycle' is Figure 1.7, found on page 8.

4.2.1. Phase A: 1965 to 1979 – pre-attachment phase

According to the research conducted by Israel and Dunsbergen (1999), phase A of the inlet development involves a clockwise migration of the main Borndiep channel, which erodes sections of the ebb delta and increases flow through the Akkepollegat channel. The significance of this stage is the proposed erosion of the ebb delta releasing sand from storage that can be transported with the tidal currents. Ultimately, due to the combined tidal currents and predominant north-westerly wave direction, sand accumulates on the eastern side of the ebb delta and forms a broad shoal.

The rapid changes in morphology during this phase are recorded in the bathymetry dataset. In the bathymetry map of 1971 (Figure 4.1) the shoal approaches the shoreline from the eastern ebb delta with an almost E-W orientation, while its eastern edge shows dispersal towards the

shoreline and attachment around transect 5. By 1975 (Figure 4.2), re-working of the sediments by waves causes the shoal to align with the curved shoreline in a SW-NE orientation.

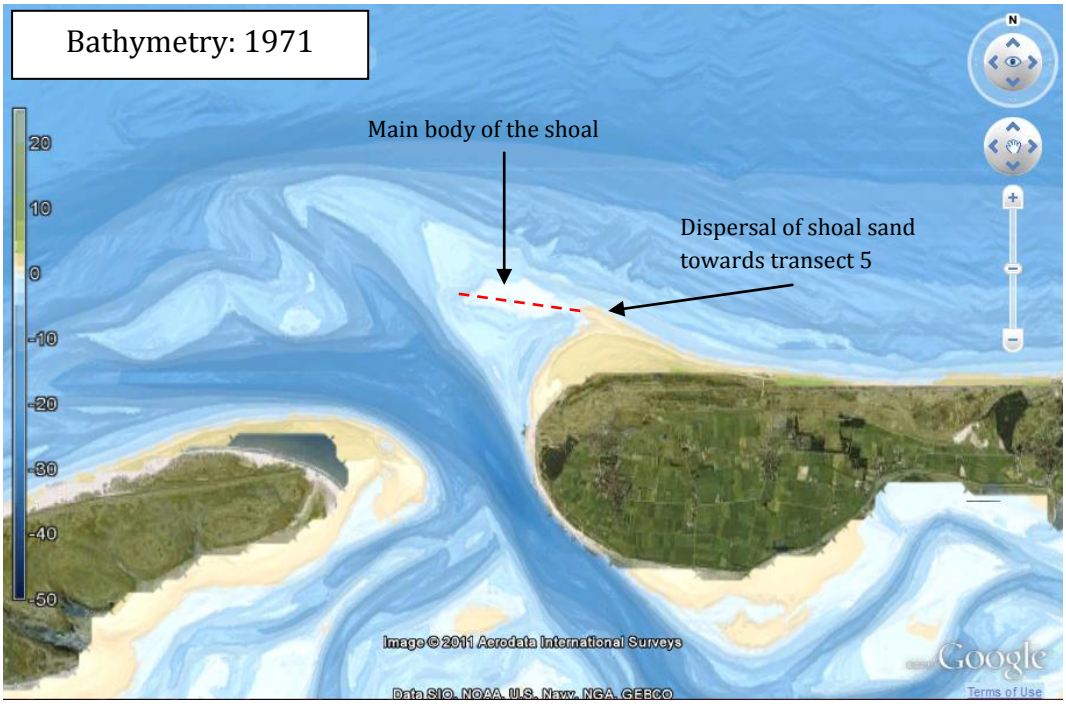

Figure 4.1: Bathymetry map of 1971: The shoal is visible as a shallower area to the north-west of the beach; the main ebb channel is the Westgat.

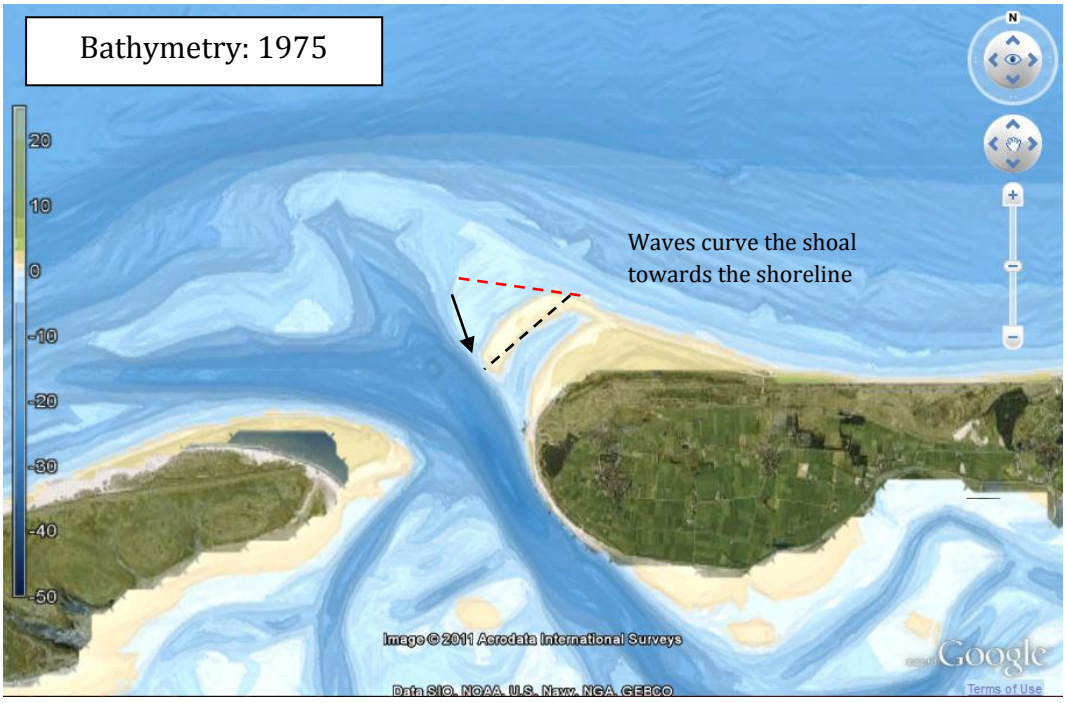

Figure 4.2: Bathymetry map of 1975: the shoal is re-shaped by waves as it nears the shoreline, becoming more elongated and curved in form; the main ebb channel remains the Westgat while the Boschgat becomes deeper and more smoothly connected to the Borndiep.

4.2.2. Phase B: 1980-1992 – shoal attachment and dispersal

In relation to Ameland's northern coastline, the main morphologic event taking place during this phase is the attachment of the ebb delta shoal to the shoreline (Figure 4.3). This is achieved through a combination of wave action and tidal flow that acts to push the shoal towards and along the shoreline. Other significant but less relevant events, from a beach morphology perspective, occur as the inlet undergoes a gradual transition from the initial single ebb channel orientation to a two-channel orientation. The two channels drain the east and west sides of the tidal basin. This change in channel formation and flow pushes the Borndiep closer to the western edge of Ameland, causing localised erosion to the beach (Israel and Dunsbergen, 1999).

In this phase the shoal will migrate to and join with the rest of the shoreline, contributing its volume to the beach and the island as a whole (Figure 4.4). One of this research's main objectives is to quantify the volume that is added to the beach during this phase. Further, the evolution of this volume of sand through time is quantified in terms of its dispersion throughout the coastal zone (within the boundaries of the data). While it is expected that the majority of significant morphologic change will occur at transects 3 and 4, the downdrift locations at transects 5, 6, 7 and beyond may also begin to show signs of accretion or erosion depending on the influence of the shoal.

Figure 4.3 shows an area of deeper water located immediately between the shoal and the beach, which did not appear in the map of 1975 (Figure 4.2). Further, the shape of the shoal appears disintegrated when compared with the previous 1975 map.

Figure 4.3: Bathymetry map of 1981: The shoal merges with the shoreline and begins to disperse, while the main ebb flow switches from the Westgat in the west, to the Akkepollegat in the north.

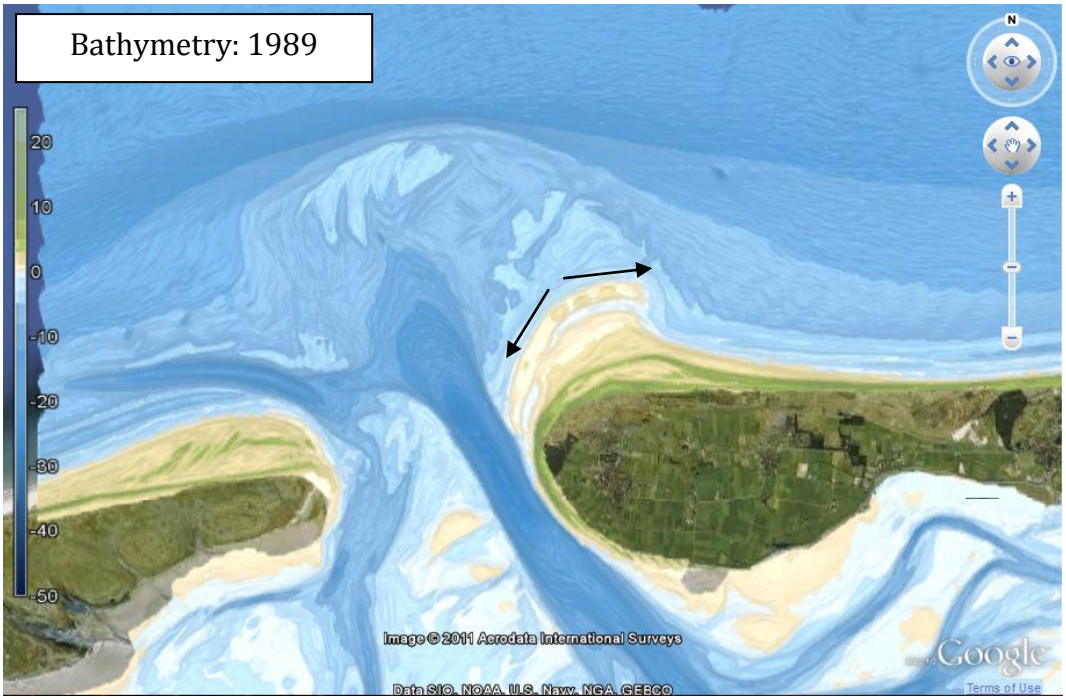

Figure 4.4: Bathymetry 1989: The newly-attaching shoal is dispersed in the alongshore direction towards both the inlet and downdrift; the two-channel situation exists in the inlet.

4.2.3. Phase C: 1993-2004 – coastal dispersal

By phase C, the orientation of the Borndiep reaches a critical point with tidal flow that it breaches the Koffieboonplaat dividing the two ebb channels and re-forming the connection with the Westgat (as seen in Figure 4.5). As flow is increased through the Westgat, the Akkepollegat flow is reduced and this allows for the reformation of the previously-separated ebb delta (dominant diverging flow through the Akkepollegat divided the ebb delta across the shoal). Sedimentation at the delta toe, enabled by the ebb flow, causes an increase in delta bed level. The eastern delta builds at depths greater than -5 metres NAP, where wave action is as yet unable to form shoals. Figure 4.6 and Figure 4.7 show the increasing bed level of the ebb delta between the years 1996 and 2002, indicating that rapid sedimentation takes place during this phase.

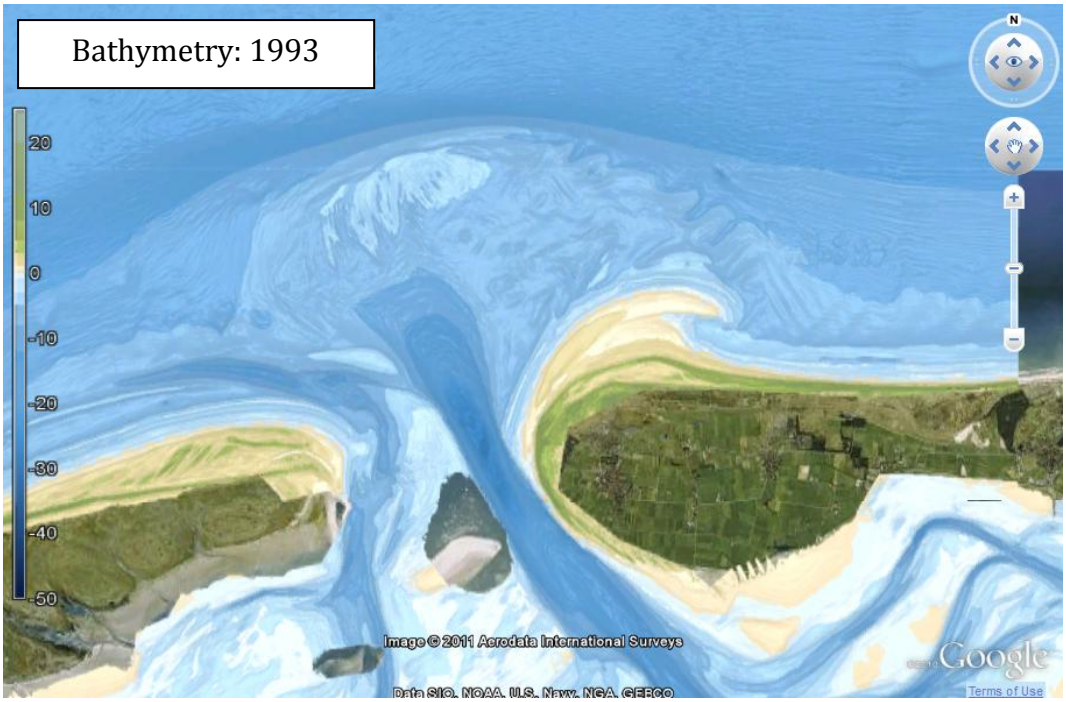

Figure 4.5: Bathymetry map of 1993 - The attachment shoal is flattened against the western shoreline as the Borndiep rotates to a northerly orientation, while the eastern end of the shoal arches eastward along the coast.

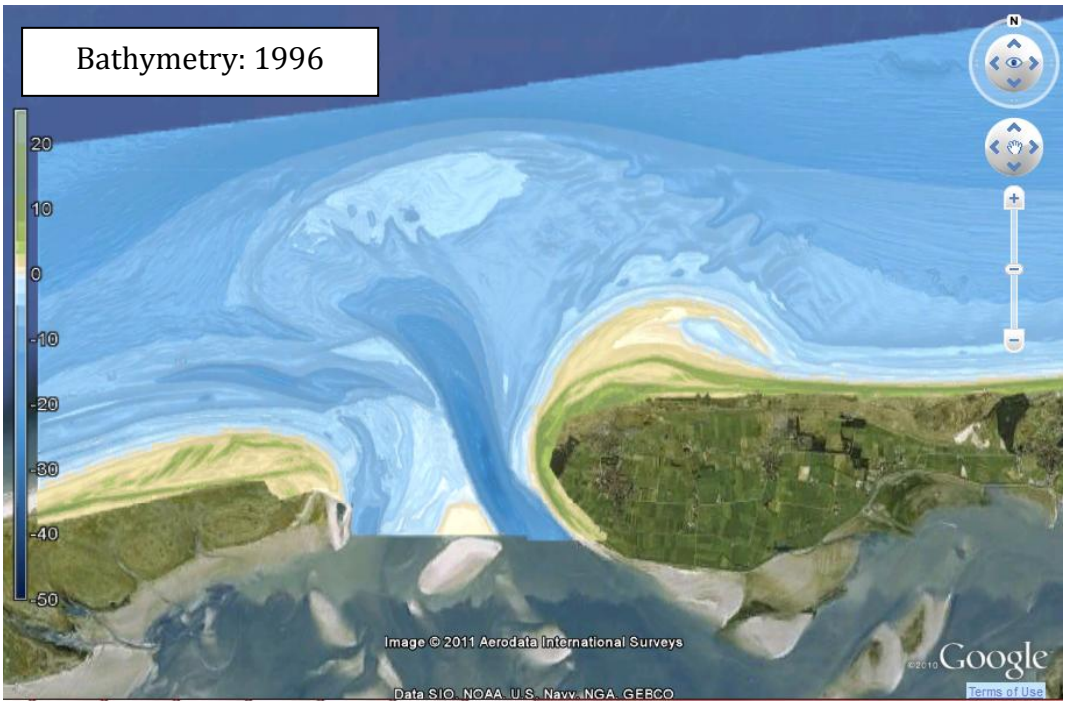

Figure 4.6: Bathymetry map of 1996 - The eastern side of the shoal is curved alongshore and toward the coastline under the influence of both wave- and tidally-driven forces; the Akkepollegat deposits sediment at the ebb delta toe.

Figure 4.7: Bathymetry map of 2002 – a tidal lagoon is created between the former shoal and the beach, while sedimentation occurs across the whole ebb delta causing the bed level to rise.

4.2.4. Phase D: 2005– to present – sand wave propagation

In the final phase of the four proposed stages of the Ameland Inlet development, a single-channel morphology develops in the inlet throat that directly connects the main Borndiep channel to the Westgat. The Borndiep increases its efficiency by straightening its connection to the Westgat, and in doing so erodes the westerly beaches of Ameland. Continued accumulation on the easterly ebb delta permits its building upwards to a critical height, after which shoals are able to form and ultimately migrate towards the northwest coast. By this point the cycle has once again reached the initial phase A configuration and a full cycle is complete. The bathymetry map of Figure 4.8 does not yet show the same configuration as the initial phase A, suggesting that if the cycle were to begin anew then further developments that strengthen the Borndiep connection to the Westgat are taking place.

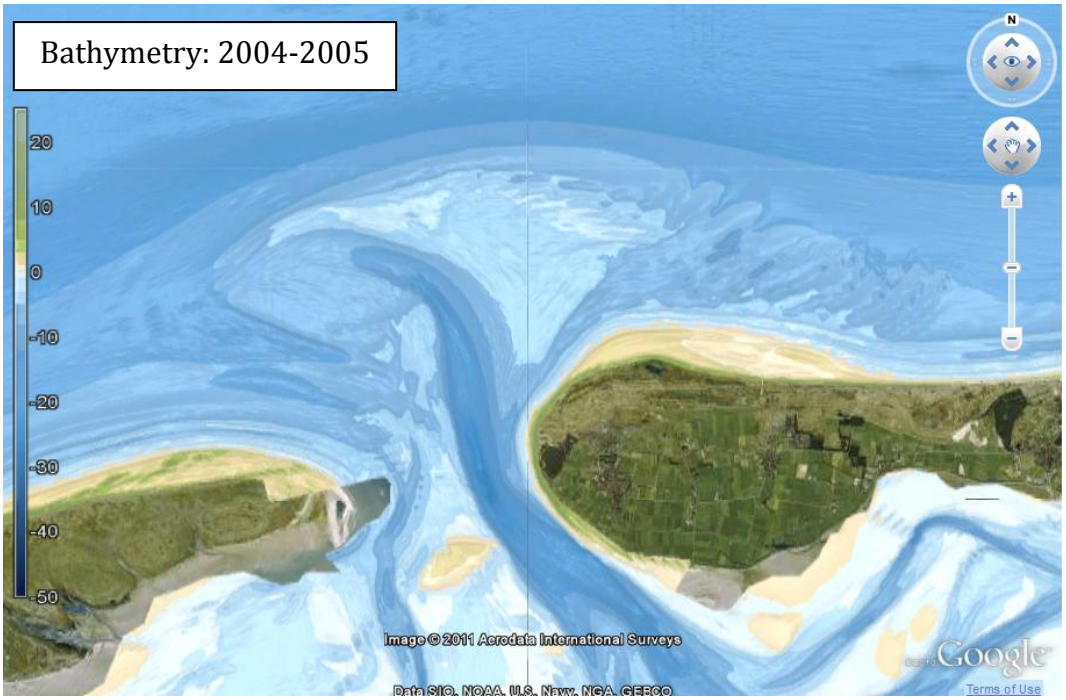

Figure 4.8: Bathymetry map for 2004-2005 - The former shoal is almost completely incorporated into the beach and is being dispersed towards the southwest and east by sediment transport in a bifurcating pattern from the north-west.

4.3. Long-Term Behaviour of Beach Width

For the purposes of this study, beach width has been calculated as the distance between two points in each profile: the dune foot (in most profiles this is chosen as +3 metres NAP) and the estimated high tide position (+1 metre NAP), as indicated by the HWM. The horizontal distance between these two points results in an estimated beach width for a certain year. The results are presented in a set of graphs, each depicting the evolution of the position of dune foot and high water per year and per transect, i.e. the first year of the record has dune foot position at 0, with subsequent deviations recorded as the difference from 0 (likewise for estimated high tide position).

Due to the amount of variation in beach widths and the explanation required, the transects will be discussed individually, beginning with those nearest to the inlet (see Figure 2.1; page 28).

4.3.1. Transects 3 and 4

The seemingly chaotic pattern of beach width seen in transects 3 and 4, with large fluctuations occurring throughout the period 1965-2010, is a product of the complicated migration, attachment and subsequent dispersal of the 1980s Bornrif shoal. In the beginning of the period, these transects display similar patterns of beach width reduction as the position of the high tide mark moves inland. The beach at transect 4 responds slower to erosion than transect 3, as beach width at 4 remains around 800 metres for the period 1968-1979, while ongoing erosion at 3 reduces beach width by 400 metres in the same period. By 1980, with the approach and

attachment of the shoal and associated wave-sheltering reducing wave-driven erosion on the beach, the width of the beach increases (Figure 4.3; page 62).

The presence of a deep area from 1981-1985 prevents the shoal from migrating onshore at transect 3 until 1986, after which beach width increases to its widest (≈800 m) in 1990. The fluctuating pattern seen in both transects 3 and 4 is due to this staggered migration and attachment phase, resulting in a similar pattern but occurring in different years, for example the deep region in the nearshore at transect 3 (Figure 4.3; page 62) does not appear in the profile of transect 4 so the shoal attaches earlier here than at transect 3, hence transect 3 maximum width is lagged behind transect 4 as the deep region closes.

Subsequent dispersal of the shoal sand is producing fluctuating beach widths as there is a point when the beach appears quite flat and it is difficult to discern a high tide position. This is particularly true for the period 1982-1987 for transect 4, where large fluctuations in beach width come about through the rapidly changing (eroding, adjusting) morphology following the shoal attachment phase.

The maximum beach width occurs in 1990 for transect 3 (832 m) and in 1992 for transect 4 (1123 m), which coincides with the full attachment of the shoal to the beach. The sand from the shoal is also dispersed vertically, but landward, in the profile which sees a raising of the beach level and an increased apparent width, despite the fact that the shoal/beach is eroding and shoreline moving landward. Thus, this maximum beach width is an ephemeral occurrence, lasting no longer than the time it takes to erode the shoreline which, according to the data, is around 4-8 years for transects 3 and 4 respectively.

In terms of erosion rate, this means that between 1990 and 1994 the high water position at transect 3 retreated landwards at a rate of about 150 m/year. Similarly, between 1992 and 2000 the high water position at transect 4 retreated landward by approximately 70 m/year. In the years since, the erosion rate has averaged 15 m/year and 8-9 m/year for 3 and 4 respectively. The extreme erosion at transect 3 is reflected in the very close lines of HWM and dune foot in the graph. The future of the beach and dunes at these transects is precarious if erosion continues at this rate, however planned beach nourishments at these locations may slow the decline in beach width, although temporarily.

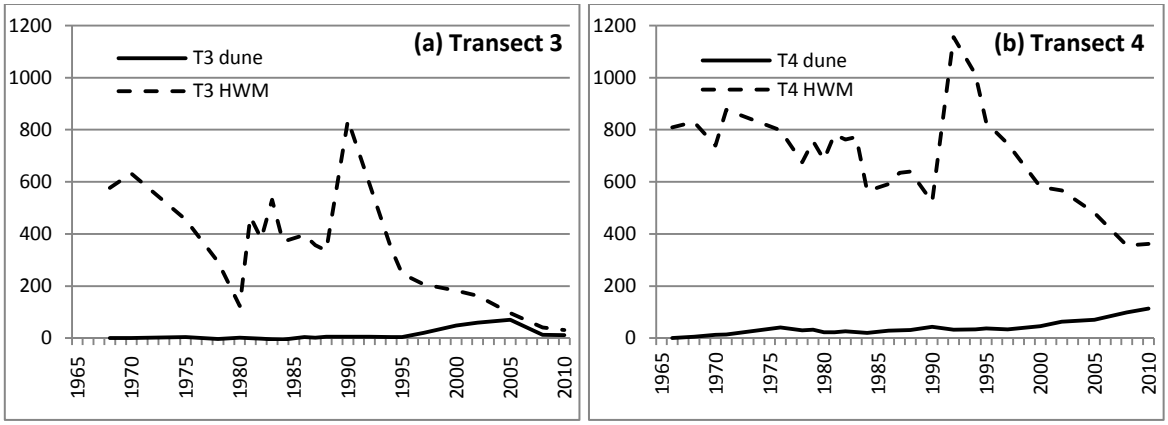

Figure 4.9 HWM and dune foot position through time, (a) Transect 3, (b) Transect 4.

4.3.2. Transects 5 and 6

Transect 5 has a muted response in comparison to transects 3 and 4, although there are similarities with transect 4. Prior to the shoal attachment, the beach widens with an increase of volume presumably derived from the shoal and alongshore dispersal. By 1984 this accretion trend changes to erosion as the HWM retreats landward at a rate of 15 m/yr, until 1989 when this trend is suddenly reversed as the shoal is dispersed towards transect 5. The overall response is one of accretion and beach widening, and the net gain in width over this period is around 400 metres.

The two transects 5 and 6 have markedly similar profiles, despite the fact that transect 6 undergoes a different development to transect 5.

Between 1983 and 1988, the level of the beach at transect 6 gains 0.5-0.7 metres elevation, and between 1986-1988 the HWM migrates rapidly landward by 50 metres. A 2-metre high berm-like feature develops on the foreshore in the intervening period, suggesting that sand being eroded is transported up the foreshore as well as downdrift. These dynamic changes to the beach precede the downdrift migration of the shoal, which appears suddenly in the profile of transect 6 in 1992.

Transect 5 maximum beach width occurs in 2002, extending 675 metres from the dune foot. Likewise, transect 6 is at its widest in 2006 when the beach width reached over 770 metres from the dune foot. In both transects the peak width appears suddenly but decreases slowly, and is seen to increase again slightly in the last few years.

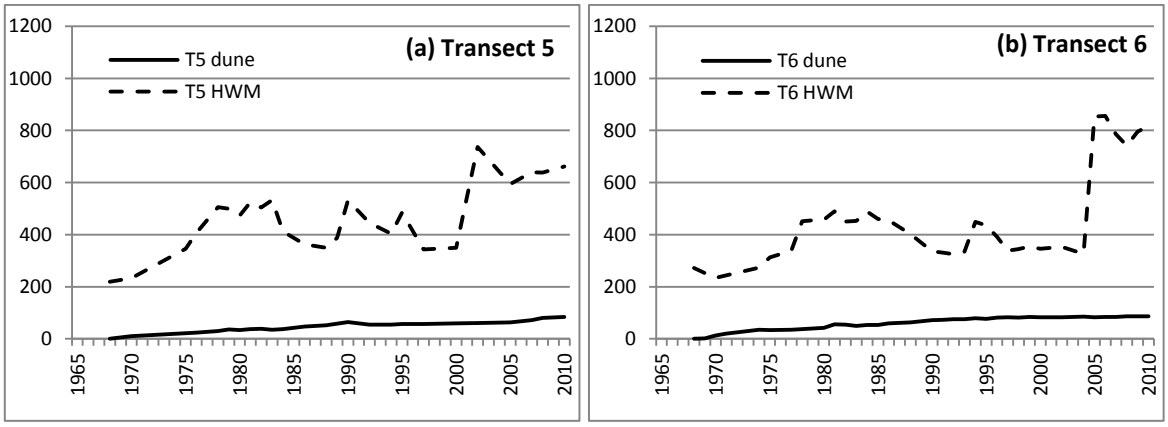

Figure 4.10 HWM and dune foot position through time, (a) Transect 5, (b) Transect 6.

4.3.3. Transects 7 to 10

The transects in the most distant part of the study area from the inlet each display their own variability, similar to each other but significantly time-lagged. To begin with, transect 7 had a complicated history involving a tidal channel which means that it doesn't follow the pattern of the other transects.

From the start of the record transect 7 is accreting, with beach width increasing year on year and dune foot position moving seawards. Little change occurs in the beach width between 1967

and 1975, however between 1975 and 1979 the HWM migrates seaward at a rate of 20 m/year; between 1979-1980 the HWM shifts position by another 70 metres seaward. This sudden short-term increase in beach width occurs in association with accretion on the foreshore of the profile, which is disturbed by large fluctuations in the submerged lower profile leading up to 1980. The HWM then remains steady for several years with slight fluctuations. By 1986 however the trend is reversed and the HWM retreats landward; 35 m/year from 1986 to 1988, which is comparable to the accretion trend of 1979-80. Between 1994 and 1996 the attachment shoal/spit appears in the lower foreshore of the profile, existing around -2 to 0 m NAP.

The declining trend of beach width is a reflection of the interaction between the attachment shoal dispersing as a spit across the foreshore, creating a tidal lagoon feature that fronts the beach. Continued dispersal of the spit closes the distance between it and the beach. Erosion of the beach at transect 7 could therefore be a result of tidal forces acting within an increasingly smaller lagoon entrance, causing the erosion of the beach and possibly the spit before it connects to the beach itself.

Transects 8, 9 and 10 have a somewhat less complicated history, as seen in the graphs as a fairly straightforward pattern of stable coastal position until the passage of the sand wave in a time-lagged manner. Beach nourishment took place along this stretch of coastline (transects 7 -10 and beyond) in 1996, which is clearly seen in the trend as a sudden jump in HWM and dune position. The HWM suddenly migrates seaward by approximately 60 metres from the pre-nourishment position of transects 8 to 10. The efficacy of the nourishment is seen, however, in the decrease of beach width once again in the following 2-3 years, but it stops short of returning to the pre-nourishment situation.

There are, however, smaller events that cause an increase in the beach width. The period between 1980 and 1995 sees a gradual increase and decrease in beach width at transect 8 which does not cause an associated migration in dune position (other than long-term trend), as seen in the nourishment with a change in dune position (Figure 4.11 [b]). The fact that the dune remains more or less the same indicates that it is the beach that is increasing width for several years, before returning to the previous shoreline width. The same feature can be seen in transect 9 and, to a lesser degree, transect 10 between the years 1985-1995, likewise in transect 7 from 1975 to 1995 (Figure 4.11 [a-d]). The same time-lagged response, similar to the passage of the sand wave, suggests that this feature is also a sand wave-type feature migrating downdrift.

There are two plausible reasons as to the origin of this smaller sand wave: either it is the remnant of a small shoal that migrated from the eastern ebb delta at an earlier time (before the record), or it is the result of dispersal following a beach nourishment. According to Cheung et al (2007), sand mining of the shoal took place in 1979 and 1980 whereby 2.5 Mm^3 of sand was removed and replaced elsewhere (0.2 Mm^3 south of the bar; 2.2 Mm^3 downdrift). The suggestion is that the smaller sand wave event seen propagating alongshore, preceding the main sand wave event, is a portion of this displaced sand.

Dividing 2.2 Mm^3 by 3000 m (estimated alongshore distance of the shoreline from transect 5 to 8) shows that the total dispersed volume of this sand spread across the 3 km stretch of the beach, would equal roughly 730 m^3 per metre width. A check of the cross-sectional volume at each transect shows that the jump in volume following 1980 equals around 400-600 m^3. It wouldn't be unreasonable to make the connection between this beach nourishment derived

from sand mining the shoal, and the small sand wave seen in the profiles of transects 6-8 from 1980 onwards.

The maximum beach width reached at each transect varies considerably, affected by increased longshore drift and the passage of the sand wave. Transect 7 reaches its maximum before the eastern transects, peaking in 1985 with a width of ≈370 metres from the dune foot. It is only by 2004 that transect 8 reaches its maximum width (750 metres), hinting at the slow rate of longshore drift in addition to the complex wave-tidal interaction at the tidal channel on transects 6-7. Beach width at transect 8 remains narrow due to the forcing of the entry channel to the lagoon against the dune foot. When this channel closes, the maximum width of the beach is reached.

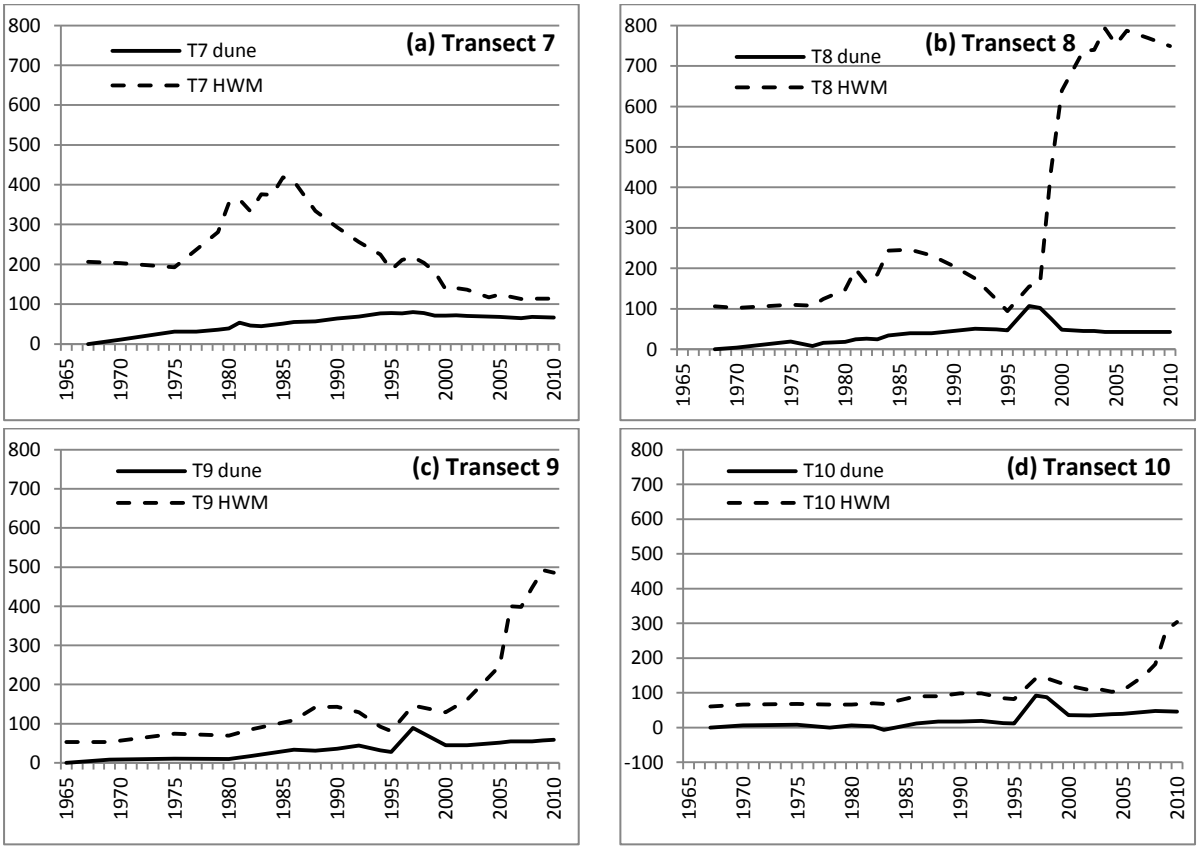

Figure 4.11 HWM and dune foot position through time, (a-d) Transects 7-10.

By this point it is possible to see that the sand wave is attenuating, or in other words, it is decreasing in cross-shore amplitude as it progresses alongshore. Figure 4.12 presents the range of beach widths that occur during the 45-year record, showing clearly the attenuation of the sand wave as it passes each transect. Transect 9 therefore may have already reached its maximum width, around 425 metres, or will reach it in the coming 2-3 years. Likewise for transect 10; the same pattern of suddenly increasing width suggests that its peak is due to occur sometime in the next 5-10 years. It is however difficult to estimate the rate of sand wave transport at this part of the coast, because the attachment shoal and tidal channel of the lagoon affected sand dispersal and the otherwise 'normal' response to the shoal. Figure 4.13 presents

the data of maximum beach width as a function of time, and shows the progression of peak beach width from one transect to the next. The lagoon feature disturbed the 'normal' trend by preventing the beach width at transect 7 from becoming wider, and thus causing the peak to occur much earlier than other transects.

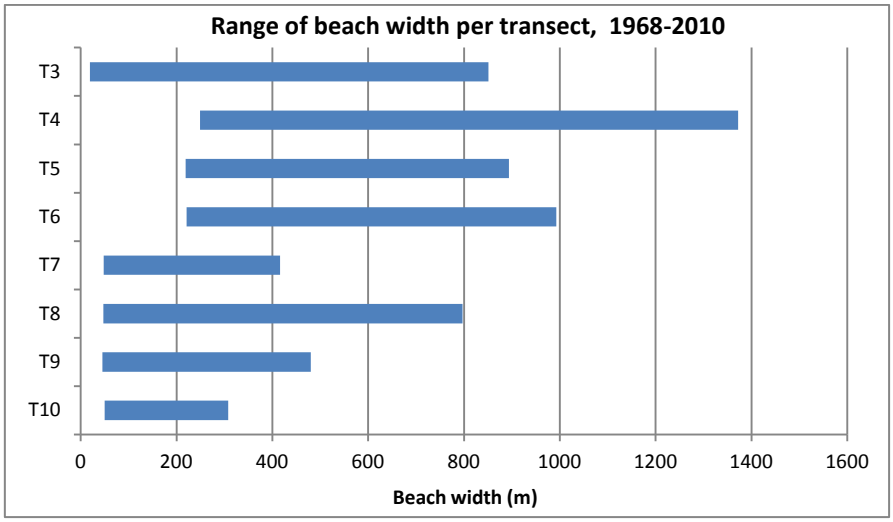

Figure 4.12: Range of beach width from 1968-2010 - the largest range occurs at transect 4, where the shoal attached to the beach, while transect 10 is yet to reach its maximum.

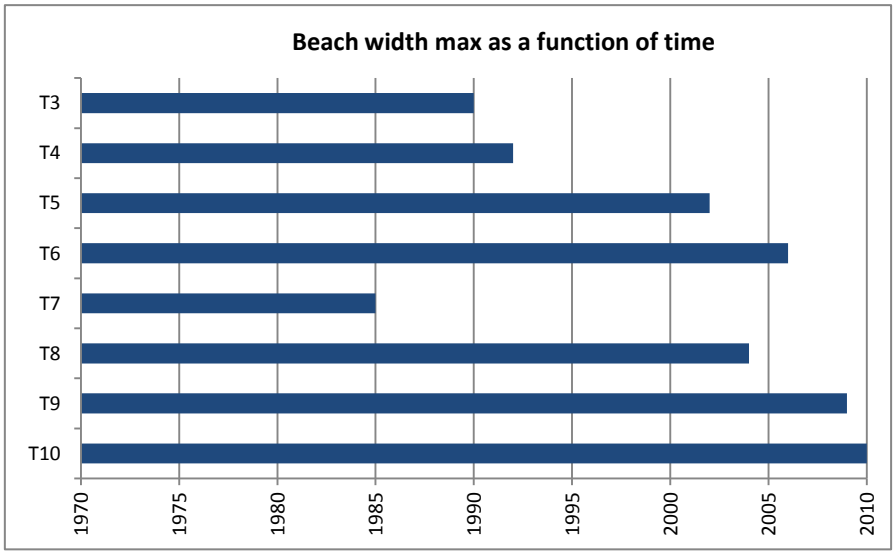

Figure 4.13: The maximum of beach width per transect as a function of time – the progression of the sand wave peak in beach width is interrupted at transect 7 due to the complicated situation of the shoal-spit and lagoon creation.

4.4. Long-Term Behaviour of Beach Volume

4.4.1. Transect 3

In the immediate period before the shoal attaches to the beach, a gradual increase in beach volume occurs for both transects 3 and 4 (Figure 4.14). The earliest data from before 1980 is limited in its seaward extent, so volume calculations during this period only relate to the volume between +2.5 m and -3 m NAP, indicated in the graphs as two separated parts of the volume line. It is, however, possible to see the trends of increasing volume despite the incompatibility with the rest of the data.

For transect 3 the volume peak occurs in 1982 with 8400 m^3, then the trend is a steady decline in the period following, to 680 m^3 in 2010. The decline in volume can be explained in three parts: 1981-1985, the presence of the deep nearshore region; 1986-1995, shoal attachment and dispersal; 1996-onwards, persistent erosion related to low ebb delta elevation.

Before the shoal attaches to the beach at transect 3, it is prevented from migrating by the presence of a 14 metre-deep region, possibly an offshoot from the Borndiep channel. Meanwhile the seaward-facing side of the shoal, the top of which is around +1 m NAP, undergoes rapid erosion due to its exposure to wave energy. Between 1982 and 1984, the shoal is reduced by 38% of its cross-sectional volume, decreasing from 4300 m^3 to 2650 m^3. The percentage net loss totals 18% and 20% (of the original 1982 volume) for 1983 and 1984 respectively.

By 1986 the deep nearshore region has been infilled and the shoal becomes almost fully part of the beach. In this second 'part' of the erosion trend, net loss from the beach as a whole averages around 400-600 m^3/m/yr at transect 3, for the period 1986-1995. This trend is clearly visible in the profiles as a rapid landward retreat of the foreshore, with an additional elevation increase. The top of the shoal in 1986 was just at 0 m NAP, while in 1992 the shoal remains visible as part of the beach but the 'top' is now at 1.6 m NAP and a distance of 900 m further landward than in 1986 (Figure 4.15).

From 1995 onwards the erosion trend levels out at around 200 m^3/m/year. Beach nourishment at transect 1 through to 3 (Rijkwaterstaat, 2006) in 2004 appears to make little difference to the overall erosion trend, and by 2008-2010 further erosion removes almost all the nourishment sand and erodes into the dune foot. To make a comparison with the beginning of the record in 1982, only 8% of the total beach-shoal volume remains at transect 3 in the present day (Figure 4.16).

Comparing the two trends of volume and width, a time lag exists between the peak of beach volume and that of beach width, whereby peak width occurs 8 years after the volume peak. This lagged response occurs because beach width is measured from the +1 m NAP position, and it takes 8 years for cross-shore sediment transport to transfer sediment from the lower foreshore towards the HWM. By the time beach width maximum is reached, the peak volume is already in decline with longshore transport processes dispersing the sediment alongshore.

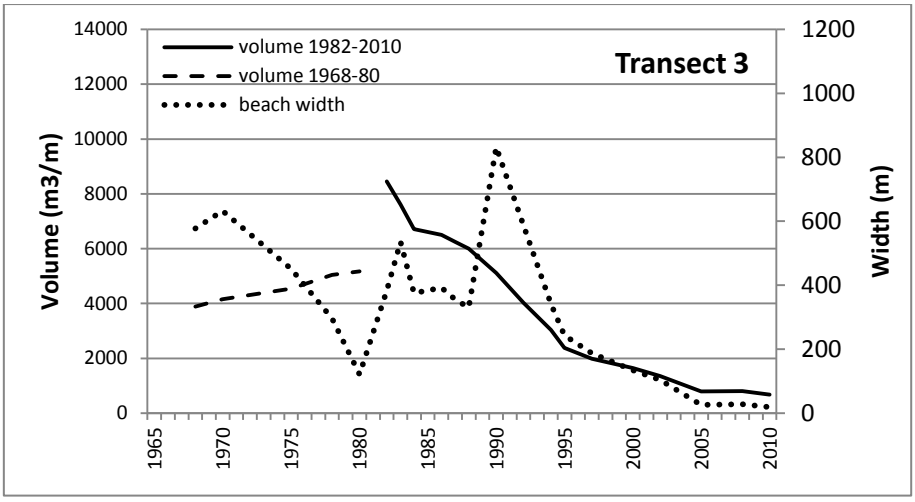

Figure 4.14 Beach volume and width through time for Transect 3 (N.B. the dashed line indicating volume from 1968-1980 is due to insufficient data for comparison with subsequent years).

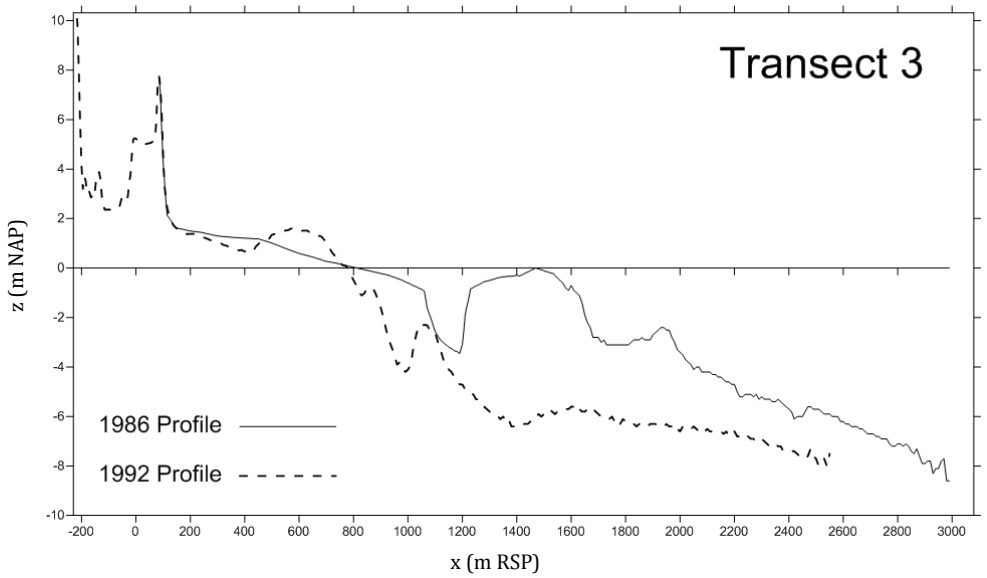

Figure 4.15: Cross-shore profiles of transect 3, during 1986 and 1992.

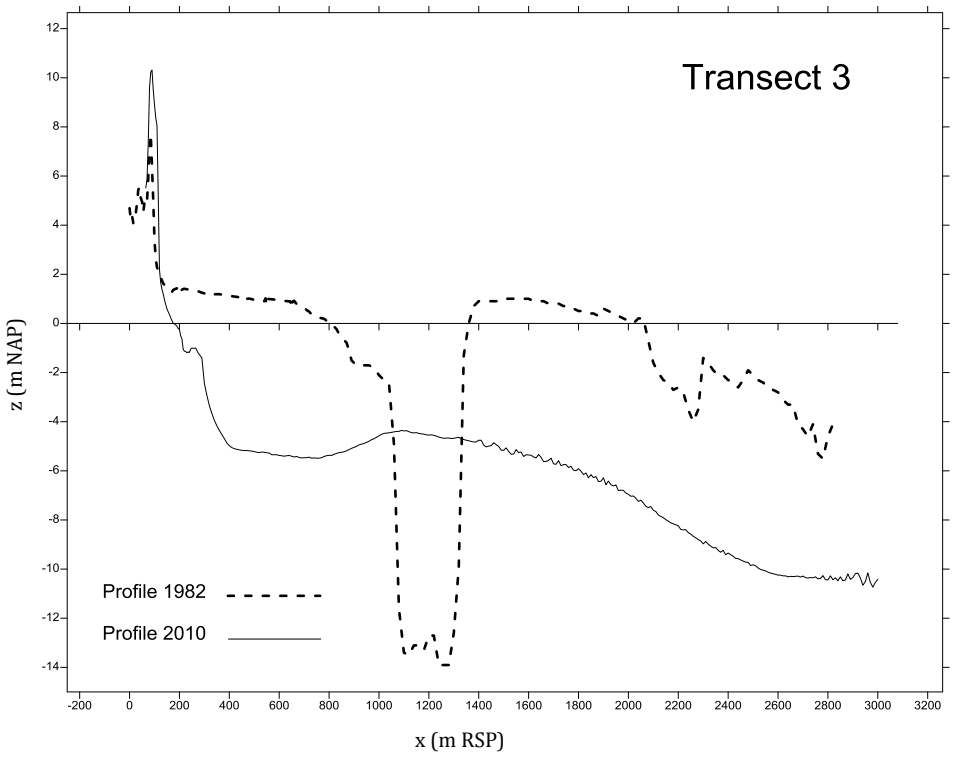

Figure 4.16: Cross-shore profiles of transect 3, comparing the bed levels during 1982 and 2010.

4.4.2. Transect 4

As indicated previously, the attaching shoal first connected with the beach in the area of transect 4 and likely did so at the very beginning of the Jarkus record (late 1960s). Beach width during the start of the record until 1982 remains stable at approximately 800 metres from the dune foot. The earliest records are limited in their seaward extent, but it is possible to see the shoal approaching and joining the beach between 1976 and 1979 (Figure 4.17). This leads into the increased volume seen in the following years, with peak volume occurring in 1984 with 9500 m^3. The volume added from the shoal at this transect is a little over 2000 m^3, between 1982 and 1984.

It is possible that errors in volume calculation appear during this period, however, as parts of the profile have not been sufficiently surveyed. This is probably due to the depth of the water being too deep for surveying by foot, but too shallow for a boat. Unfortunately this means that unnaturally straight sections of the profile appear and introduce unavoidable errors into the dataset. These sections are restricted to the area where the shoal is beginning to attach to the beach, so data is lost at this point but otherwise the profile is complete. This affects profiles from 1981, 1983, 1986, 1987, and 1988.

As most of the shoal isn't sufficiently surveyed for several years, it is difficult to tell when it fully attaches to the beach. The seaward side erodes during this time and the foreshore retreats landwards. From 1990 to 1995 the foreshore retreats by approximately 500 metres: as this is mostly below the +1 m NAP boundary it is not as clearly seen in the beach width measurements. Once again the erosion pattern of backwards retreat and upward building is seen in these profiles (Figure 4.18). The associated volume change is a loss of approximately 1500 m^3/m in this five-year period.

In the years following the merging of the shoal with the beach, there is a persistent net loss of cross-sectional volume that is approximately 400-500 m^3 per year until 2000, resulting in a loss of half of the volume of the beach as measured in 1984. In the last ten years, 2000-2010, the rate of erosion decreases slightly to around 200-300 m^3/m/year. The change in profile between 1980 and 2010 is shown in Figure 4.19.

The peak volume is achieved in the middle of the Jarkus record as the shoal merges fully with the beach. Consequently beach width maximum is lagged behind volume peak due to the volume held below the +1 m NAP boundary for width. Similar to transect 3, the time lag is also 8 years between peak volume and peak width.

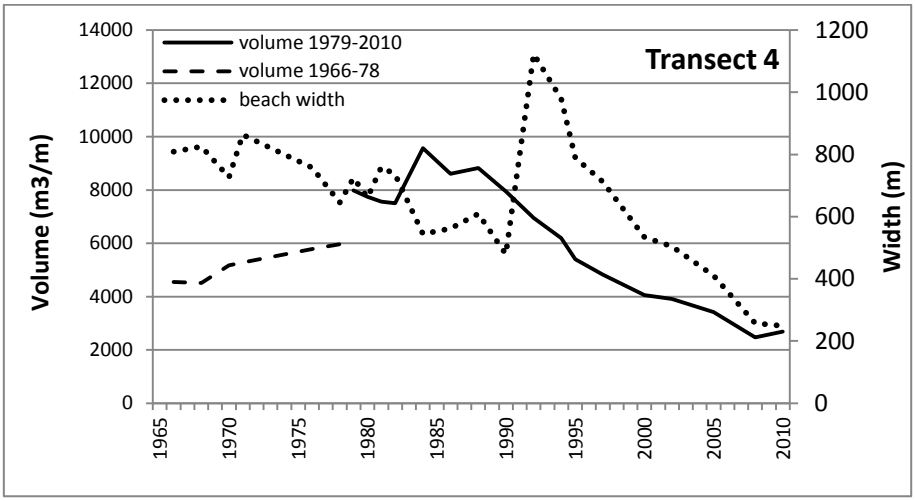

Figure 4.17: Profile volume and beach width through time for transect 4.

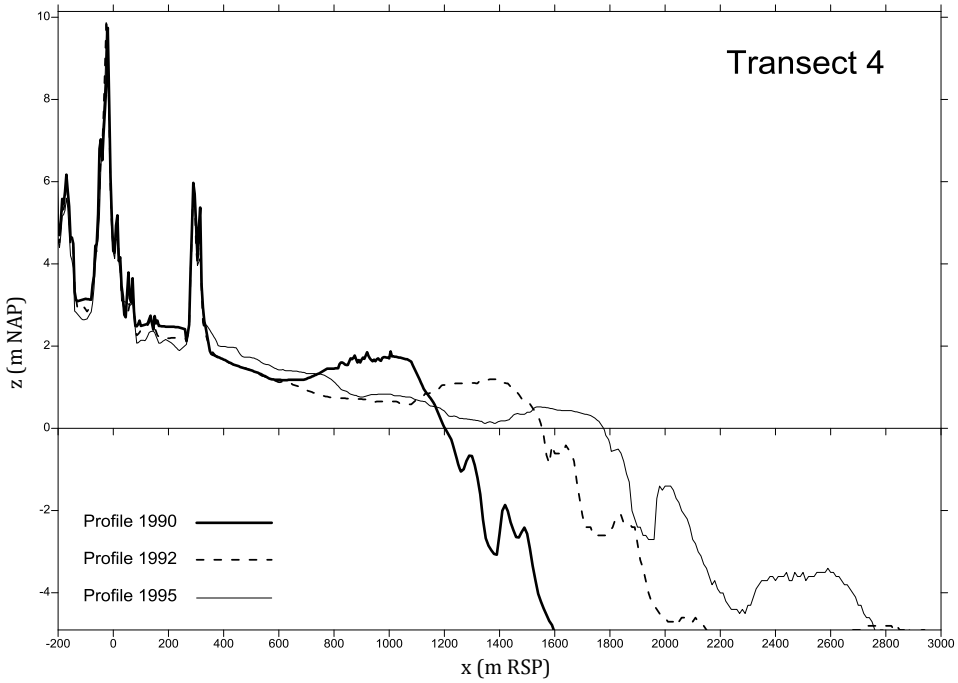

Figure 4.18: Cross-shore profiles of transect 4, indicating the rapid retreat of the beach between 1990 and 1995.

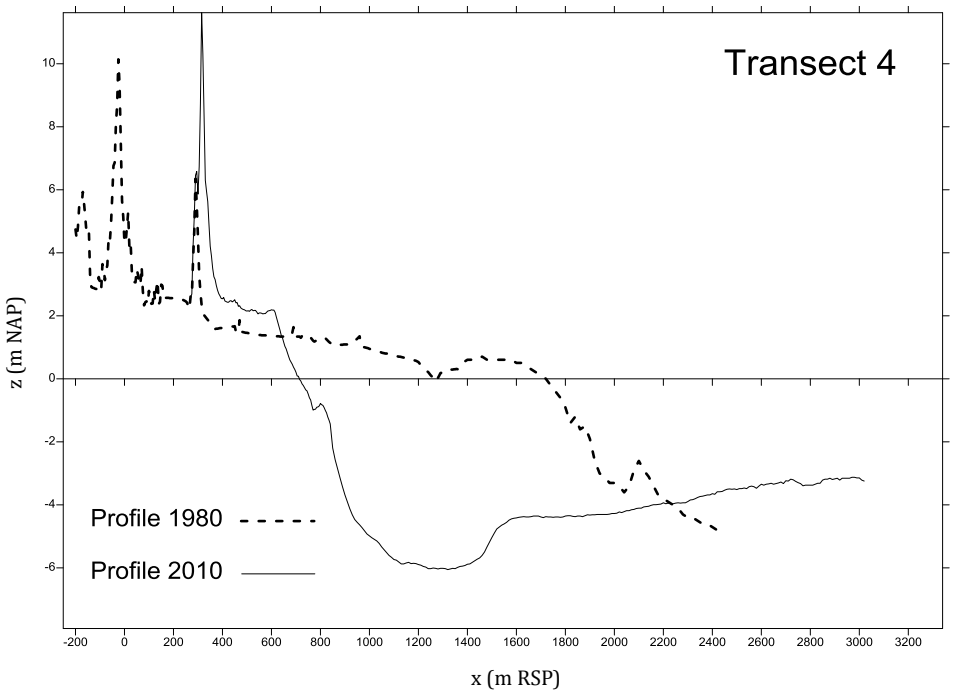

Figure 4.19: Cross-shore profiles for transect 4 for 1980 and 2010, highlighting the landward retreat of the attached shoal and the higher beach elevation in 2010.

4.4.3. Transect 5

Not unlike the previous two transects, transect 5 also had a steady volume increase in the earliest years of the record, peaking suddenly with the appearance of the shoal in the profile, and decreasing in the subsequent years. Volume calculations were carried out between contours +2.5 m and -5 m NAP (Figure 4.20).

In the profile for 1970 large-amplitude nearshore bars can be seen which are different from the previous year's profile. By 1975 similar fluctuations can be seen as low in the profile as -7 m NAP, but have an amplitude (or height) of about 2 metres and appear to be the nearshore bars that are expected to exist on this coastline. As shoal attachment is taking place at transect 4 between 1975-1979, it would be logical to expect some transfer of sand from the shoal towards the beach before and during this period. This results in an increase in longshore drift and volume at transect 5 increases from 4300 m^3 in 1970 to 5100 m^3 in 1981, with 25% (200 m^3) of this added volume occurring in 1980. The higher proportion of added volume in 1980 may reflect increased efficiency in erosion at transect 4 following full shoal attachment, and further, transect 4 experiences a coincidental loss of volume around this time.

The majority of the volume of sand from the shoal does not make an appearance in this transect profile until 1989, and is preceded by a trend of erosion since 1983 that reduces the cross-sectional volume by 800 m^3. The sudden appearance of the shoal (Figure 4.21) contributes 5600 m^3 between 1989 and 1991, raising the total volume to its peak of 10,400 m^3.

Shown in the graph of volume and beach width (Figure 4.20), after the shoal appears in transect 5 there is a prolonged period of decreasing volume that begins rapidly but slows in recent years. The main reason for the volume increase in 2010 is the appearance of a new shoal between -3 m and -5 m NAP, at a distance of about 1200 metres from the beach, which contributes 1300 m^3 to the total cross-sectional volume. Maximum beach width is achieved during this period as the

attached shoal from 1991 is eroded in the same backwards and upwards manner as in previous transects: after reaching this peak, erosion slows and the position of the beach is more stable.

The development of this transect from 1970 to 2010 (Figure 4.22) has resulted in a net gain of cross-sectional volume totalling 2300 m^3 (excluding the new shoal, net gain is 980 m^3) and has seen a progradation in both the shoreline and the dunes.

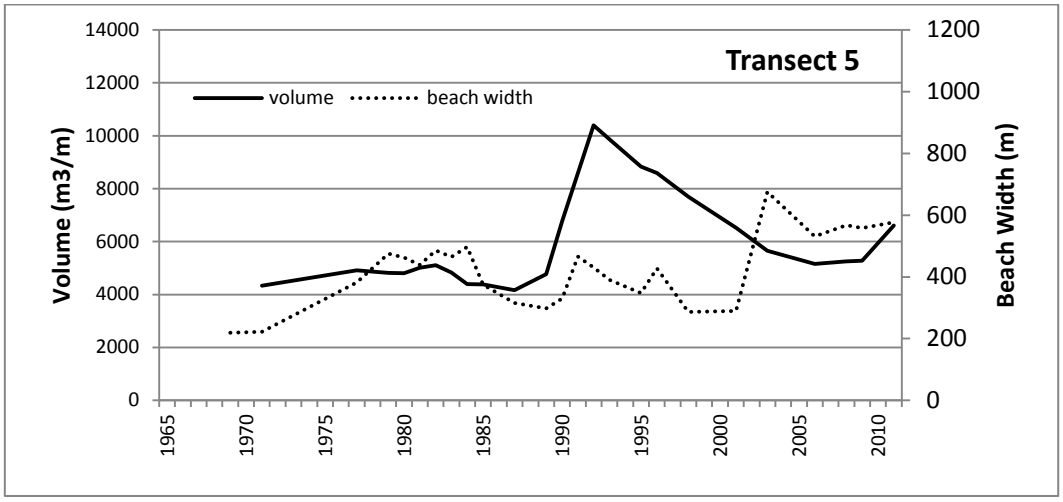

Figure 4.20: Profile volume and beach width through time for transect 5.

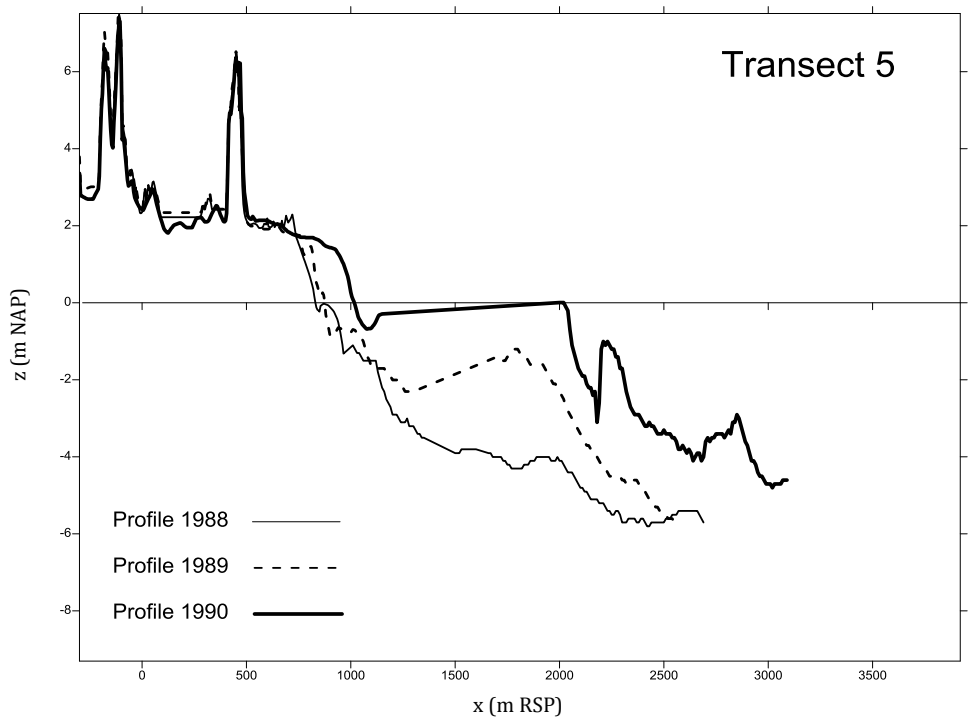

Figure 4.21: Cross-shore profiles for transect 5 showing the rapid appearance of the sand wave in the profile between 1988 and 1990 (N.B. the flat sections of profiles 1989 and 1990 are a result of interpolated data).

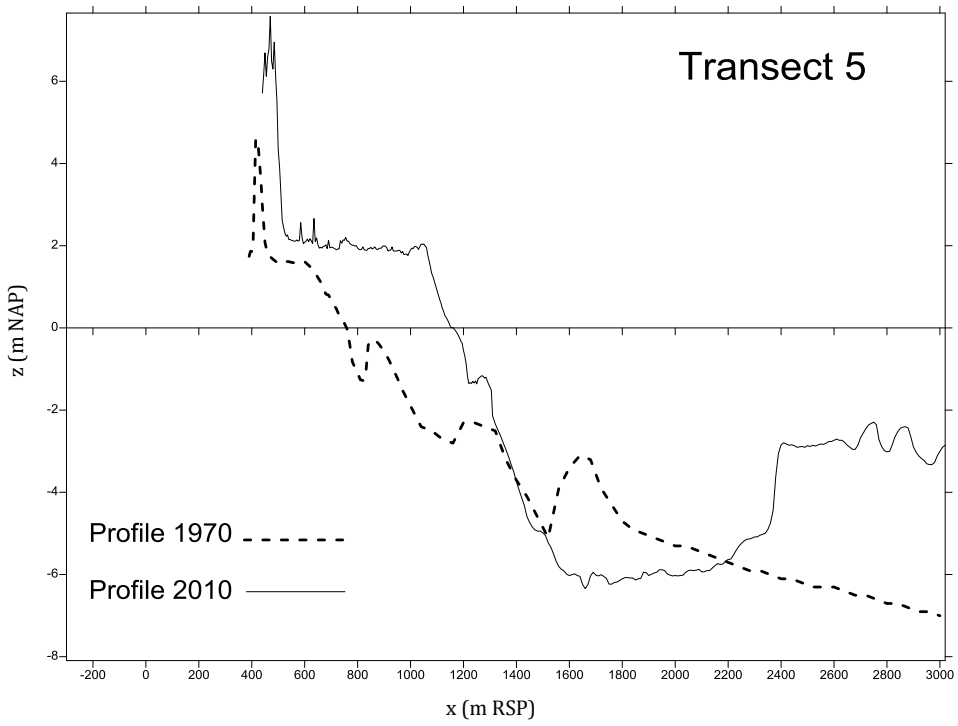

Figure 4.22: Cross-shore profiles for transect 5 for 1970 and 2010.

4.4.4. Transect 6

The same characteristic pattern appears in transect 6 as it did in the previous profiles: the earliest part of the record shows volume increase towards a main peak volume, dropping off afterwards slowly (Figure 4.23). Volume calculations used the main dune foot contour +3 m NAP in conjunction with the -6 m NAP contour, the apparent closure depth within 3 km of the coastline.

The early increasing trend is interrupted by a small "jump" in the trend which is likely to be associated with a beach nourishment scheme in 1980, whereby sand from the shoal was placed downdrift to alleviate erosion (Cheung et al, 2007). Volume in 1980-81 increases by 600 m^3 in two years to 6480 m^3, as the profile shows the beach gaining in overall elevation by 0.25 m and becoming smoother at the foreshore area (removal of the berm). The height of the nearshore bars also increases by approximately 0.5 m (Figure 4.24).

Recovery following the nourishment is rapid, with erosion narrowing the beach width and raising the height of the berm and foreshore. The level of the beach is lowered but does not return to pre-nourishment level, and it is raised further with the input of sand that builds on the berm/foreshore zone.

In 1990-91 there are signs of lower foreshore disturbance that takes the form of wide flat bars, and with the appearance of the shoal in 1992, it is assumed that these disturbances are due to alongshore sediment transport. The subsequent volume peak occurs in 1994 with a volume of 10,800 m^3 and it remains high for several years as a lagoon opened up between the beach and the spit, preventing the spit from migrating much further landward. It is assumed that longshore drift continues to provide sand to the shoal/spit, as waves are now breaking on the

spit rather than the beach itself. Volume reductions, therefore, are associated with direct volume transfer of the spit instead of the beach, which has become a wave-sheltered environment exposed only to shallow wind waves with limited erosive power.

By 2005 the spit has tracked landwards and upwards enough to expose the top surface above +1 m NAP, and it has joined sufficiently to the original beach to be deemed one unit. Particularly since 2000 the spit was losing volume of around 300-500 m^3/m/year, and by 2005 it had a total net loss of 3300 m^3/m since its peak in 1994.

The subsequent years indicate continued erosion at the beach of transect 6, and it appears stable in the short-term with an increasing foreshore/berm feature indicating erosion is still taking place. However, by 2008 an offshore (2000 m distance from dune foot) shoal began to appear with an accretionary gain of 2000 m^3/m between the years 2008 and 2010 (Figure 4.25). Existing around -4 m to -6 m NAP, this newly forming shoal is comparable in volume to the beach and it is yet to be seen how this shoal will develop in the coming years, as previous bathymetric records did not record shoals in this location, or were insufficient in extent to pick it up. Possibly this is a so-called "saw-tooth" bar which develop on the downdrift sides of ebb tidal deltas and migrate obliquely to the coast.

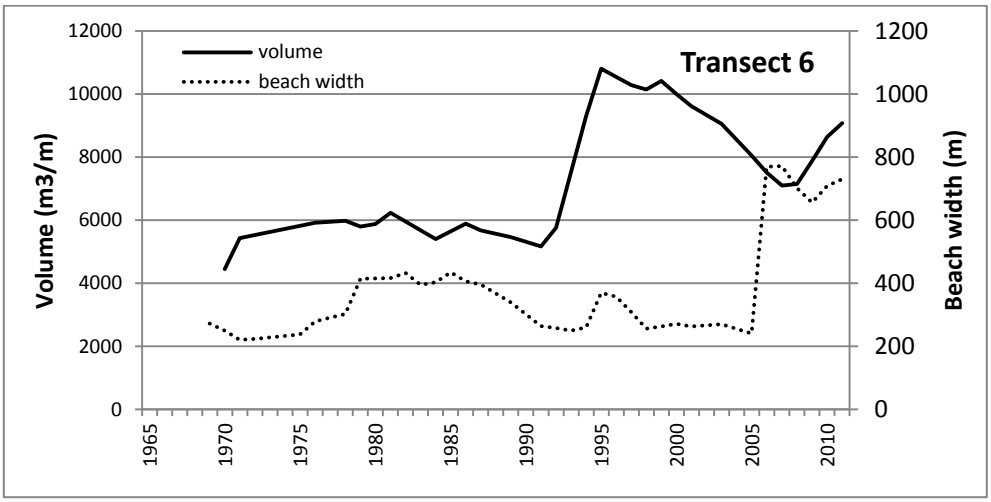

Figure 4.23: Profile volume and beach width through time for transect 6.

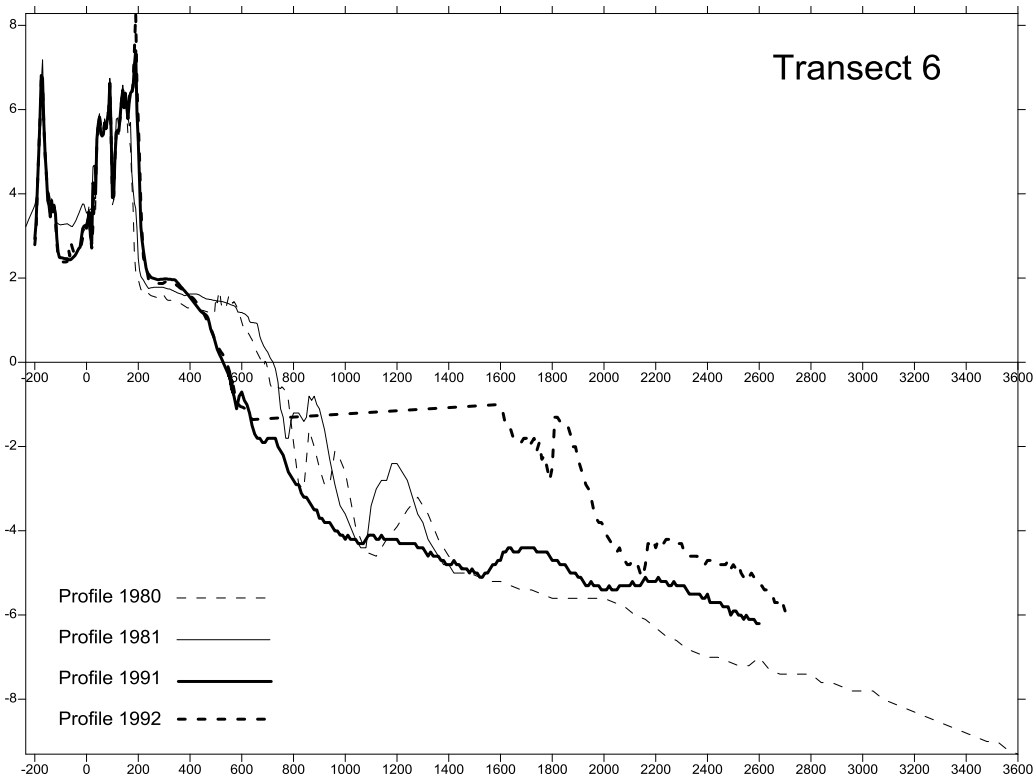

Figure 4.24: Cross-shore profiles for 1980 to 1992 – the profile of 1981 shows a small accretion across the whole profile since 1980, possibly due to an early beach nourishment, while profiles 1991 and 1992 show the sudden arrival of the shoal.

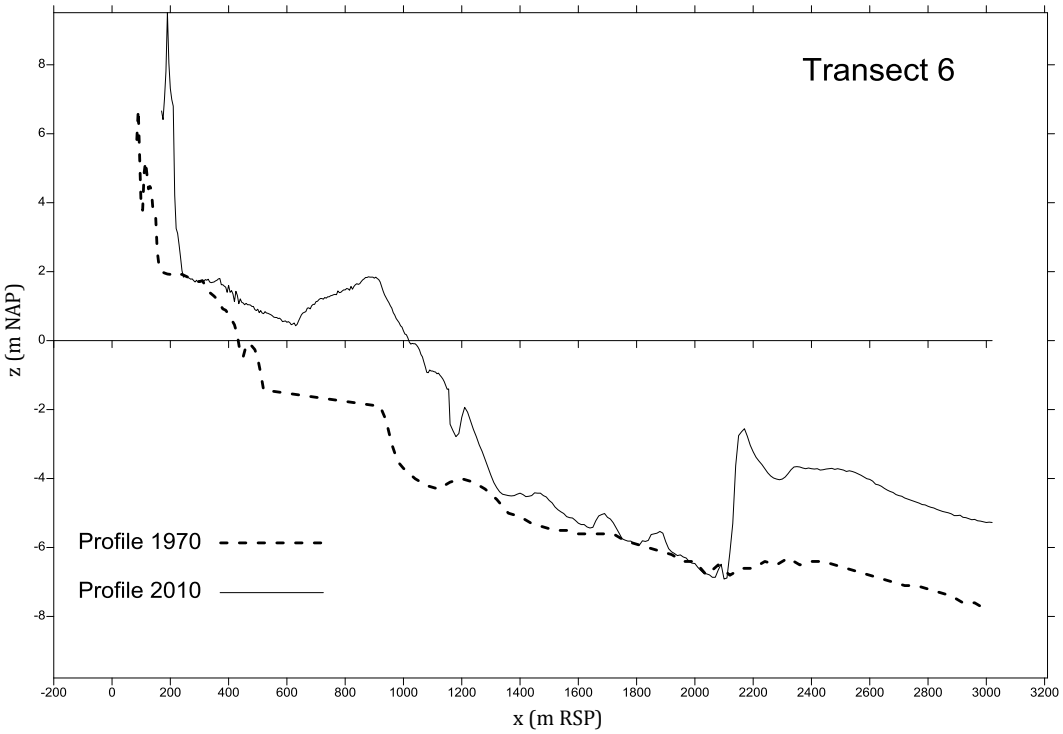

Figure 4.25: Cross-shore profiles of transect 6 for 1970 and 2010.

4.4.5. Transect 7

Unlike the transects that are located closer to the inlet, the volume and width trends of transect 7 are less complicated and have fewer fluctuations than those updrift. This is also seen in the last three transects to be discussed in the next sub-section. The same steadily increasing trend in volume is followed by a brief period of erosion which precedes the main body of sand from the shoal (Figure 4.26). The dispersal of this sand occurs much slower than its arrival at this part of the coast.

After a period of increasing volume to 1984, an erosion trend develops. The rate of erosion is about 80-160 $m^3/m/yr$ for the following years, except in 1989-90 when it suddenly increases to 300$m^3/m/yr$, slowing again in 1991 to 80 $m^3/m/yr$. The erosion trend is halted in the same year (1994) that bars appear in the lowest part of the profile, between -4 m and -6 m NAP, representing 1300 m^3 of additional sand to the profile (Figure 4.27). After the spit reaches the transect in 1995-96, it seems that sediment transport is still occurring continuously as beach-shoal volume remains high to the peak in 2000 (9675 m^3/m) before beginning to decline in volume in 2001. From the sequence of profiles it looks as though the rate of alongshore drift for both the approach of the shoal/spit, and its decline, have both slowed compared to the response in previous transects. It takes about 4 years for the peak volume to occur, and at least 10 years for the volume to return to the pre-shoal level with an average erosion rate of 275 $m^3/m/yr$.

The last point about transect 7 is the disparity between the trend in volume and beach width: volume increases as the shoal/spit is dispersed into transect 7, but because volume calculations are made between contours +3 m and -6 m NAP the 'actual' beach measurements do not take into account the fluctuations in morphology under +1 m NAP. The shoal does exceed the 1 m NAP boundary in the later profiles but it is not included in beach width measurements due to the depth of water and distance between it and the beach.

Figure 4.28 contains the profiles for 1970, representing the start of the record, and 2010. The profile of 2010 shows that overall accretion has occurred, and also the remnant morphology of the lagoon on the backshore is present. A wide depression between 200-600 m leading to a much higher berm indicates that the lagoon is still partially active, but wave action is primarily occurring on the outer berm at around 650 m.

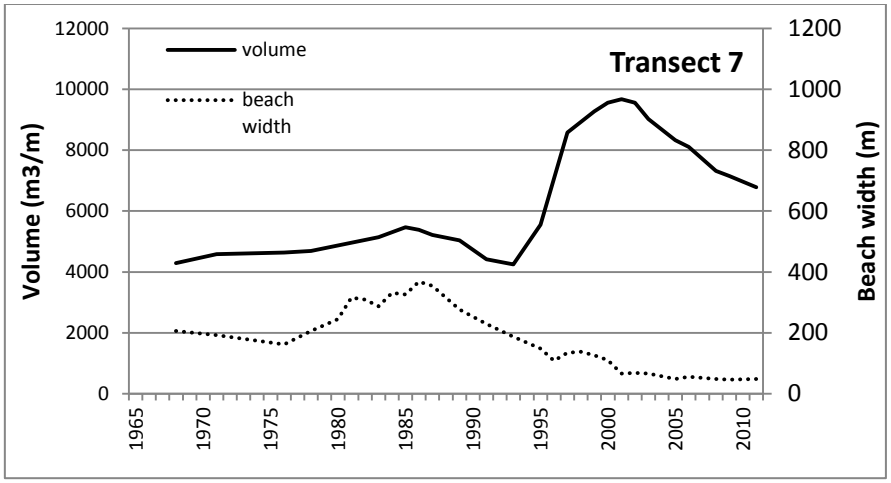

Figure 4.26: Profile volume and beach width through time for transect 7.

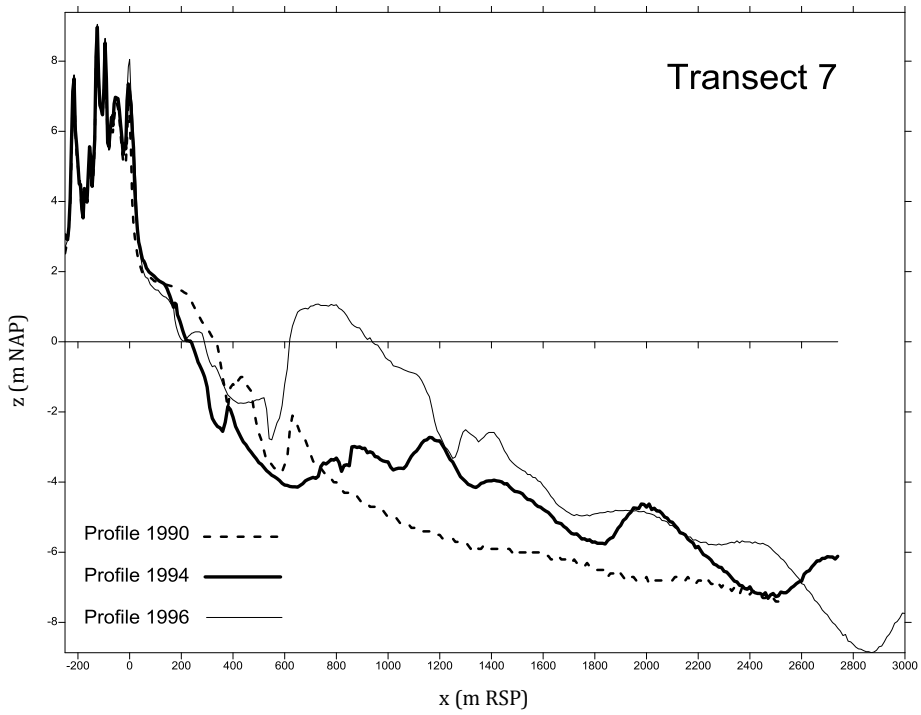

Figure 4.27: Cross-shore profiles of transect 7 indicating the appearance of the sand wave between 1990 and 1996.

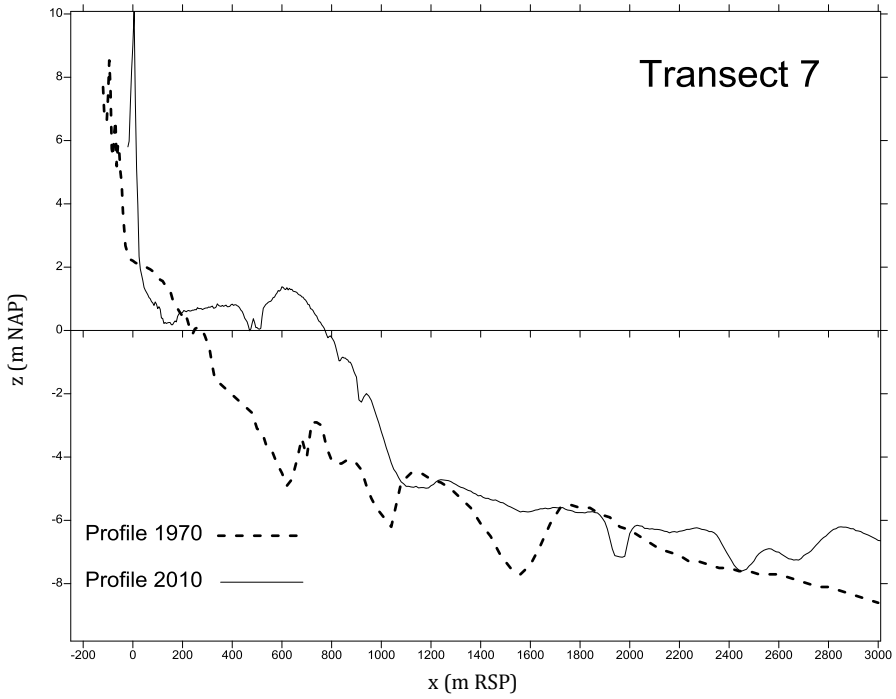

Figure 4.28: Cross-shore profiles of transect 7 at the beginning (1970) and end (2010) of the record.

4.4.6. Transects 8, 9 and 10

In the furthest three transects from the inlet, the response to inlet dynamics is time-lagged relative to the attachment of the shoal in the 1980s, and the effect of the complicated morphological development updrift is diminished. Transects 7 to 10 are 4-7 kilometres from the first transect which means that it takes longer for the sand wave to propagate to this point. However, this does not mean that there is little impact on the coastline, as the same trends of gradually increasing volume and beach width are seen, but these increases are comparatively muted when compared to more updrift locations (Figure 4.29 to Figure 4.31).

The profiles for transect 8 show increasingly fluctuating foreshore and nearshore bars, down to -6 m NAP, from 1997 onwards (coinciding with the 1996 beach nourishment) (Figure 4.32). The volume gain for the entire profile in 1997 (including nourishment) is 800 m^3/m. Volume increases for the following seven years, at an average rate of 585 $m^3/m/yr$, but with the greatest intensity between 1998-2000 when accretion rate varied from 800-1300 m^3/m. The volume peak occurs in 2004, with 7770 m^3/m.

This same pattern occurs in the profiles for transect 9 and 10 also, where the dispersal of sand from the former shoal takes place much more slowly and volume builds gradually from the foreshore. In the 9 year period from the onset of increasing volume to the volume peak in 2010, transect 9 had an average accretion rate of 240 $m^3/m/yr$ (in the first 4 years this rate is 400 $m^3/m/yr$, slowing in the last 5 years). The same can be said for transect 10, which experienced at first an accretion rate of 400 $m^3/m/yr$ but this slowed to around 200-300 $m^3/m/yr$ before the most recent volume calculation in 2010.

This shows, in contrast to the near-field transects, there is no sudden increase in volume from one year to the next: instead beach volume increases gradually over several years, with this period of time increasing from 7 years at transect 8, to 9 years for transect 9 (Figure 4.32). The assumption is that transect 9 has already reached its peak volume, but if it is yet to increase then the rate of sediment transport is still slower than at transect 8. It is most likely that transect 10 has not yet reached its peak volume, but will probably do so in the next few years.

Another contrast to the near-field locations is that beach width and volume are now in phase, and the previous time lag between peak volume and peak width is gone. This is due to the gradual arrival of the sand wave volume allowing time for cross-shore transport of sand to the +1 m NAP (HWM) level.

The beach nourishment that was discussed in Cheung et al (2007), whereby sand mining of the shoal took place to nourish the downdrift coast, is visible in the last three transects for an extended period after the nourishment was carried out in 1981. Transects 8 to 10 show a slightly increasing volume between 1981 and 1988, which is detected in the profiles as beach widening and increase in beach elevation in combination with increased foreshore bar fluctuations. The 1996 beach nourishment, however, does not appear distinctively as a large volume increase (probably as it was a beach nourishment, therefore not a relatively large volume). It also coincided with the approach of the sand wave, which begins at transect 8 in 1996 (1998 for transect 9; 2001 for transect 10).

Figures 4.33 to 4.35 indicate the net change in the profile from the beginning to the end of the record, all of which show accretion over the time period.

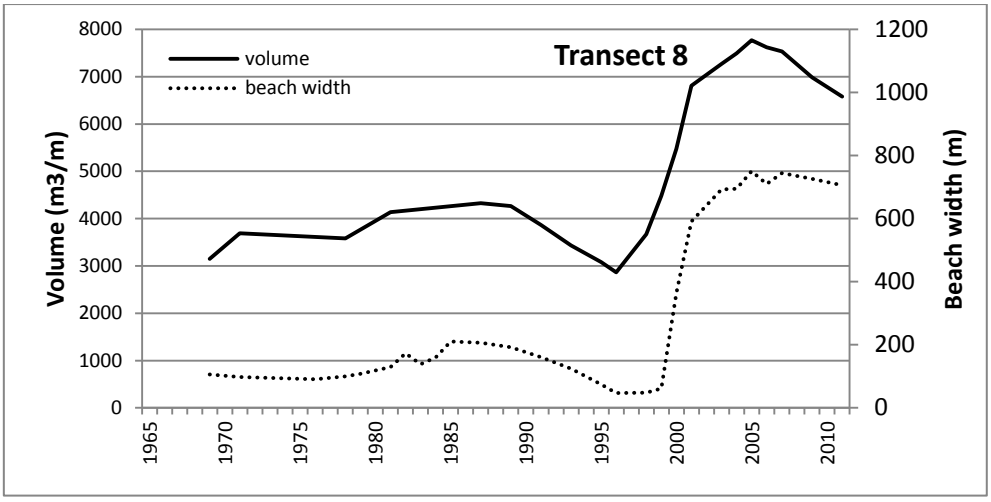

Figure 4.29: Profile volume and beach width through time for transect 8.

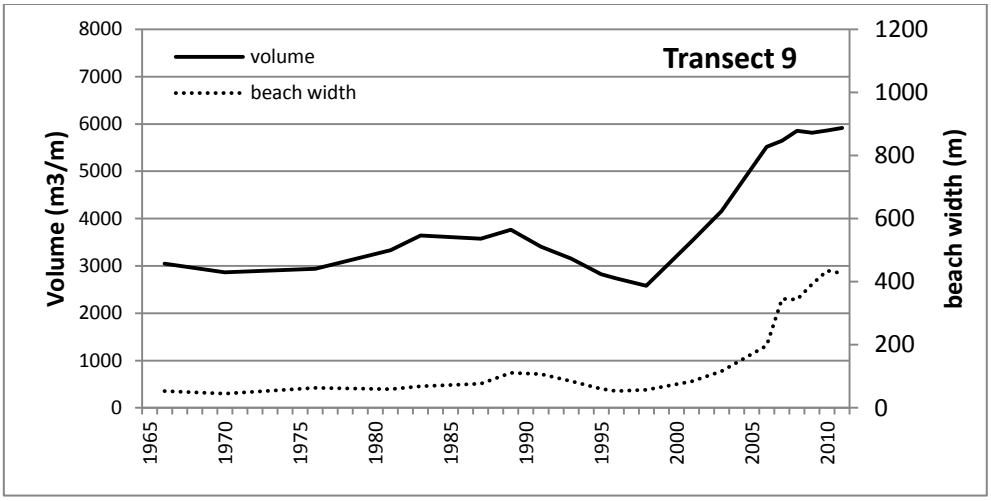

Figure 4.30: Profile volume and beach width through time for transect 9.

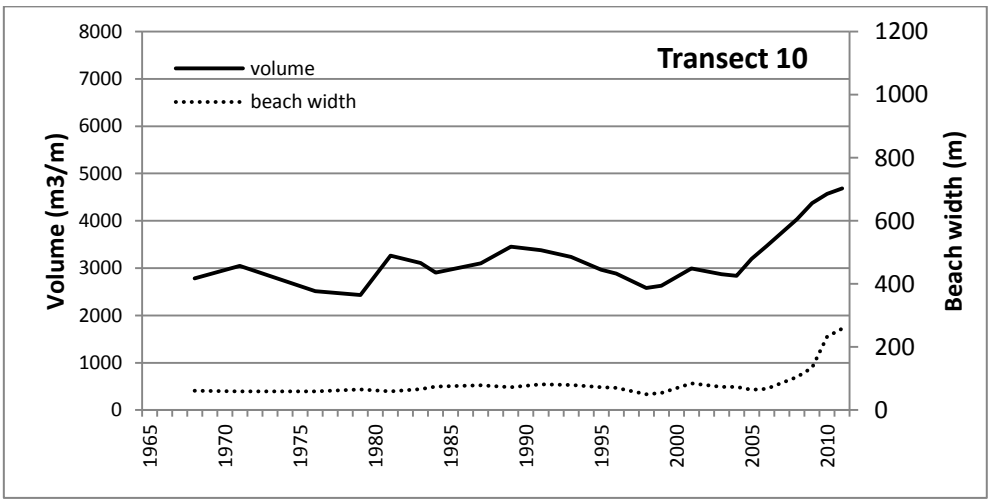

Figure 4.31: Profile volume and beach width through time for transect 10.

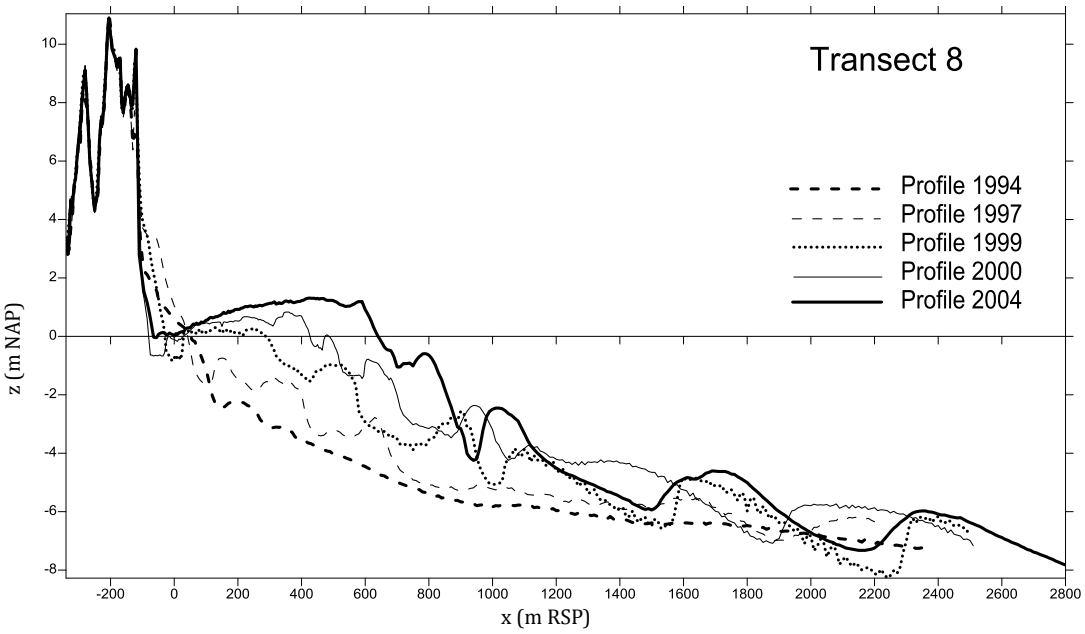

Figure 4.32: Cross-shore profiles of transect 8 showing the gradual appearance of the sand wave between 1994 and 2004.

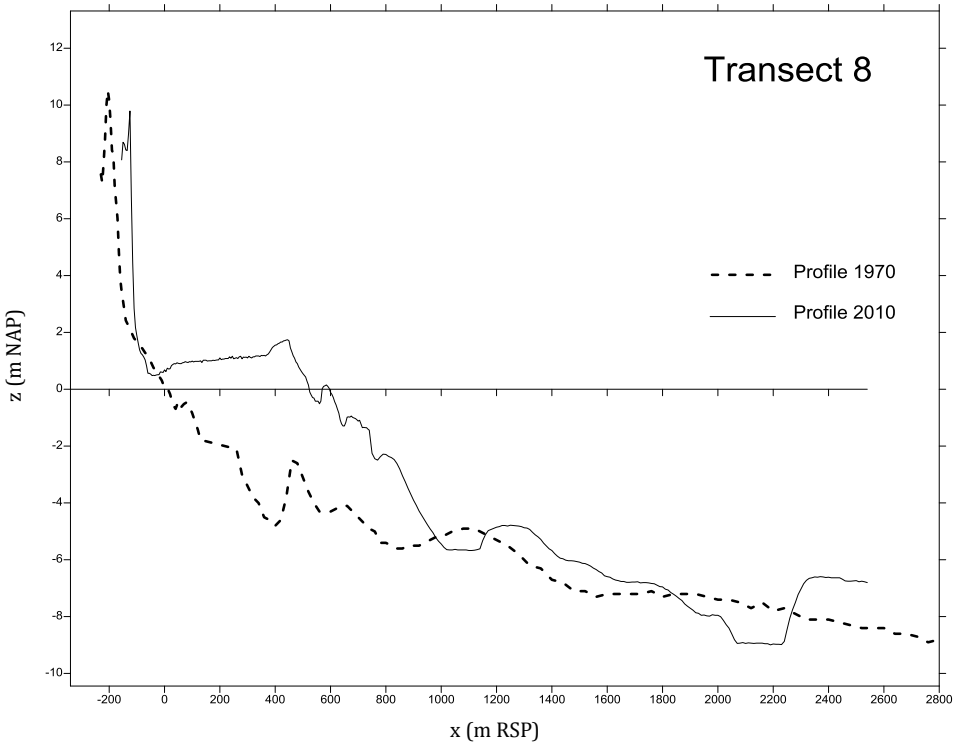

Figure 4.33: Cross-shore profiles for transect 8 from the beginning (1970) to the end (2010) of the record.

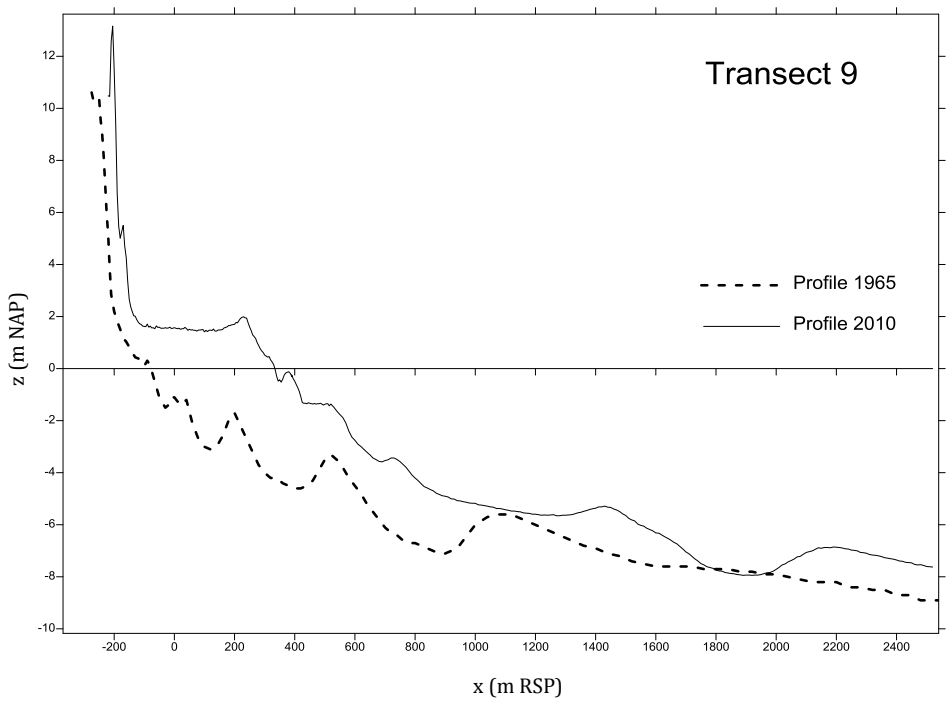

Figure 4.34: Cross-shore profiles of transect 9 from the beginning (1965) to the end (2010) of the record.

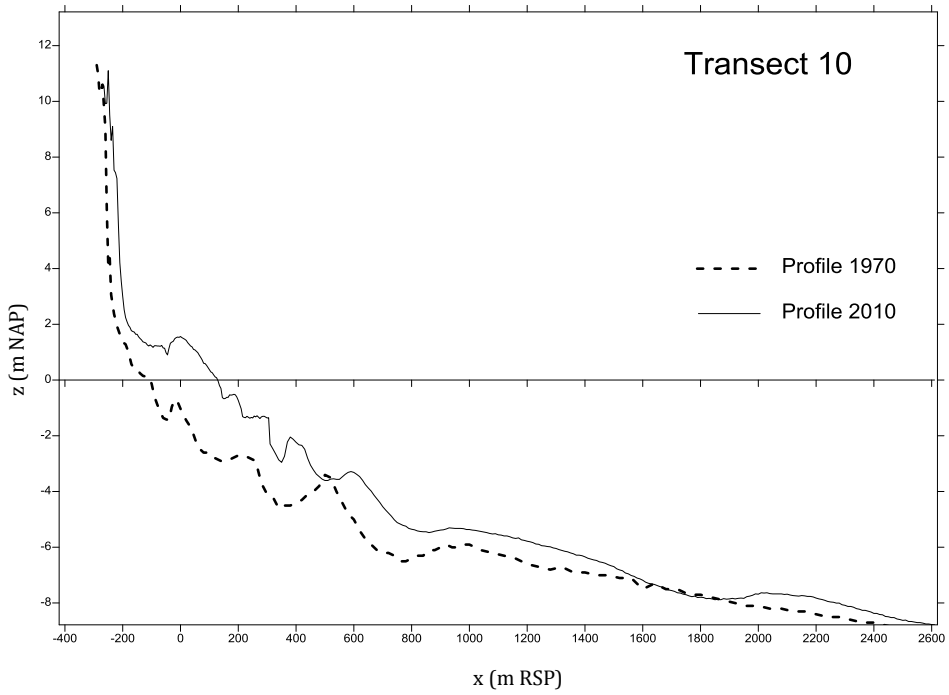

Figure 4.35: Cross-shore profiles of transect 10 from the beginning (1970) to the end (2010) of the record.

4.4.7. Sand Wave Volume Attenuation

To better understand the fluctuations in beach volume (change in volume amplitude of the sand wave) along the shoreline, an average beach volume was derived from the years preceding the peak volume associated with the sand wave. The preceding years often show a steady-fluctuating volume which increases suddenly in a clearly-defined peak year, making it easy to distinguish pre- and post-sand wave years. It was not possible within the limits of the dataset to define an average pre-sand-wave beach volume for transect 3.

Table 12: Profile volume per transect

Transect number	**4**	**5**	**6**	**7**	**8**	**9**	**10**
Peak volume (m^3 per m)	9562	10389	10805	9673	7767	5913	4686
Average volume (m^3 per m)	7696	4858	5681	4888	3848	3253	2976
Difference Peak - Average (m^3 per m)	1866	5531	5124	4785	3919	2660	1710
Difference as % of average volume	24	114	90	98	102	82	57

Table 12 contains the quantification of the volume that is contributed by the shoal to the beach, by determining the peak volume and subtracting the average beach volume. For most of the transects, the progression of the sand wave contributes 100% of the previous average beach volume, therefore doubling the cross-sectional volume. Taking a closer look at the figures, the actual volume added to the beach (difference of peak minus average) becomes smaller with distance from the inlet. Transects 9 and 10 highlight this attenuation of the sand wave as it is dispersed alongshore to these transects: comparatively less volume is transported to these inlet-distant locations than the near-field locations. This is an expected result as cross-shore sediment dispersal will also take place during the time it takes for the shoal sand to disperse. Indeed this has occurred, as will be shown in the next section concerning dune development.

4.4.8. Summary

The analysis of beach cross-sectional volumes between 1965 and 2010 has shown that the downdrift beach undergoes dramatic changes when the Bornrif shoal migrated towards and joined with the north-western coast of Ameland.

The volume peak when the shoal attaches to transect 3 in 1982 totals 8400 m^3/m, but rapid erosion between 1986 and 1995 was approximately 400-600 m^3/m/yr, slowing to around 200 m^3 per year after 1995. The same progressive erosion trend is observed at transect 4, which experiences a similar erosion trend of about 400-500 m^3/m/yr until 2000, which then reduces to around 200-300 m^3/m/yr over the last decade. With the rapid changes in volume occurring to the foreshore, cross-sectional volume fluctuates faster than the HWM and a time-lag of 8 years appears with beach width following volume.

An extreme erosion trend occurs at transect 3 and the most recent measurements from 2010 indicate that the beach width now is at its narrowest from the whole 45-year record. This erosion trend only occurs at this transect, which suggests there are other factors in play which enhance erosion at this location. The bathymetry maps of Figure 4.2 (page 61) and Figure 4.4 (page 63), which show the alignment and extension of the shoal to the west as well as the east,

are interpreted as indications of a bifurcation in sediment transport at transect 3. Sediment from the shoal is transported in an alongshore direction primarily to the east, but also towards the west and into the inlet itself. This results in the extreme erosion trend. Further, as Figures 4.2 to 4.4 do not show increased beach width on the beaches to the west of transect 3, it is assumed that sediment transported in this direction is either re-cycled back towards the ebb delta (i.e. FitzGerald, 1984) or it enters the inlet basin. This is contrary to the view of Kana et al (1985), as the diverging wave pattern does not lead to re-nourished beaches on both sides of the shoal.

Table 12 shows that the volume that comprises the sand wave at transects 5 and 6 equals the average total cross-sectional volume of the beach: the beach volume at these transects doubles with the passage of the sand wave. Further, the time lag between volume and width increases to 11 years at both 5 and 6. The sheer volume involved in this sand wave, enough to double the volume of the beach, causes this time lag as wave dynamics only slowly disperses sediment in the cross-shore direction.

When the sand wave progresses beyond transect 5, it becomes like a spit and is stretched across in front of the coastline (see Figure 4.5 [page 64] and Figure 4.6 [page 64]). This response is due to the interaction of tidal forces at the inlet enhancing eastwardly-directed sediment transport, and also due to the wave-sheltering effect of the ebb tidal delta. As the spit/sand wave lengthens alongshore, it is curved by waves inwards towards the coastline at transect 7, where it forms a tidal lagoon. The presence of this lagoon means that there are now beaches which have been cut-off from normal coastal processes, and beach width at transects 6 and 7 remains constant through time. The sand wave continues to propagate alongshore, and the erosion trend at transect 6 since 2000 has been 300-500 $m^3/m/yr$.

The sand wave reaches transect 7 partly as the spit, and the tidal channel maintaining the lagoon remains close to the shoreline at this location. Before the sand wave arrives, there is a volume trend of erosion between 1984 and 1994 (80-160 $m^3/m/yr$), followed by a more gradual appearance and peak volume of the sand wave in 2000. It takes approximately 6 years from the first increases of beach volume before the peak volume occurs, which suggests that the sand wave is attenuating in form. There is no time lag difference between volume and peak at transect 7 as the tidal channel cut off the beach from normal coastal processes.

By the time the sand wave appears at the most westerly transects, its progression alongshore has resulted in a time lag in both its appearance at the transects and also in the peak volume. By 1996, there is a ≈16 year time lag from the first attachment of the shoal, to its appearance as a sand wave at transect 8. Further, at transect 8 it takes seven years from the first appearance of the sand wave in the profile to its peak volume in 2004, at 7770 m^3/m. This is in contrast to the near-field sites whereby sudden volume increases from one year to the next marked the peak volume. The attenuation of the sand wave at these distant transects means that the transfer of sand from the updrift locations takes place much more gradually than at the near-field sites. Additionally, beach width and volume at these transects is now in phase with each other, while at the near-field transects there was a time lag between peak volume and beach width.

4.5. Long-Term Behaviour of Dune Development

4.5.1. Introduction

As part of the tidal inlet and barrier island system, the dunes also have a role in long-term development particularly when it involves sediment bypassing. Dunes act as a long-term store for sediment in the coastal zone, so accretion and erosion either locks up or releases this sand from this storage. In the Netherlands, the dunes also act as the first line of defence against storm surges and it is important that they are maintained either naturally or by nourishment.

Dune growth is related to sediment availability (of the right size), wind velocity and direction, beach width, humidity, and the presence of vegetation to allow accumulation, among other factors. Cross-sectional volume of the foredune, its height, and the dune foot position give enough information about the dimensions of the active dune at a given time, as each is inherently linked to the other. For each transect this data has been collated and analysed for patterns and trends in dune development.

4.5.2. Cross-Sectional Volume and Dune Foot Position

Figure 4.36 shows graphs for dune volume (m3/m/yr) and the change in position of the dune foot through time, at transects 3 to 10. The position of the dune foot is displayed in such a way that its position at the beginning of the record is zero and each subsequent year is a deviation from zero. Dune volume indicates the cross-sectional volume of the foredune for a given year.

In every graph, dune volume and dune foot position have each increased over time, reflecting the 'healthy' nature of the dune system that results from the influx of sand from the Bornrif shoal. Dune building indicates the prevalence of not only alongshore transport, but also cross-shore transport.

The dune foot at transect 3 very suddenly retreats landwards between 2005-2008 due to the narrowness of the beach and the exposure to wave attack during storms. The cross-sectional profile is affected only slightly, but the long-term trend of dune-building (which slowed in the last decade) ceases to continue as dune erosion occurs. An aerial photograph taken in 2007 captures the dune erosion at transect 3, where it is possible to see an erosion scarp and slumping that resulted from undercutting of the dune foot (Figure 4.37). The narrowness of the beach and the distance of the HWM from the dunes highlights the susceptibility of these dunes to further erosion, if left untended.

Beach nourishment schemes are clearly marked in the graphs of transects 8, 9 and 10, where the dune foot position is advanced by around 40 metres seaward. The subsequent rapid landward retreat of the dune foot position in the following years shows that this type of nourishment is only a short-term solution to dune erosion, as within 5 years the dune foot has almost reached its pre-nourishment position at each transect.

Table 13 provides detailed volume data per transect, by calculating the difference in dune volume from the first and last record in the Jarkus dataset. The data show that approximately 200-300 m^3/m are added to the dunes over the respective periods of analysis. Estimated rate of change highlights a spatial variability in the alongshore direction: the lowest rates of change are found in the same locations as the highest amounts of variability due to the dispersal of the shoal, namely transects 4 to 8. This may be a consequence of wave and tidally driven dispersal

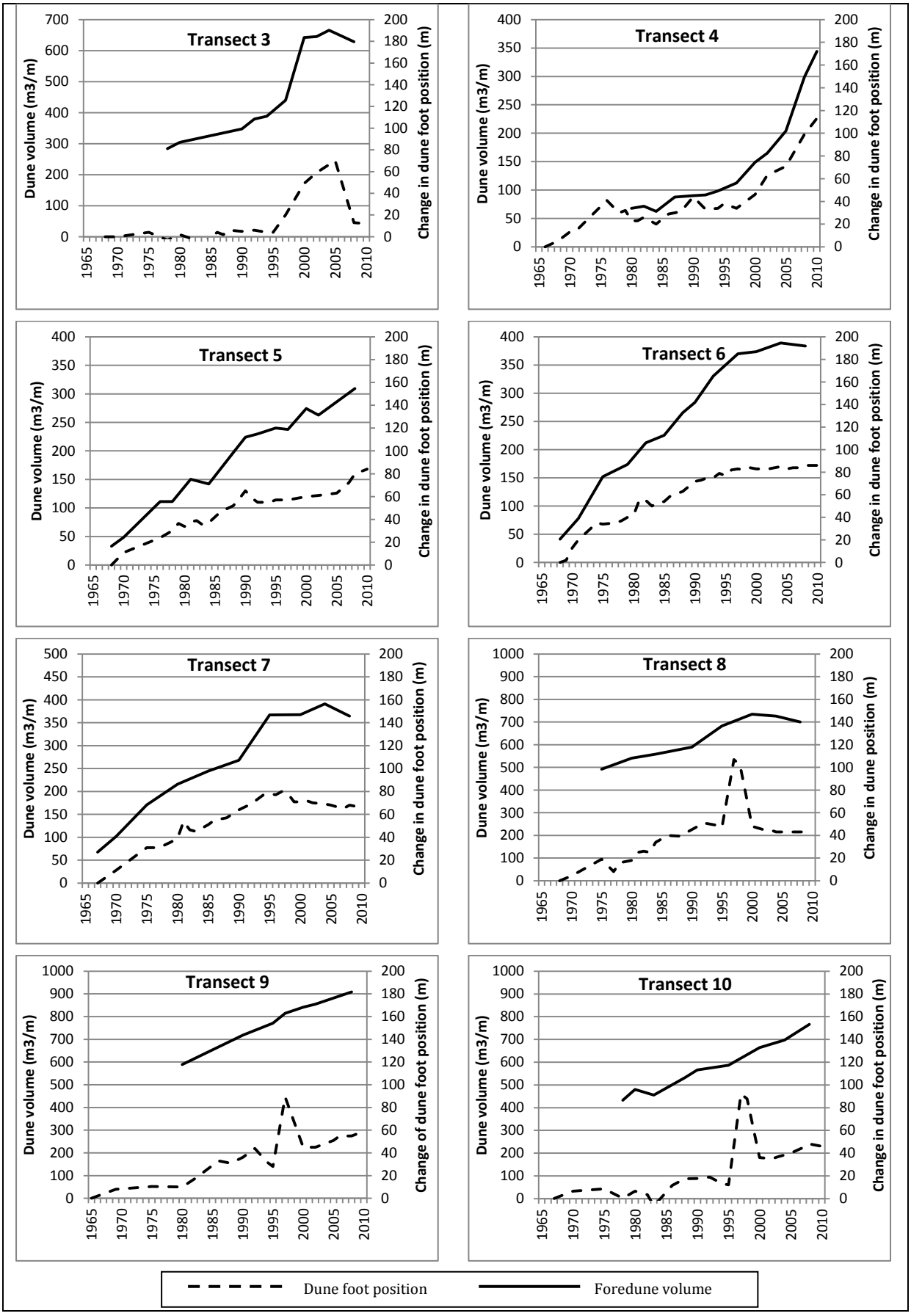

Figure 4.36: Foredune volume and dune foot position through time for each transect 3 to 10.

dominance over cross-shore dispersal. Additionally, transects 3.8–10 have undergone beach nourishments in the past which adds further sand to the upper beach near the dunes. The initial volume at the start of the record is also higher at these transects than at the others. It would be expected that excess sediment placed on the beach during nourishments would be blown towards the dunes, but also the cross-shore shift in the +3 m NAP dune foot contour (Figure 4.36; transects 8-10) indicates that sediment is placed at the dune foot itself.

Figure 4.37 Aerial photograph taken in 2007 at RSP 3. Note the erosion scarp and slumping that suggests undercutting by waves. (KustFoto.nl, retrieved 2011).

Table 13: Dune volume development from the beginning to end of the record.

	Year	Dune volume (1) m3/m	Year	Dune volume (2) m3/m	Difference m3/m	Rate of change (m3/m/yr)
Transect 3	1978	284	2008	629	345	11.50
Transect 4	1980	68	2010	344	276	9.20
Transect 5	1968	33	2008	309	276	6.90
Transect 6	1968	41	2008	384	343	8.58
Transect 7	1967	67	2008	364	297	7.24
Transect 8	1975	492	2008	700	208	5.94
Transect 9	1980	589	2008	909	320	11.43
Transect 10	1978	432	2008	767	335	11.17

4.5.3. Dune Height

Dunes prograde in a seaward direction with the accumulation of sand on the seaward side. This leads to not only an increase in volume, but naturally an increase in dune height. To give an indication of dune development from the start to the end of the record, Table 14 contains height data from the first year of dune data and also the last. The difference in height is calculated and an estimated rate of change is provided.

Presumably due to the vast volume of sand available, the orientation of the dunes with the prevalent north-west wind, and the extreme width of the beach, dune height at transect 4 increases by much more than the rest of the coastline with an estimated accumulation rate of 0.20 m/yr. This produces a dune height that is 8.6 metres higher than at the beginning of the record. Further, dune height is also the lowest at this part of the beach at the beginning of the record. Possibly its exposed position, open to wind from a wide area, contributes to and inhibits its development through time. Data from before this record began would be required to confirm this suggestion.

All transects experienced increased dune height between the period of 1965-2010, coinciding (as expected) with the previously discussed increases in dune volume and prograding dune foot. The furthest transects had comparatively low rate of change, which is likely due to the interplay of beach width and morphology that results from the passage of the sand wave. The lowest rate of change is seen at transects 7 and 8 (0.02 m^3/m/yr) which had a consistently narrow width beach that was affected by erosion from the tidal channel in 1999-2000.

The green beach between transects 6 and 8 probably plays a role in limiting the supply of sand towards the foredunes. This green beach is the remnant of the lagoon area and is partially vegetated and badly drained, which leads to increased sediment trapping.

Table 14: Dune height development from the beginning to the end of the record.

	Year	Dune height (m)	Year	Dune height (m)	Difference	Rate of change (m/yr)
Transect 3	1968	7.0	2010	10.3	3.3	0.08
Transect 4	1966	3.0	2010	11.6	8.6	0.20
Transect 5	1968	4.5	2010	7.6	3.1	0.07
Transect 6	1968	6.6	2010	9.5	2.9	0.07
Transect 7	1967	6.2	2010	7.0	0.8	0.02
Transect 8	1968	10.0	2008	10.8	0.8	0.02
Transect 9	1965	10.5	2010	13.1	2.6	0.06
Transect 10	1967	11.9	2008	13.8	1.9	0.04

5. Discussion

5.1. Short-Term Morphological Development

During a 6-week period of fieldwork, the short-term fluctuations of the downdrift beach were measured and the coastal indicators of beach width, volume, slope and spatial change were analysed. Two locations were measured: transects 3.8 to 5.2, the near-field site, and transects 9.20 to 10, the far-field site. A comparison is made between the near-field location which has a wave-shadow effect from the ebb delta, and the more exposed downdrift site where the presence of the ebb delta is reduced.

Clear trends appeared across each of the coastal indicators for transects 3.80 to 5.20 (near-field site). The greatest variations in profile occurred between 3.80 and 4.02, and each transect showed a trend of accumulation at the berm and landward-moving profiles. The volume trends also suggested a similar pattern, whereby the average gains and losses over the campaign period indicated a division at 4.20: the transects west of 4.20 underwent average loss of volume over time, while the transects to the east experienced an average gain. The largest decrease in net volume occurred at transect 3.80 (-19 m^3/m) followed by transect 4.02 (-16 m^3/m). The total net foreshore volume reduction over this period is 9100 m^3 between 3.8 and 4.20, whereas the net foreshore volume increase between 4.4 and 5.2 is 12500 m^3.

An alongshore pattern appears in foreshore slope, with the lowest slope occurring at transect 4.20 (-0.013) while relatively steeper slopes occur on either side. The steepest foreshore slopes were found to appear at the westerly transects, with slopes averaging at -0.018. In the eastern transects of 4.40 to 5.20, slope has a higher value than at 4.20 but is less than the transects in the west, averaging about 0.015.

Lastly, the clearest indication of the variations between transects 3.80 to 5.20 is shown in Figure 3.18 and Figure 3.19 (page 56), figures which indicate the spatial differences in volume loss and gained during the measurement campaign. The proportion of the area between each transect that undergoes loss or gain between the start and the end of the campaign, is shown as a percentage per transect. Greatest loss occurs at transect 3.80, while greatest gain occurs at transect 4.80. An alongshore decline in erosion occurs between these transects.

All of these indications add further weight to the theory of a bifurcation in sediment transport: extreme erosion occurring on the westernmost transects is observed from the short-term patterns of high profile variability, the consistent steepness of the foreshore, and high proportion of overall erosion at these transects. The wide, flat beach at 4.02 to 4.20 appears to be the dividing point for sediment transport (see Figure 2.3; page 30), where net loss in volume occurs to the west and net gain occurs to the east. It is probably at this location where the divergence of wave crests occurs, as this section of the beach is oriented SW-NE and therefore is parallel to the prevalent wave direction from the NW.

The far-field beach at transects 9.20 to 10 has a trend of sediment re-distribution throughout the profile, resulting in a net accumulation on the backshore and net erosion on the foreshore. Overall, the cut and fill analysis showed a net erosion loss of -5500 m^3 for this 1 km stretch, otherwise the balance of erosion and accretion suggests primarily re-distribution is occurring rather than a net loss of sediment. Observations during fieldwork suggest that accumulation of

sand on the dunes may account for the apparent loss of sediment during this time. There is no alongshore pattern of erosion and accretion like at the near-field location.

5.2. Long-Term Morphological Development

Considering the cyclical nature inherent in the tidal inlet system and morphology, one of the main objectives of this study is to determine whether there is also a cyclical component in beach morphology evolution. Consequently, the following discussion is sub-divided roughly into decade sections, where each section will summarise and evaluate the area of study as a whole unit within the period. Each section corresponds to proposed morphological phases as discussed in Israel and Dunsbergen (1999), a widely-cited article that examines the morphological cycle of the inlet itself. Using these phases as a framework for morphological changes sets the whole system into context of not just a singular beach, but rather a complex system of interacting forces resulting from inlet dynamics.

5.2.1. Phase A: 1965 to 1979 – pre-attachment phase

It would be expected that during this phase of development, transects 3, 4 and possibly 5 would show accretion offshore as sand is brought to the eastern ebb delta shoal. The bed elevation will rise to above -5 metres NAP and the form of the shoal will be visible. The focus of the Israel and Dunsbergen research is on the inlet and no mention is made of the Ameland coastline itself, however it would be expected that the shoal would provide an area of wave-sheltering to the beach to the immediate east of the shoal. This effect may appear as beach widening close to the shoal attachment site, but it may be complicated by the dispersal of sand from the shoal as it progresses towards the beach. Beyond RSP 3 to 6 it is unlikely that the shoal will have an impact on beach morphology due to the slow rate of change involved with sediment transport mechanisms.

Initial results indicate that the aforementioned expectations have partially been met. A shoal/swash bar that first appeared in the beginning of the record (1968, transects 3, 4) can be identified in transects 3 and 4. In this first period of a roughly a decade, transects 3 and 4 do not reach any lower than -3 to -4 metres depth to a distance of 1500-2000 metres from the RSP line. This is in accordance with the findings from Israel and Dunsbergen (1999) regarding the accumulation and build-up of the eastern ebb delta shoal. Between 1968 and 1978 the shoal approaches the beach and by 1976 (not before 1971, but data is limited in this period), attaches to the coastline at transect 4 and, crucially, not at transect 3. The shoal is said to have joined with the beach when there is no longer a significant depth of water or distance between the shoal and beach proper, i.e. by 1971 there remains a water depth of -3 m and a distance of 150 metres between contours of -1 m NAP; by 1976 the water depth is ≈1 m between the two features and the distinction between beach and shoal is less defined.

The shoal merged with the coastline initially at transect 4, then was re-shaped by waves in both the easterly and westerly directions. Its form as it merged with the coast was distinctly crescentic (see Figure 4.2). This development echoes the observations made by Kana et al (1985) in Figure 1.12 (page 19), whereby the outer edges of migrating shoals are curved towards the coast by wave refraction. Wave refraction around the shoal sets up an alongshore

pattern of erosion either side of the shoal, with accretion taking place where the shoal merges with the beach. Prior to attachment at transect 4, there is a period of coastal retreat and beach width reduction (1971 to 1979) shown in Figure 4.17, which could be interpreted as a shoreline response to the changed morphology and wave refraction.

This erosion trend can be attributed to wave refraction as wave crests become aligned to the shoal to the west of transect 5 and 6, which is observed by Kana et al (1985) at Dewees Inlet in South Carolina, USA (see Figure 1.12). This sets up an alongshore pattern of accretion at the attaching shoal and erosion on either side. While an erosion trend is distinguished at transect 5, on the other side of the shoal at transect 3 the area of deeper water complicates the process and it is not clear if the response is the same.

Transect 3 during this period undergoes rapid backshore morphology evolution. In the beginning of the record in 1968, transect 3 has a distinctly convex backshore which dipped into a 100 metre-wide channel of 1 metre depth very nearby to the dune foot. In the subsequent ten years the backshore experiences accretion and the channel is infilled rapidly. The beach shape takes on a more usual form, sloping from the dune foot to the water's edge. The shoal is seen just offshore and it makes a landward progression of ≈200 metres between 1970 and 1975. By 1978 the top of the shoal accumulates sufficiently through swash action to +0.7 m, while remaining in the same position as 1975. At this time, there still remains several hundred metres between the shoal and the beach, but the beach widens by 60 metres in the three years before 1978.

Transects 5 and 6 only show accretion in the seaward direction (beach widening) in these years before the shoal merges fully with the beach. This suggests a dispersion of sand alongshore before the shoal/swash bar ceases migration, and perhaps an influence of wave sheltering.

From transect 7 onwards through to transect 10 (stretch of coastline of approximately 3 kilometres length) only slight changes in the profile occur, almost exclusively in the lower foreshore with few significant morphological developments occurring on the subaerial beach during this time. Profile deviations mostly occur between 0m and -6m depth and beyond this depth the morphology smoothes out as waves are no longer disturbing the seabed. The form of the lower foreshore suggests migrating bars are the main cause of profile change. There are often multiple bars in the lower foreshore, of varying amplitudes, existing only until around -6m depth.

As the furthest reaches of the beach (until transect 10) are in the tail-end of the penultimate shoal attachment event from the 1930s, the profiles were examined for a residual sediment transport and to see if there is an accretion or erosion trend which may suggest downdrift movement of sand to sediment-starved locations. It was, however, not possible to identify any significant trend in the furthest profiles in the earliest data sets, suggesting that all additional sand from the previous cycle had dispersed. The beach during this phase seems to be stable in the short-term, aside from expected annual deviations.

5.2.2. Phase B: 1980 to 1992 – shoal attachment and dispersal

Transect 3 underwent dramatic morphological change during this phase. Between 1980 and 1981 a channel fronting the shoal increased its depth from -3m to -15m and effectively cuts off

the beach and the shoal at this point. The alongshore extent of this deep region (1981: transects 2.60; 3.01) (1982: transects 1.02; 3.01) is limited and does not appear in the data any further east than transect 3.01. Indeed by 1982 the most westerly points at transect 1 to 2 show the existence of the Borndiep to depths of greater than 28 metres, migrating eastwards against Ameland's west coast, as discussed in Israel and Dunsbergen (1999). The limited extent beyond transect 3 suggests that the presence of the deep region on the northwest beach is restricted, perhaps to a off-shoot or bend in of the Borndiep or Oostgat rather than a full breakthrough across the Bornrif shoal. Sand mining said to have taken place in 1981 (Cheung et al, 2007) is another possible reason for this deep region. Nevertheless, its presence in the profile at transect 3 indicates a separation of the beach from the shoal at a point in time when the rest of the shoal is attaching at transect 4. Recovery and infilling of this opening is steady in the following years and by 1986 the depth of this point in the profile is once again -3m. Throughout this phase and until 1986, volume is lost from the shoal while infilling occurs in the channel.

During the first phase, it was discussed that the shoal attached to the northwest beach at transect 4. In the following years until 1984 the beach is adjusting to the new sand volume and rapid dispersal takes place. By 1984 smaller swash bars are still migrating off the Bornrif and contributing to the beach volume, which sees an increase of 2000 m^3 at RSP 4 between 1982 and 1984. Subsequent years show that this is the final 'package' or migration of the swash bars for this stage of the cycle.

After the shoal merges with the beach, it acts as a sand wave which is dispersed in an alongshore easterly direction, as dictated by the prevalent wave direction and enhanced by tidal propagation from the west. Transects 5 and 6, located to the east of the shoal attachment site, show a trend of erosion in the years prior to the (sudden) appearance of the sand wave in their profiles. The sand wave appears as a sudden (year-to-year) increase in volume and is distinct in the profile as a large deviation from the normal bed level. With volume peaks occurring in 1992 and 1994 respectively, the sand wave is progressively moving from its attachment zone and is preceded by an erosion trend of roughly 130 $m^3/m/yr$.

Transects 7 to 10 show a small deviation in their normal trends between 1980 and 1990, which has been attributed to a small nourishment from sand mining that occurred when the shoal was attaching to transects 3 and 4 (Cheung et al, 2007). Otherwise, beach volume and width at these inlet-distant locations remains in a steady or stable condition during this phase. This beach is not yet affected by the shoal processes.

5.2.3. Phase C: 1993 to 2004 – alongshore dispersal and spit development

By at least 1993, transects 3 and 4 both show that the nearshore section of the profiles has lowered in elevation to below -5 metres NAP, while the beach formed from the shoal attachment shows a landward-directed erosion trend.

At transect 6 a complicated morphology develops as the shoal becomes like a spit, and curves in the alongshore but slightly landward direction, forming a lagoon between the spit and the beach. While the spit gains in height in the following years, it is prevented from migrating landward by the interacting forces on the tidal lagoon which fill and drain it with each tidal cycle. The result is that the spit remains more or less stationery for almost a decade while the lagoon gradually fills with sediment. The seaward edge of the spit is eroded while the landward edge progresses slowly.

Transect 7 is located approximately at the point where the tidal channel entered the lagoon and thus this part of the beach was subject to greater erosion with the meandering of this channel. This is clearly indicated in the years between 1999 and 2004 where a sharp reduction in beach width is seen in the profiles.

The Rijkswaterstaat undertook a beach and dune nourishment scheme during 1996 between transects 7.00 and 11.20 to counteract the ongoing erosion problem (Rijkswaterstaat [kustlijnkaarten], 1998). The immediate effect of the nourishment can be seen in the beach profiles of the subsequent years as a sudden seaward movement of both the dune foot (+3 metres NAP) and the estimated high water mark (+1 metre NAP). It is interesting to note that transect 7 does not show a change in beach profile associated with a nourishment scheme, despite being mentioned in the Rijkswaterstaat report of 1998. It is possible that this part of the beach was left out of the nourishment scheme due to the shoal/spit feature spreading alongshore, as by 1996 this feature appears in the lower foreshore profile for transect 7. The beach at transect 7 is eroded by 23 m/yr and 40 m/r in 1998-99 and 1999-2000 respectively, as the channel between the beach and the former shoal becomes narrower and erodes the beach.

The sand wave propagates through transects 7 to 10 during this phase, and is distinctly marked by a short period of erosion followed by a longer period of increasing beach volume and width.

Profiles of transect 8 indicate landward-moving bars formed around -6 metres NAP from 1998 onwards, coinciding with general volume increase across the foreshore profile as sediment moves alongshore from transect 7. The beach trend by 1998 is one of erosion and steepening due to the interference by the tidal channel against the dunes, and by 2000 the beach width has narrowed dramatically to around 20 metres (from ≈60 metres). However, by 1997 the sand wave has already reached the lower foreshore of transect 8 and increases both the volume and beach width in the subsequent years.

From 1996, the volume increases due to the combination of a beach nourishment at the same time as the sand wave arrives at this transect. The marked erosion trend in volume and width in particular, are dramatically reversed with the passage of the sand wave. The foreshore zone within 800 metres of the dune foot develops gradually over this time with increased sand volume. By the end of this phase the profile volume has more than doubled in 10 years, but has also experienced a dramatic accretion (nourishment) and erosion (tidal channel).

The beach nourishment in 1996 does not appear to increase the overall profile volume of transect 9. This is because the nourishment sand was placed high on the beach at the dunefoot where it is included in the calculations for dune volume rather than the beach volume, using the estimated boundary of +3 metres NAP. There is, however, an increase in the beach width and dune position which indicates the effect of the nourishment scheme, but the 'total volume' for the transect is not affected. In fact, even after the nourishment, there is still a lower total volume than before the nourishment. The arrival of the sand wave at this transect, starting in 1999, is preceded by an eroding trend for around 10 years, which might account for the eroding trend in the previous years with the nourishment.

The same kind of trends exist for transect 10 as they do for transect 9. At transect 10, a gradual erosion trend precedes the first appearance of the spit in 2000, in the form of migrating swash bars in the lower profile that are indicative of a gradual bit-by-bit sediment transport.

5.2.4. Phase D: 2004 and onwards – sand wave propagation

Towards the end of the last decade (i.e. in 2007), measurements at near-field transects 3 and 4 show that the eastern ebb delta is indeed building upwards and increasing its previously lowered surface to greater than -5 metres NAP. This evolving morphology can also be seen clearly in the bathymetry map for 2004-2005, which shows a landward-directed accretion on the eastern side of the ebb delta, originating from the outer delta.

Sediment dispersal dominates the morphology of the near-field beaches during this phase. Sediment is accumulating on the eastern ebb delta, but the most north-westerly beaches at transects 3 and 4 are eroding strongly and a landward-directed trend in the HWM is detected. Sediment dispersal from the west towards the east has already been identified and continues during this phase. Beach erosion at transects 3 and 4 is particularly extreme, and indications from the dataset show that this section of beach is at its most narrow from the whole 45-year period. Persistent erosion related to low ebb delta bed level in combination with a diverging sediment transport around the shoal has led to the narrowing of the beach since the shoal attachment. This is in line with the observations of Hicks et al (1999), who stated that downdrift beaches are starved of sediment during the period that the ebb delta is accumulating.

The last 10 years of the dataset also records the reduction and near-closure of the tidal channel/lagoon feature that was present for several years between transects 6 and 7. The spit that created the lagoon merged with the coastline and a channel opened up that remains today. During the fieldwork conducted in September to November 2010, it was observed that a "green beach" exists now between transects 6 and 7, where seawater reaches the 'old' beach but is insufficiently connected to the sea. Indeed for much of the beach between transect 5 and 6 there is dense low vegetation and a protected habitat for birds, which indicates the lack of contact with the sea and coastal processes. With this lagoon semi-closure the beach volume peak at transects 5 and 6 has only recently occurred, and therefore sediment dispersal in the following years will erode along this part of the beach.

A clear trend of the shoal's easterly-directed dispersal is reflected in the morphology of increasing beach width with time, in an alongshore direction. The propagation of the shoal as a sand wave can be seen as 'peaks' in beach width and volume, often with volume peaking before beach width (as volume includes water depths where alongshore sediment transport is taking place). In this phase we see transect 8 peaking in volume, with transects 9 and 10 estimated to hit peak volumes sometime in the next few years.

The trend on the far-field eastern transects of 8-9-10 shows progressive accretion on the foreshore. Accretion along this section of the beach is a gradual process of a slowly widening beach and volume. This is in contrast to earlier dispersal nearer the attachment zone where a singular mass appeared abruptly in the beach profile. This suggests that the erosive power is less with distance from the shoal and the inlet, or that more sediment is being held up at the updrift locations rather than transported downdrift.

There is clear evidence that the main dispersal mechanism occurring on the North Sea coast is the propagation of a sand wave from the shoal at transects 3 and 4 during phase B, towards transect 8 to 10 in phase D. An alongshore trend in increasing (then decreasing) cross-sectional volume and beach width is immediately preceded by an erosion trend. The sand wave form then becomes attenuated in amplitude as it progresses alongshore. This is typical sand wave behaviour as portrayed by Schwartz (2005) (see Figure 1.15). Further, the dispersal of the shoal

sand is seen to act as a singular mass of sediment moving alongshore, as opposed to a diffusive process throughout the coastal zone, which further cements the sand wave theory.

The paper by Hicks et al (1999) observed that a multi-year pattern on the far-field beaches is phase-locked to the bypassing cycle, although lagged in time. This same pattern has been shown to also occur on this stretch of coastline between 1965 and 2010. The attachment of the shoal in the early 1980s on the near-field beach induces a sand wave alongshore, which reaches transect 10 after a period of approximately 30 years. Further, the time lag shown between beach volume and width, which is several years at the near-field transects, decreases in the far-field transects to the point where there is no lag between volume and width.

5.3. Properties of the Coastal Profiles

Research question 1: How much sand was added to the beach when the shoal attached to the shoreline?

a. How does the downdrift beach volume change over time?

In order to address this question, the trend of beach volume had to be defined in terms of the appearance of the shoal and the inclusion of its sand volume to the beach. Over time, peaks of cross-sectional volume occurred as the bulk of sand from the former shoal was dispersed in the alongshore direction as a sand wave. An average of the pre-shoal volumes was calculated, and deducted from the cross-sectional volume of the transect peak. With this data, a percentage could be calculated to present the shoal-contributed volume as a proportion of the "original" average volume.

The results were surprising, and showed that for most of the central transects (RSP 5-8) the shoal volume added was equal or higher than the total volume of the beach: a doubling of the average volume. Particularly for transect 5, an increased volume of 114% occurred at the time of its peak. The bulk of the shoal volume attenuates through time, as it progresses from one transect to another: therefore, a comparatively smaller sand volume is transferred to the furthest transects than at those nearest the inlet. The budget of the sand wave is conserved, but it becomes more spread out along the coast with time. Thus, individual transects distant from the inlet experience smaller volume and beach width changes. In addition to the attenuation, some volume loss occurring over time can be attributed to cross-shore re-distribution.

Transects 3 to 7 are seen to undergo the most amount of change during the 45 year record, while transects 8 to 10 are affected in a gradual manner. According to the Fenster and Dolan (1996) classification for the spatial extent and magnitude of inlet influence, the long-term analysis has shown that transects 3 to 7 are dominated by these inlet processes, while transects 8 to 10 are influenced.

b. How do properties of coastal profiles change in time and space?

The trend appearing in the volume fluctuations occurs alongshore in a time-lagged fashion, whereby the alongshore dispersal of shoal sand takes place sequentially from one transect to another with distance from the inlet. Beach width is seen to follow a similar pattern between adjacent transects. A time lag between beach volume and width peaks occurs in transects 3 to 6,

ranging from 8 to 11 years in phase difference. This time lag is due to the volume of sediment involved and time period required for this sediment to reach the +1 m NAP position which defines the lower boundary for beach width. At transect 7 this volume-width time lag does not occur, as the beach is separated from normal coastal processes by the alongshore development of the spit. At transects 8 to 10, no time lag occurs. At this point the volume of sediment transported along the coast is attenuated and the volume peak takes several years to occur, in which time sediment is transported in the cross-shore direction towards +1 m NAP.

In transects 3 and 4 there is a period of beach narrowing before the shoal attachment, after which the shoal merges with the beach and is dispersed. During this period of dispersal a wide flat beach exists just under +1 m NAP, therefore causing the fluctuations in HWM position during this time. Long-term erosion occurs at these transects in the following period, and the beach is eroded dramatically.

c. Where in the profile does most change occur?

In the short term, the cut/fill analysis showed that for both locations (RSP 3-5, 9-10) there was widespread surface change. Surface change at RSP 3.6-5.2 and 9-10 showed a coupling of increased loss, decreased gain at the westerly transects, with a switch to decreased loss increased gain in the easterly transects. This alongshore loss-to-gain (west to east) pattern suggests that wind erosion over the wide beach is transporting sand from the foreshore and backshore towards the dunes and easterly parts of the beach. Dune build-up over the long-term reflects a steady input of wind-blown sand from the beach, indicating that this is a persistent process in both the long- and short-term.

In the long-term data, covering the foreshore as well as the beach, more change to the profile occurs in the foreshore and nearshore environments. This is expected as these form the most active part of the profile exposed to constant wave energy.

d. Is there a cyclical component to volume fluctuations over time?

In the sense of a cyclical component being a deviation and subsequent return from the normal volume, this is not quite visible in the morphological data except at transects 3 and 4. The cyclical component hypothesised was stemmed from similar studies (e.g. Schiermonikoog) which indicated a cyclical fluctuation in HWM and dune foot in the long-term, and also resulted from sand bypassing processes at a tidal inlet. In order for a cyclical trend to be identified, it would be necessary to have morphological data that extends further in time than the Jarkus data offers.

Israel and Dunsbergen (1999) suggested a cycle of approximately 50-60 years for the channel development in the Ameland inlet, and it is assumed that a similar cycle is observed on the downdrift beach. In the transects that underwent significant morphological development (3 and 4) a cyclical component is identified. These transects are in the location where the shoal merged with the beach and thus they responded to it from the earliest years of the dataset. In the subsequent years since the shoal migrated into these profiles, the cross-sectional volumes have increased, peaked and decreased with the dispersal of the attachment shoal. Considering the situation of the beach at the beginning of the record, erosion has returned both the volume and width to its previous pre-shoal level, and even has exceeded this further. Additionally, Figure 4.9

(page 67) appears to indicate that a trend of erosion is superimposed upon the cyclical behaviour. Both the maximum and minimum volumes (beach widths) have occurred over the course of the last 45 years, so a morphological cycle of around 20 years can be identified at transects 3 and 4.

e. During a previous shoal attachment, did the shoreline respond in the same way as currently?

Unfortunately the Jarkus dataset does not extend far enough back in time to determine whether the shoreline responded in the same way to the last major shoal migration event. Israel and Dunsbergen (1999) inferred that the last major shoal event occurred in 1926, and proposed the beach morphology of 1950 (widespread sediment dispersal) would be the situation of 2010. Therefore, morphological data for at least the period 1925-1950 would be required to properly address this question. However, systematic profile data is just not available for this early period.

5.4. Sediment Dispersal

Research question 2: How is sediment dispersed on the coastline following attachment of the shoal?

a. What is the main mechanism by which the attaching shoal is dispersed?

When the attaching shoal merged with the beach in the early 1980s, it become elongated and aligned to the coastline. Part of the shoal was transported by wave and tidal forcing towards the inlet (see following question), while the majority of the shoal merged and began dispersing alongshore towards the east. A sand wave form developed, preceded by a trend of erosion for a period of around 5 years prior to the appearance of the sand wave at each transect (4 to 7). This erosion trend is attributed to sediment starvation as normal longshore drift processes do not operate around the sand wave. As the sand wave progressed alongshore, it developed into an alongshore spit due to the relatively strong influence of eastward-directed tidal forces. As it became further from the sheltered area nearest the ebb delta, wave forcing curved the spit in towards the coastline, where it formed a lagoon. The development of this lagoon occurred around 20 years after the main attachment of the shoal. The sand wave is attenuated in form, and spread across a wide alongshore width. This attenuation is shown in transects 8 through to 10, where the changes in beach width and volume are reduced compared with the near-field beaches. The volume reaching transect 9 is half of that which was added to transect 5 (from 5000 m^3/m to around 2600 m^3; Table 12). The attenuation trend is typical of sand wave behaviour (Schwartz, 2003), and while the volume of the sand wave is conserved the volume is spread over a wider alongshore width and thus smaller changes are seen in the downdrift transects.

b. Can a diverging sediment transport be identified from morphological changes?

A secondary direction of alongshore dispersal has been discussed in literature such as Cheung et al (2007) and Rijkswaterstaat (2010), whereby the prevailing north-westerly waves approach the beach and diverge towards the east and west. This sets up a bifurcation in

sediment transport around transect 4. Both directions of sediment transport are enhanced by tidal flow, but the dominant longshore drift direction is from west to east as shown by the sand wave development.

The bifurcation in sediment transport has been proved in both the short- and long-term data. In the short-term data, transects 3.8 to 4.20 underwent considerably more variation than the other transects, experienced more erosion, and had a consistently steeper foreshore (0.018) than at the rest of the beach. A similar erosion trend was not observed at any other location on the beach, near- or far-field, which suggests that a bifurcation in sediment transport enhances erosion at these transects. An alignment of the shoreline orientation following the attachment of the shoal, particularly observed in the bathymetry maps for 1989, 1993 and 1996 (see Figure 4.4 to Figure 4.6), hints towards a bifurcation in sediment transport which permits this re-shaping of the shoal.

5.5. Dune Development

Research question 3: What is the impact of fluctuating beach volume on dune development?

a. Does a phase of shoreline accretion and beach widening correlate with dune building processes and vice versa?

There does not appear to be a clear correlation between the dynamic beach width and the slower-responding dunes. This is a factor of time mainly, as the beach is responding at a much faster rate than the dunes do and perhaps covering a longer period of time would indicate a correlation between beach width and dune position. That said, there is a persistent dune foot progradation through time and the short-term data indicated a pattern of accumulation on the backshore, which adds volume to the dunes in time.

b. How much dune advance has there been since attachment of the shoal?
    i. Have dunes increased in height and/or advanced towards the shoreline?
    ii. What is the change in volume of the dunes since attachment of the shoal?

The historical morphological data has shown that at each transect, dune volume and dune foot position has prograded during the period 1965-2010. Dune volume increases by 200-300 m^3/m over this period. The trend in dune foot position is one of advance towards the shoreline, with an average total shift of around 60 metres cross-shore movement for each transect, with the exception of transect 4 which has a shift of up to 120 metres. Dune foot position only mirrors the HWM in exceptional circumstances, such as beach nourishment and erosion at transect 3. Beach nourishment occurs in transects 7-10 and is clearly detected when comparing beach width with dune foot position. The long-term erosion trend in transect 3 removes much of the original beach width and shoal sand, that the dune foot is threatened with wave erosion from storm events and has been eroded in recent years.

Lastly dune height has increased in each transect over the period 1965-2010. The greatest rate of height increase occurs at transect 4, which sees an estimated 0.20 m/yr added each year. Initially the dunes were much lower here, and its exposed position facilitated more sediment input towards the dunes.

c. Is there evidence of aeolian processes dispersing sand cross-shore and contributing to dune formation?

Aeolian cross-shore dispersal processes are evident in both the short- and long-term beach profile datasets, and also are suggestive from the ongoing dune building and progradation of the dune foot.

6. Conclusions

The hypothesis stated that insufficient dispersal of the shoal volume from the westerly beaches was enabling erosion at further downdrift locations. The results of beach volume analysis has shown that a significant volume from the sand wave is yet to reach the eroding locations of central Ameland, and is still dispersing from transects 9-10. It remains to be seen how much of the original volume will nourish the distant beaches, as the attenuation of the shoal between transect 4 and 10 has decreased the available volume for dispersal. While near-field transects such as 5 and 6 received over double the original volume of their beaches (≈5000 m^3/m) when the sand wave progressed through, transect 9 only received an 80% increase in volume (≈2600 m^3/m) and 10 currently has around 60% increased volume. It is likely, therefore, that the rest of the beach to the east will again only receive a small proportion of the overall shoal volume as it spreads out alongshore. It is expected that through time erosion of the near-field transects will provide more littoral drift sand.

This research has shown that, through time, the shoal is dispersed in such a way that "peaks" in volume occur successively from one transect to another. This appears to be the passage of a sand wave, an irregularity in beach form that moves alongshore as a singular mass in the direction of net littoral drift and which can be tracked downdrift as the propagation of an accretion/erosion wave (Schwartz, 2003). This same pattern can be detected in the morphology, particularly from beach width, where the sudden appearance of the main shoal volume is preceded by a period of erosion. This erosion is a result of a ceasing in the normal littoral drift as the shoal volume draws nearer, and wave refraction around the shoal may also play a role. However, a time lag occurs between the peak volume and peak width in the record, where beach width lags behind volume. This difference ranges from 8-11 years at transects 4 to 7, but when the sand wave reaches transects 8 to 10 this time lag does not occur.

The extreme erosion trend at transect 3 indicates a bifurcating sediment transport, the evidence for which is shown in both the short-term fieldwork data and also the long-term data. The erosion trend since 1995 levelled at 200 $m^3/m/yr$, and the current width of the beach is its lowest for the entire record. This means that nourishing the beach at this transect is probably ineffective in the current phase, and awareness should be made of the forces acting at this location when considering nourishments in the future.

The natural state of the beaches is difficult to discern from the nourishment projects that have taken place for decades. It is likely that erosion trends will be slowed or reversed by persistent nourishment schemes with the intention of preventing encroachment on the "fixed shoreline", the BKL. The impact on the natural beach morphology is yet to be evaluated and particularly concerns the coastline further downdrift of nourishment sites, where the erosion trend is not as severe as the central portion of the island. Indeed, as the shoal sand wave reaches the nourishment locations over the coming years, there may in fact be an excess of sediment as the volume contained in the sand wave is probably not considered during nourishment decision-making.

Based on the cyclical nature of the inlet system it is expected that the current eastern ebb delta accumulation will build for the coming decade, resulting in the formation and migration of another Bornrif shoal in the 2020s. The central section of Ameland's north coast will experience

the slow, attenuating passage of the previous shoal and the associated trend of erosion followed by accretion.

7. References

BRUUN, P. and GERRITSEN, F., 1959. Natural bypassing of sand at coastal inlets, 1959, Journal of Waterways and Harbor Division, pp. 75-107.

CHEUNG, K.F., GERRITSEN, F. and CLEVERINGA, J., 2007. Morphodynamics and sand bypassing at Ameland Inlet, the Netherlands. *Journal of Coastal Research,* **23**(1), pp. 106-118.

CLEVERINGA, J., ISRAËL, C.G. and DUNSBERGEN, D.W., 2005. De westkust van Ameland: Resultaten van 10 jaar morfologisch onderzoek in het kader van de Rijkswaterstaat programma's KUST2000 en KUST2005. RIKZ/2005.029. The Netherlands: Rijkswaterstaat RIKZ.

COOPER, J.A.G., MCKENNA, J., JACKSON, D.W.T. and O'CONNOR, M., 2007. Mesoscale coastal behavior related to morphological self-adjustment. *Geology,* **35**, pp. 187-190.

DAVIDSON-ARNOTT, R.G.D. and VAN HEYNINGEN, A.G., 2003. Migration and sedimentology of longshore sandwaves, Long Point, Lake Erie, Canada. *Sedimentology,* **50**, pp. 1123-1137.

DAVIS JR, R.A. and BARNARD, P., 2003. Morphodynamics of the barrier-inlet system, west-central Florida. *Marine Geology,* **200**, pp. 77-101.

DEAN, R.G., KRIEBEL, D.L. and WALTON, T.L., 2006. Cross-shore Sediment Transport Processes, In: King, D., Coastal Engineering Manual, Part III Chapter 3, Coastal Sediment Processes, Engineer Manual 1110-2-1100. EM 1110-2-1100 (Part III). Washington D.C.: Coastal & Hydraulics Laboratory, US Army Corps of Engineers.

DEAN, R.G. and WORK, P.A., 1993. Interaction of navigational entrances with adjacent shorelines. *Journal of Coastal Research Special Issue,* **18**, pp. 91-110.

FENSTER, M. and DOLAN, R., 1996. Assessing the impact of tidal inlets on adjacent barrier island shorelines. *Journal of Coastal Research,* **12**(1), pp. 294-310.

FITZGERALD, D.M., 1996. Geomorphic variability and morphologic and sedimentologic controls on tidal inlets. *Journal of Coastal Research Special Issue,* **23**, pp. 47-71.

FITZGERALD, D.M., 1988. Shoreline erosional-depositional processes associated with tidal inlets. In: D.G. AUBREY and L. WEISHAR, eds, *Hydrodynamics and Sediment Dynamics of Tidal Inlets: Lecture Notes on Coastal and Estuarine Studies.* New York: Springer-Verlag, pp. 186-225.

FITZGERALD, D.M., 1984. Interactions between the ebb-tidal delta and landward shoreline: Price Inlet, South Carolina. *Journal of Sedimentary Petrology,* **54**(4), pp. 1303-13182.

FITZGERALD, D.M., KRAUS, N.C. and HANDS, E.B., 2001. *Natural mechanisms of sediment bypassing at tidal inlets.* ERDC/CHL CHETN-IV-30. Vicksburg, MS.: US Army Engineer Research and Development Center.

FITZGERALD, D.M. and PENDLETON, E., 2002. Inlet formation and evolution of the sediment bypassing system: New Inlet, Cape Cod, Massachusetts. *Journal of Coastal Research Special Issue,* **36**, pp. 290-299.

FITZGERALD, D.M., PENLAND, S. and NUMMEDAL, D., 1984. Control of barrier island shape by inlet sediment bypassing: East Frisian Islands, West Germany. *Marine Geology,* **60**, pp. 355-376.

GAUDIANO, D.J. and KANA, T.W., 2001. Shoal bypassing in mixed energy inlets: Geomorphic variables and empirical predictions for nine South Carolina inlets. *Journal of Coastal Research,* **17**(2), pp. 280-291.

GOLDSMITH, V., BYRNE, R.J., SALLENGER, A.H. and DRUCKER, D.M., 1975. The influence of waves on the origin and development of the offset coastal inlets of the southern Delmarva peninsula, Virginia. In: L.E. CRONIN, ed, *Estuarine Research.* New York: Academic Press, pp. 587.

HAYES, M.O., 1980. General morphology and sediment patterns in tidal inlets. *Sedimentary Geology,* **26**, pp. 139-156.

HAYES, M.O., GOLDSMITH, V. and HOBBS, C.H., 1970. Offset Coastal Inlets: Forms of Sediment Accumulation in the Beach Zone, *Proceedings 12th Coastal Engineering Conference (ASCE),* 1970, , pp. 1187-1200.

HAYES, M.O. and KANA, T.W., 1976. *Terrigenous clastic depositional environments.* Technical Report No. 11-CRD. Columbia, South Carolina: Department of Geology, University of South Carolina.

HICKS, D.M., HUME, T.M., SWALES, A. and GREEN, M.O., 1999. Magnitudes, spatial extent, time scales and causes of shoreline change adjacent to an ebb-tidal delta, Katikati Inlet, New Zealand. *Journal of Coastal Research,* **15**(1), pp. 220-240.

HUBBARD, D.K., 1977. *Variations in tidal inlet processes and morphology in the Georgia embayment.* Technical Report No. 14-CRD. Coastal Research Div., Dept. Geol., University of South Carolina, Columbia: .

ISRAËL, C.G. and DUNSBERGEN, D.W., 1999. Cyclic morphological development of the Ameland Inlet, The Netherlands, Proceedings IAHR Symposium on river, coastal and estuarine morphodynamics, Department of Environmental Engineering, University of Genoa, 1999, , pp. 705-714.

KANA, T.W., 1995. Signatures of coastal change at mesoscales, Coastal Dynamics '95, Proceedings of the International Conference on Coastal Research in terms of Large Scale Experiments. New York (ASCE), 1995, , pp. 987-997.

KANA, T.W., HAYTER, E.J. and WORK, P.A., 1999. Mesoscale sediment transport at Southeastern U.S. tidal inlets: Conceptual model applicable to mixed energy settings. *Journal of Coastal Research,* **15**(2), pp. 303-313.

KANA, T.W., WILLIAMS, M.L. and STEVENS, D., 1985. Managing shoreline changes in the presence of nearshore shoal migration and attachment, *Proceedings Coastal Zone 1985 (ASCE New York),* 1985, , pp. 1277-1294.

LOUTERS, T. and GERRITSEN, F., 1994. *The Riddle of the Sands.* RIKZ- 94.040. Ministry of Transport, Public Works and Water Management, Directorate-General of Public Works and Water Management, National Institute for Coastal and Marine Management (RIKZ).

MICHEL, D. and HOWA, H.L., 1997. Morphodynamic behaviour of a tidal inlet system in a mixed-energy environment. *Physical Chemical Earth,* **22**, pp. 339-343.

MORANG, A. and PARSON, L.E., 2002. Coastal Terminology and Geologic Environments, In: Morang, A., Coastal Engineering Manual, Part IV Chapter 1 , Coastal Geology Part III. Engineer Manual 1110-2-1100. Washington, DC.: U.S. Army Corps of Engineers.

O'BRIEN, M.P., 1931. Estuary tidal prisms related to entrance areas. *Civil Engineering,* **1**(8), pp. 738-739.

OERTEL, G.F., 1977. Geomorphic cycles in ebb deltas and related patterns of shore erosion and accretion. *Journal of Sedimentary Research,* **3**, pp. 1121-1131.

OERTEL, G.F., 1975. Ebb-tidal deltas of Georgie estuaries. In: L.E. CRONIN, ed, *Estuarine Research.* Academic Press, New York, pp. 267-276.

OERTEL, G.F., 1972. Sediment transport of estuary entrance shoals and the formation of swash platforms. *Journal of Sedimentary Petrology,* **42**(4), pp. 857-863.

ROBIN, N., LEVOY, F. and MONFORT, O., 2009. Short term morphodynamics of an intertidal bar on megatidal ebb delta. *Marine Geology,* **260**, pp. 102-120.

SCHWARTZ, M.L., ed, 2005. *Encyclopedia of Coastal Science.* The Netherlands: Springer.

SHA, L.P., 1989. Variation in ebb-delta morphologies along the west and east Frisian Islands, the Netherlands and Germany. *Marine Geology,* **89**, pp. 11-28.

SHA, L.P. and VAN DEN BERG, J.H., 1993. Variation in the ebb-tidal delta geometry along the coast of the Netherlands and the German Bight. *Journal of Coastal Research,* **9**(3), pp. 730-746.

STIVE, M.J.F., AARNINKHOF, S.G.J., HAMM, L., HANSON, H., LARSON, M., WIJNBERG, K.M., NICHOLLS, R.J. and CAPOBIANCO, M., 2002. Variability of shore and shoreline evolution. *Coastal Engineering,* **47**(2), pp. 211-235.

VAN LEEUWEN, S.M., VAN DER VEGT, M. and DE SWART, H.E., 2003. Morphodynamics of ebb-tidal deltas: a model approach. *Estuarine, Coastal and Shelf Science,* **57**, pp. 899-907.

WALTON, T.L. and ADAMS, W.D., 1976. Capacity of inlet outer bars to store sand, *Proceedings of the 15th Coastal Engineering Conference, Honolulu (ASCE),* 1976, , pp. 1919-1937.